UNIVERSITY OF CALGARY

Bearing Capacity of Tapered Piles

by

John Tristan Spronken

A THESIS

SUBMITTED TO THE FACULTY OF GRADUATE STUDIES IN

PARTIAL FULFILLMENT OF THE REQUIREMENTS FOR THE DEGREE OF

MASTER OF SCIENCE

DEPARTMENT OF CIVIL ENGINEERING

CALGARY, ALBERTA

NOVEMBER, 1998

Abstract

This thesis summarizes the findings of load tests conducted on model tapered, partially tapered, and straight piles. All piles were 50.8 mm in diameter with the tapered piles reduced to 25.4 mm diameter at the toe. The piles were driven into a medium-dense pluviated sand bed under 3 different pressure regimes: no additional pressure, surcharged, and surcharged with confining pressure.

Test results showed that bearing capacity increased with increasing volumetric displacement, taper angle, percentage of pile tapered, confining pressure, and depth of driving. Tapered piles provided equal or greater bearing capacity under no additional pressure condition and significantly greater capacity under the surcharged with confining pressure condition. The surcharged condition yielded unreliable results.

End bearing in all conditions was reliably estimated by a double passive pressure method. The bearing capacity could be reliably determined using pile driving formulae.

Acknowledgements

I wish to extend my thanks and gratitude to Dr. R. C. Joshi for his guidance and patience throughout this entire period. In addition I wish to thank Mr. Don McCullough whose technical expertise, historical knowledge and numerous timely equipment repairs were invaluable in the completion of this project.

Finally, I wish to thank my family for the support and encouragement that they provided me for the duration of this project.

To My Parents

Table of Contents

List of Tables

List of Figures

Chapter 1

Introduction

1.1 General

Piles are used to transmit loads to a deeper, and stronger soil stratum when the surface soil strata is incapable of supporting the superstructure. This may be due to insufficient strength in the surface layer of the soil or to unacceptable settlement. Piles generally support vertical compressive loads, but tensile and lateral loads may result from external sources such as wind, earthquake, waves and machinery or internally from the movement of the soil itself.

The use of piles as a means of supporting structures has a long history throughout the world. In 200 BC the Han Dynasty in China was known to have used timber piles as supports for bridges (Mohan, 1988). Most of the structures in the city of Venice, Italy are entirely supported by piling, some of which is hundreds of years old. Prior to the late 19th century, piling was based upon a trial and error basis or upon previous experience in the particular region. Geotechnical engineers have learned a great deal about pile foundations during the past century, but there remain many aspects of their design and behaviour yet to be explored and explained.

Early piles were generally made from wood due to the availability of timber and the lack of materials such as concrete and steel. However, the strength, long term reliability, and

availability of concrete and steel often make them a better alternative for the massive structures which are constructed today in the modern world

Piles can be summarized into three major classifications: cast-in-place piles, driven closed ended piles or open ended piles. The decision to use one type of pile versus a different type encompasses factors such as the location of the building site, the type of soil, the required depth of the pile, the required bearing capacity, the equipment available, the site conditions, and local practice.

Closed ended piles are the most common types of piles available on the market. These piles can be formed out of wood, steel, or concrete and are generally driven into the soil. The steel piles are usually pipe piles, which have a hollow circular cross-section with a thick plate or a driving shoe at the toe. Precast concrete piles typically come in sections with circular, hexagonal or square cross-sections.

Open ended piles are similar to closed ended steel piles, but, as the name implies, they do not have a plate or driving shoe at the pile toe. This facilitates the driveability due to a decrease in the resistance at the toe of the pile. Upon completion of driving, the soil from the hollow portion inside the pile is sometimes removed and filled with concrete to increase both the bearing capacity and also the ultimate strength of the pile itself. Studies (Klos and Tejchman, 1977; Smith 1995), though not conclusive, have shown that it may not be necessary to fill open ended pipe piles with concrete in order to achieve a bearing

capacity similar to that of closed ended piles. Other low displacement steel piles include standard H or I sections.

Cast-in-place piles are a form of non-driven closed ended piles. The pile is formed by augering a hole in the ground, placing the required reinforcing steel in place, and filling the hole with concrete. After the concrete has set the pile behaves in a manner similar to closed ended piles. The depth of excavation, the soil characteristics, or the presence of water may necessitate the insertion of a steel sleeve or casing into the augered hole in order to prevent the collapse of the soil.

The ultimate bearing capacity of piles has been the focus of many studies (Skempton, Yassin and Gibson, 1953; Meyerhof, 1956; Nordlund, 1963; Vesic, 1967; Mansur and Hunter, 1970; Touma and Reese, 1973; Mitchell and Solymar, 1984; Olson and Long, 1989). Both theoretical and empirical methods have been developed by engineers in order to determine the bearing capacity of piles in a wide range of soils. These methods have proven to be reliable, but the inconsistent nature of soil leads to a degree of uncertainty. This has resulted in the inclusion of generous safety factors into the design process. The safety factors are further increased due to the limited data that can be deduced from normal field tests, the many variables encountered when dealing with different soil strata, and the selection of the appropriate empirical coefficients. These unknowns are not as great for driven piles due to the feedback provided during the driving process. Test piles may be installed to improve the accuracy of the design, but this practice is both expensive

and time consuming. Thus test piles are generally installed only on major projects.

Laboratory testing attempts to improve the reliability of the pile design. The validity of laboratory testing has been questioned due to scaling uncertainties and also the inability to fully replicate field conditions. However, laboratory testing has the advantage of being relatively inexpensive and offers a great deal of control on the soil and other variables. The low cost involved allows for the analysis of a wide range of variables which can later be applied to the actual field conditions.

Many attempts have been made to increase the bearing capacity of piles through modification of the pile shape while maintaining the length and diameter. Most of the explored methods deal with improving the end bearing capacity of the pile. Franki-piles and belled piles are the two most common methods of increasing the end bearing capacity of the piles. Through different means the pile base is expanded and the diameter of the pile at the toe is increased thus increasing the bearing capacity of the pile. One method uses a dynamic method which may or may not yield true pile capacities, while the other uses mechanical means to increase the base area. Both the Franki and belled piles are cast-in-place and thus preclude the use of steel or precast piles.

Little has been done to attempt to improve the shear resistance of the piles. The most common method to increase the shear resistance of the pile comes in the form of roughening the surface of the pile. Another, but largely ignored, method of increasing the

shear resistance is to taper the pile, which forms the basis of this paper. *Monotube*® has been making tapered piles since the 1920's, and numerous sources (Peck, 1958; Morrison and Robinsky 1964; Nordlund, 1964; Olson and Long, 1989; Rybnikov, 1990; Zil'berberg and Sherstnev, 1990; Kodikara and Moore, 1993) have demonstrated dramatically increased bearing capacity when using tapered piles in certain sandy soils. Yet the use of tapered piles is limited, in part, due to the lack of design methodology and widespread results from testing of such piles. Another factor hindering the acceptance of tapered piles is the general higher costs associated in the manufacturing of such piles which can possibly be overcome.

1.2 Scope of Study

An investigation of the bearing capacity of tapered and partially tapered piles both in relation to each other and also in relation to uniform diameter piles was performed. Uniform sand beds were deposited using the pluviation method. Model piles were driven into a sand bed by a hammer and pulley system with a constant drop height. The piles were tested under a constant rate of penetration by a closed loop hydraulic material testing system (MTS). The parameters of this test include: the angle of taper on the pile, the length of the pile, and the additional stresses applied to the sand bed. The tapers analyzed were 0.5°, 1° and 2°, and all the test piles underwent a change in diameter from 25.4 mm (1 inch) at the base to 50.8 mm (2 inches) at the top. This resulted in the length of the taper varying with the angle of taper. The tapered piles were compared to a 50.8 mm (2 inch) straight test pile.

1.3 Objectives

The objectives of this study were:

- To study the bearing capacity of tapered, partially tapered and untapered piles driven into a dry coarse grained soil.
- To study the effects of varied driving lengths upon the bearing capacity of the various piles.
- To study the development of the shear resistance and end bearing capacity with varying buried depth of pile.
- To study the effect of varying taper on the developed end bearing capacity of the pile.
- To compare the uplift capacity between untapered and partially tapered piles.
- To study the relation between blow counts and bearing capacity.

Chapter 2

Literature Review

2.1 General

Piles are classified as deep foundations when the length exceeds the diameter by a factor of no less than four under normal circumstances (Prakash and Sharma, 1990). Depending on the location, applied loads and soil conditions, piles can be placed vertically or slanted (battered). Their purpose is to transmit load from a structure to the load bearing soil strata in a manner which will not exceed the capacity of the soil while limiting settlements of the said structure for design requirements. Piles transmit their load to the adjacent soil through the friction developed along their sides, and through bearing along their base.

2.2 Bearing Capacity of Piles

For the design purposes of piles, the ultimate axial support load is generally presented in the form:

$$Q_{ult} = Q_p + Q_s = q_u \cdot A_p + f_s \cdot A_s \qquad (1)$$

where Q_{ult} = ultimate axial bearing capacity

Q_p = ultimate end bearing load

Q_s = ultimate shaft load

q_u = ultimate end bearing stress

f_s = ultimate shear resistance

A_p = end bearing area of the pile

A_s = area of pile shaft

As shown in the preceding equation, end bearing and shaft stresses are generally treated independent of each other. Touma and Reese (1974) concluded that these two factors are not completely independent from each other and that there is interaction between the forces beneath the pile tip and the forces on the pile shaft.

In coarse grained, i.e. cohesionless, soils (sand, gravel, and rock) the ultimate bearing capacity is largely a result of the end bearing capacity of the pile. Whereas in fine grained, cohesive soils, i.e. clays and silts, the ultimate bearing capacity is largely the result of the developed shaft resistance.

The determination of the bearing capacity of piles in sand is difficult because of the many variables involved. Installation of a pile in sandy soil causes deformation of the adjacent soil, rotation of the planes of principal stress, and differential volume changes (Hanna and Tan, 1973).

2.2.1 End Bearing Capacity

Most accepted modern methods for determining the end bearing capacity of piles follow the formula:

$$q_u = c \cdot N_c \cdot S_c + q \cdot N_q \cdot S_q + \frac{1}{2} \cdot \gamma' \cdot B \cdot N_\gamma \cdot S_\gamma \qquad (2)$$

where c = cohesion of the soil

q = overburden pressure

γ' = effective unit weight of soil

N_c, N_q, N_γ = bearing capacity factors for a strip footing

S_c, S_q, S_γ = pile shape factors

B = width of the foundation

This equation is simplified for piles through the use of several logical statements. When the depth is significantly larger than the width, as with pile foundations, it may be stated that $\gamma' B N_\gamma \ll q N_q$ and therefore becomes insignificant. This reduces the original equation to:

$$q_u = c \cdot N_c \cdot S_c + q \cdot N_q \cdot S_q \tag{3}$$

In a cohesionless soil c = 0, therefore $c \cdot N_c \cdot S_c = 0$. Since virtually all piles are circular or square S_q has a constant value and therefore has been incorporated into the N'_q values. Equation (3) is thus reduced to the form:

$$q_u = q \cdot N'_q \tag{4}$$

The earliest studies into the bearing capacity of piles (Prandtl, 1921; Reissner, 1924; Caquot, 1934; Buisman, 1935) were based on the penetration of a rigid stamp into an incompressible solid. It was therefore believed that the bearing capacity of the pile was proportional to the initial overburden pressure of the soil. Vesic (1973) further concluded

that the mean normal ground stress, σ'_o, not the initial overburden stress, σ'_v or q in equations 2 through 4, governs the bearing capacity. Vesic determined that the mean normal ground stress is related to σ'_v by the equation:

$$\sigma'_o = \frac{(1+2\cdot K_o)\cdot \sigma'_v}{3} = \frac{(1+2\cdot K_o)\cdot \gamma'\cdot H}{3} \tag{5}$$

Vesic defined the end bearing as:

$$q_u = \sigma'_0 \cdot N_\sigma \tag{6}$$

Thus equating (4) to (6) results in:

$$N'_\sigma = \frac{3\cdot N'_q}{1+2\cdot K_o} \tag{7}$$

where, σ'_o = mean normal ground stress

σ'_v = effective overburden pressure

K_o = coefficient of earth pressure at rest (= 1- $\sin\phi'$)

γ' = effective unit weight of soil

H = height of soil above pile toe

N'_σ = bearing capacity factor for mean normal ground stress

N'_q = bearing capacity factor including shape factor

ϕ' = soil internal angle of friction

In an attempt to determine the end bearing capacity of piles, various failure patterns beneath the pile tip have been proposed. The differences between the various patterns and

field testing have resulted in numerous proposals for the value of N'_q. While demonstrating the high dependence of N_q upon the ϕ' of the soil, Figure 2.1 illustrates many of the various proposed values for N'_q. Figure 2.2a shows the failure pattern beneath the pile toe as proposed by DeBeer (1945) and Jaky (1948). Berezantsev (1953, 1961) and Vesic (1963) proposed that the failure occurs only in the region directly beneath the pile toe (Figure 2.2b). As shown in Figure 2.2c, Terzaghi (1945) assumed that the failure pattern beneath a pile was identical to the failure pattern beneath a shallow footing. The major assumptions being that the soil above the pile tip was replaced by an equivalent overburden pressure while ignoring the shear strength of the soil. Figure 2.2d illustrates the failure pattern proposed by Skempton *et al.* (1953) which is represents an expanding spherical cavity. Vesic (1977) proposed a failure pattern, shown in Figure 2.3a, based upon observed failure patterns beneath pile tips of model and full size driven piles, see Figure 2.3b. The wedge I is a highly compressed region of soil directly beneath the pile tip. This wedge exists beneath the tip of the pile regardless of the initial soil conditions. The wedge pushes through loose soils without forming noticeable slip surfaces. In dense soils the wedge I pushes the shear zone II into the plastic zone III. Further advancement of the pile into the soil is made possible through the compression of the soil in zones I and II as well as the lateral expansion of the soil in Zone III.

Vesic (1967) concluded that the ultimate end bearing capacity of a pile was reached only after a settlement of approximately 25% of the pile diameter for placed piles and 10% of

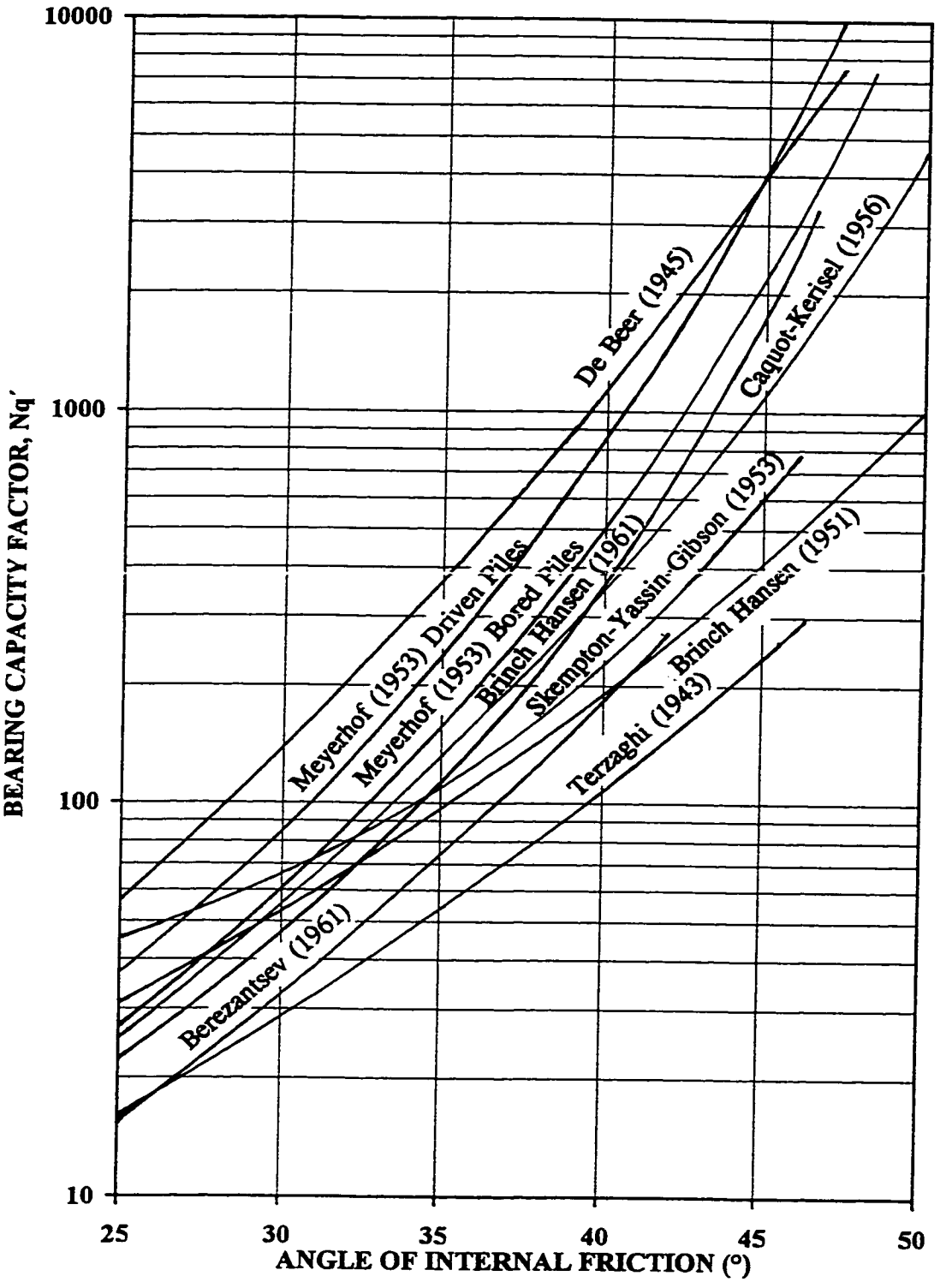

Figure 2.1 - Bearing Capacity Factor versus Angle of Internal Friction (Vesic, 1964)

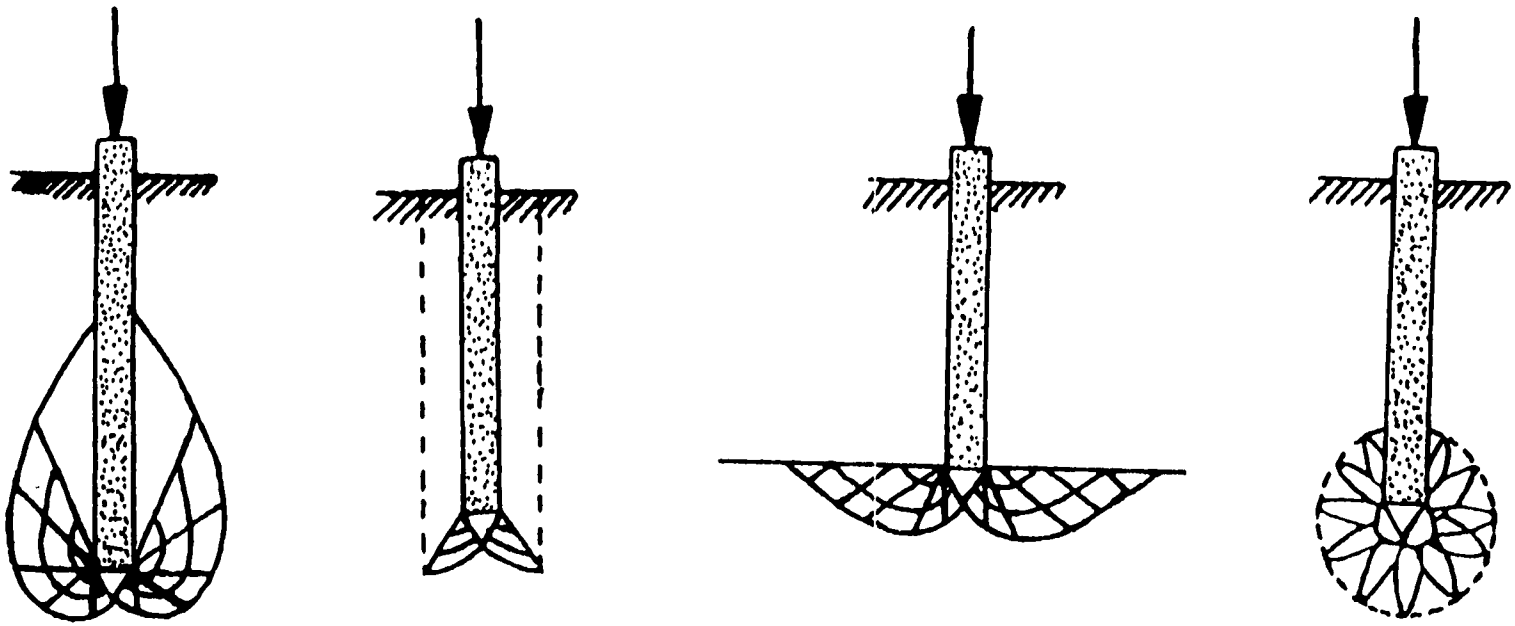

Figure 2.2 - End Bearing Soil Failure Patterns (Winterkorn and Fang, 1975)

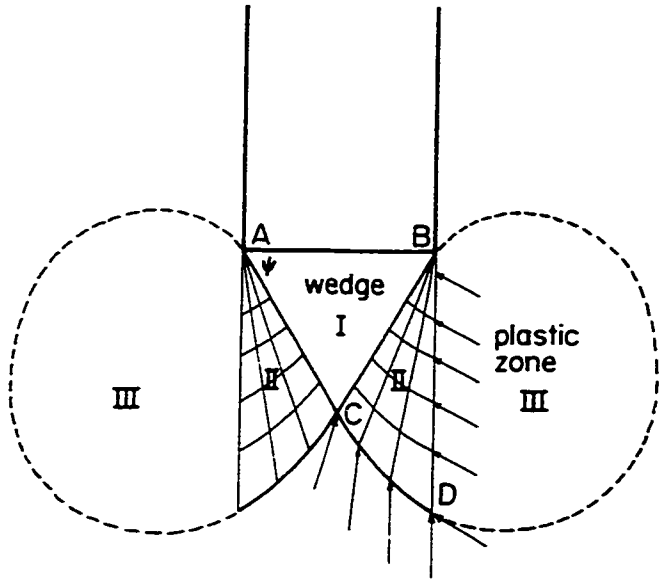

Figure 2.3a - Proposed Failure Pattern Beneath Pile (Vesic, 1977)

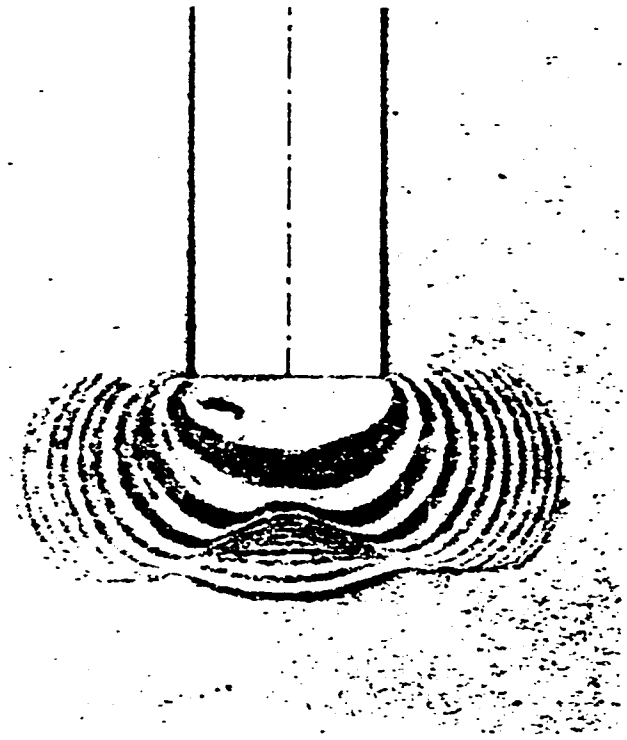

Figure 2.3b - Observed Failure Pattern Beneath Pile (Vesic, 1977)

the pile diameter for driven piles. Kulhawy (1984) arrived at values of settlement at failure of 30% and 8% for bored and driven piles respectively.

Vesic (1967) observed that the ultimate end bearing capacity of a pile increases in a linear manner which is related directly to the overburden pressure of the soil until a driving depth of four times the pile diameter is reached. Vesic (1964) had previously determined that at a depth of 10 pile diameters in loose soil and 30 pile diameters in dense soil, the end bearing capacity of the pile reaches a constant value. This maximum end bearing resistance is solely a function of the relative density of the sand and independent of the overburden pressure, σ'_v. Coyle and Castello (1981), and Meyerhoff (1983) reinforced this premise by stating that N_q varies with both the ϕ' of the soil, and the length to diameter ratio of the pile with a maximum value occurring between the depths of 10 to 20 pile diameters. On the other hand, Hanna and Tan (1973) noted that the tip resistance does not reach a maximum at these ratios, but continues to increase at a reduced rate. Several other studies (Kulhawy, 1984; Randolph *et al.*, 1994) have also concluded that the end bearing continues to increase at a decreased rate.

Based on field tests and empirical values Meyerhoff (1976) developed the following criteria,

$$Q_p = \left(0.4 \cdot \frac{\overline{N}}{B}\right) \cdot D_b \cdot A_p \leq 4 \cdot \overline{N} \cdot A_p \qquad (8)$$

where Q_p = end bearing load in tons (multiply by 100 for kN)

$\bar{N}$ = average corrected standard penetration test blow count at the pile toe

D_b = depth of driving

B = pile diameter

A_p = area of pile toe

In 1983 Meyerhoff suggested two reductions for the ultimate end bearing resistance. The first is a reduction of 33% when the pile is driven into silts instead of sand. Equation (9) describes a reduction factor for the end bearing proposed by Meyerhoff for a pile whose diameter exceeds 0.5 m.

$$R_b = \left(\frac{B+0.5}{2B}\right)^n \leq 1 \tag{9}$$

where B = pile diameter

n = 1 for loose sands

2 for medium density sands

3 for high density sands

There are basically two methods of increasing the end bearing capacity of a pile. The first method is to lengthen the pile such that it reaches a deeper and stronger strata, like a dense sand or bedrock. In regions where deeper placement is infeasible the diameter of the pile toe can be expanded.

If the pile is driven, the only manner in which the base may be expanded is through the use

of a larger diameter pile. However, bored cast-in-place piles have the option of increasing the entire diameter, or only expanding the base. Expanded base piles are classified as either belled or Franki piles depending on the method of construction. Belled piles as shown in Figure 2.4, are generally created by specialized equipment that uses two blades and a collection bucket which simultaneously allows for the formation of the bell and the removal of the soil from the hole. Engineers in the former Soviet Union attempted to form the bell through the use of explosives with varying degrees of success (Mohan, 1988).

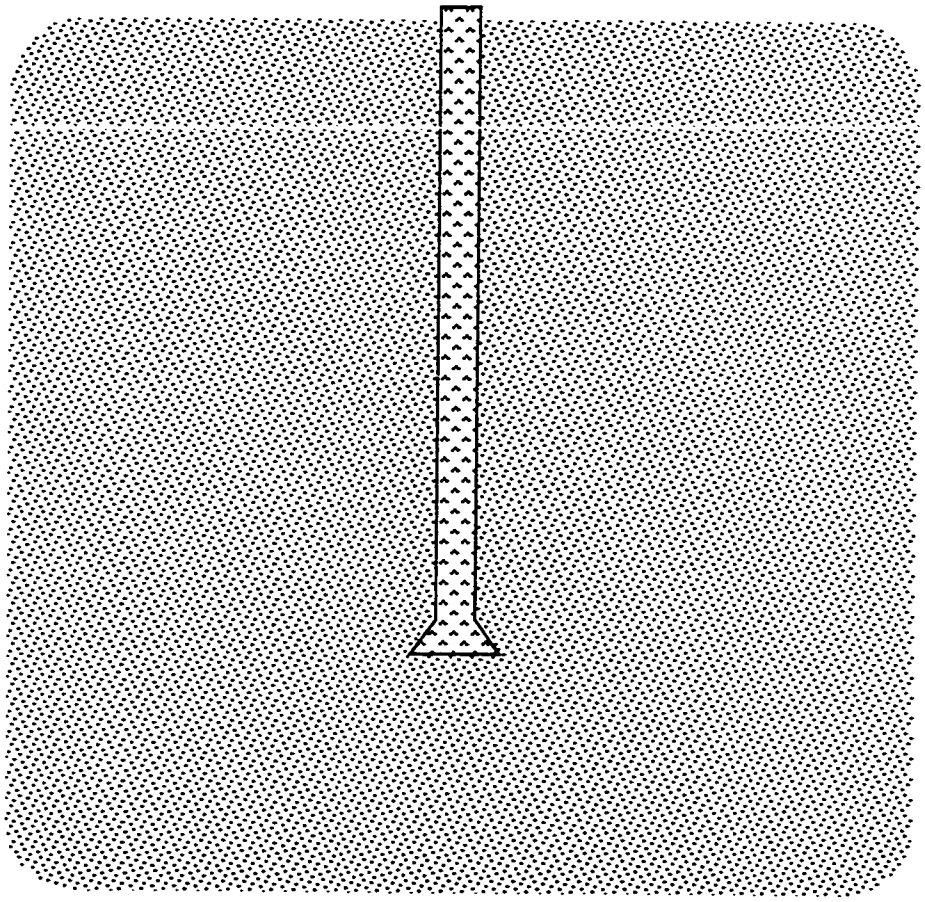

Figure 2.4 - Typical Belled Pile

Franki piles are formed by driving zero slump concrete through a rigid tube which has been driven into the ground. As seen in Figure 2.5, the completed concrete pile consisting of concrete driven out at the end of the tube and is ideally formed into a rounded expanded base.

2.2.2 Shaft Resistance

The shaft resistance of the piles is a combination of the adhesion of the soil to the pile face and the friction of the soil against the surface of the shaft. The unit shaft resistance, f_s, may therefore be described by the formula:

$$f_s = \alpha \cdot S_u + K_s \cdot \sigma'_o \cdot \tan\delta \qquad (10)$$

where, f_s = ultimate unit skin resistance

α = coefficient accounting for pile type, soil conditions and installation method

S_u = undrained shear strength of soil

K_s = coefficient of lateral earth pressure

σ'_o = mean normal ground stress

δ = angle of friction at soil-pile interface

In sand S_u becomes negligible and conversely in pure clay $\delta \approx 0$. From the comparison of many test piles installed in various clays, Vesic (1977) concluded that the values of α may vary from 0.2 to 1.5.

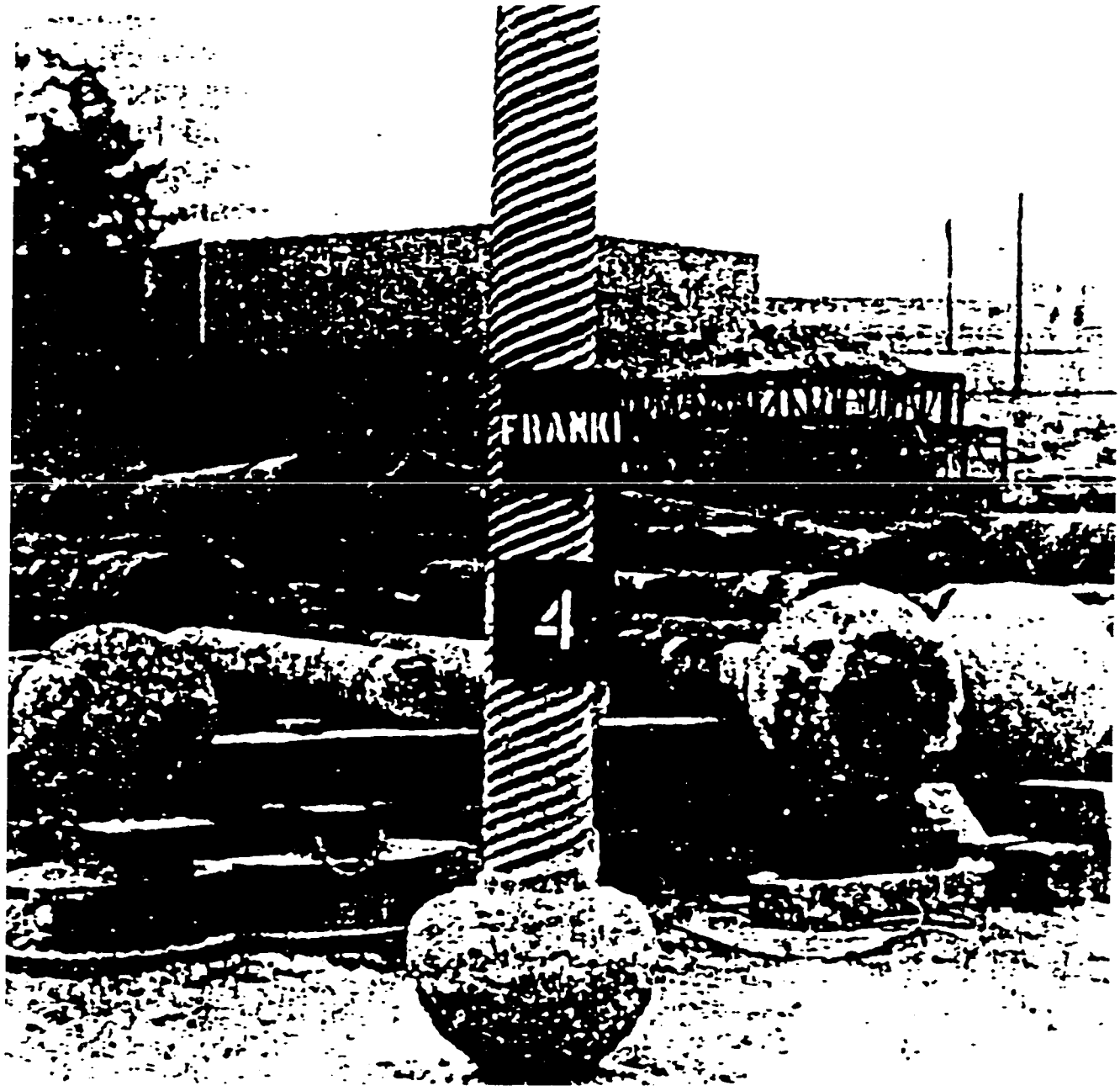

Figure 2.5 - Franki Pile (Neely, 1990)

The horizontal force in the soil, and therefore the force normal to the pile walls, is related to the vertical stress of the soil by the coefficient K_s. The range of the coefficient for a particular soil is described by three different values: K_a, K_o and K_p. K_a describes the minimum possible ratio that can exist in a soil just before failure occurs. This case most commonly occurs when dealing with a retaining wall that has yielded to a small degree. K_o describes the at rest value of the sand. K_p is the maximums possible ratio that can exist before soil failure occurs, and is equal to the inverse of K_a. Since K_p is inversely proportional to K_a, this case would be represented by pushing a wall into a soil bed. Equations (11) and (12) describe the values of K_o and K_p.

$$K_o = 1 - \sin\phi' \tag{11}$$

$$K_p = \tan^2\left(45 + \frac{\phi'}{2}\right) \tag{12}$$

Early studies (Meyerhof, 1959; Nordlund, 1963) assumed that, as the pile is driven into the ground, all displaced soil moves laterally without any vertical deformation. Thus the surrounding soil is compacted and K_s increases from the natural coefficient of earth pressure (K_o) towards the Rankine passive pressure (K_p).

Vesic (1970) and Meyerhof (1976) determined that K_z decreases from a maximum value near the top of the pile down to a minimum value near the toe. These values may vary from K_p to less than K_o. Das (1990) reported similar findings for closed ended piles, but

for low displacement piles such as H piles and open ended pipe piles, K_s is approximately equal to K_o over the entire length of the pile.

Das (1984) suggested that K_s is equal to K_o for bored or jetted piles. For low displacement piles values of $1.4K_o$ to K_o were proposed, and $1.8K_o$ to K_o for high displacement driven piles. Ireland (1957) stated that the value of K_s may approach K_p and that a design value of 1.75 should be reasonable for sands. Meyerhof (1976) proposed values of K_s in sand of 0.5 for bored piles, 0.5 to 1.0 for driven H piles and 1.0 to 2.0 for driven displacement piles. In API RP 2A (1989) standard for the American Petroleum Institute it is suggested that design values of K should be 1.0 for full displacement piles and 0.8 for low displacement piles. Bhusan (1982) proposed a value of K_s based on the relative density of the soil.

$$K_s = 0.5 + 0.008 \cdot D_r \tag{13}$$

where D_r = relative density of soil = $\dfrac{(e_{max} - e)}{(e_{max} - e_{min})} \times 100\,\%$

e = actual void ratio

e_{min} = minimum possible void ratio

e_{max} = maximum possible void ratio

Kraft (1991) described a reduction in K down from K_p that occurs during driving called "fluffing". Fluffing is comprised of two separate components. The first aspect of the

fluffing process occurs when the pressure is relieved due to the pile tip passing by the soil in question. The reduction in the value of K due to the decrease in applied load is more pronounced in dense soils than in loose soils. The other aspect of fluffing results from the additional vibrations in the soil as a result of the continuation of the driving process. The vibrations cause a greater reduction in initially loose soils than in their dense counterparts.

Peck (1958) noted that the frictional development between steel and sand is probably less than between sand and sand. Potyondy (1961) conducted the first series of tests in attempting to determine the relation between δ and ϕ' for a variety of materials. Testing showed that the ratio of δ to ϕ' was less than 1 ranging from 0.543 to 0.99. Potyondy further showed that, regardless of the material used, δ approached ϕ' as the surface roughness increased. It was concluded that since the value of δ is less than ϕ' that the failure occurred at the soil-pile interface. When δ was raised to an equal or greater value than ϕ', failure occurred in the soil near the pile, but not at the interface. Vesic (1977) reasoned that the sand at the soil pile interface is in a state of ultimate failure. Since the soil is in a state of failure the friction is independent of the initial soil density and pile material. Therefore δ can be taken as being equal to the coefficient of friction of the remolded soil, ϕ'. The values proposed by Vesic compare favorably with the values proposed by Potyondy. Various sources (Das, 1984, 1990; Coyle and Castello, 1981; Prakash *et al.*, 1990) suggest values of δ ranging between 0.5 ϕ' and 0.8 ϕ'. Kishida and Uesugi (1987) determined that δ varies linearly with the surface roughness of the steel

pile. Kraft (1991), on the basis of these and other tests (Acar *et al.*, 1982; Bozozuk *et al.*, 1979; Datta *et al.*, 1980; Yoshimi and Kishida, 1981), concluded that under normal circumstances the ratio of δ to ϕ' should be taken as 0.6 for calcareous sands and 0.7 for siliceous sands. Higher ratios could be used if proper engineering assumptions and criteria were followed.

In sands, shaft resistance is taken to increase linearly to a critical depth at which point it reaches a constant value relative to the initial sand density. Vesic (1967) places this critical depth between 10 and 30 pile diameters. From model testing in loose sand, Hanna and Tan (1973) place the critical depth at 40 pile diameters. Kulhawy (1984) proposed, that like tip resistance, an ultimate shear resistance is not reached, but that it continues to increase at a reduced rate. Kraft (1991) reinforces the Kulhawy proposal by concluding that δ decreases with depth while the contractive behaviour of the soil increases with depth. Both of these effects are related to soil arching which has the effect of limiting the developable frictional resistance. Tan and Hanna (1974) came to a similar conclusion that there is no further increase in shear capacity at large L/D values due to arching effects in the soil. Coyle and Castello (1991) concluded that the unit skin friction continues to increase with depth, but at a reduced rate.

Meyerhof (1976) based his determination of f_s on empirical correlations to field testing.

$$f_s = \frac{\overline{N}}{500} \leq 0.1\,\text{MPa} \tag{14}$$

where, f_s is in MPa

$\bar{N}$ = average corrected Standard penetration test blow count in the shear region

Hanna and Tan (1973) concluded that the shaft friction reaches a maximum value after less settlement than is required for end bearing. Vesic (1967) determined that for either bored or driven piles the settlement required to develop maximum shear resistance is 0.3 to 0.4 inches (7 mm to 10 mm), regardless of the pile diameter. Nauroy *et al.* (1988) came to similar conclusions that the ultimate skin friction was achieved after settlement of 2 mm to 6 mm for pile diameters ranging from between 20 mm and 760 mm. Testing by Kulhawy (1984) also showed similar settlements of 5 to 10 mm for the maximum shear resistance to be mobilized.

The tensile capacity of piles is developed solely through frictional resistance along the shaft unless the pile has some form of an expanded base such as a bell or a ball as in Franki piles. Hunter and Davisson (1969) concluded that the tensile capacity of piles in granular material was approximately 70% of the compressive shear force developed. More recently, Randolph *et al.* (1994) estimated the tensile shear capacity of piles was closer to 80% that of the compressive capacity.

Methods of increasing the shear capacity of piles have been limited in both theory and application. As previously stated the surface roughness of the pile has an effect on the maximum shear resistance that may be developed. The greater the roughness, the greater

the developable shear resistance. The other studied method is to taper the pile, this is done to increase the ultimate shear capacity by increasing the normal force on the sides of the pile.

2.3 Residual Stresses

Upon completion of driving the axial force in a pile is not equal to zero. Several researches (Smith, 1962; Hunter *et al.*, 1969; Tan and Hanna, 1974; DeNicola and Randolph, 1993) have demonstrated that after driving the residual stresses in a pile can be significant. If the residual stresses are not taken into account, the bearing capacity of the pile does not change, however they do affect the percentage of the load taken in end bearing versus shear which may become critical when scaling the pile to a different length. Briaud *et al.* (1984) theorized that the residual point load in sands can reach significant levels due to the fact that friction loads require less movement to be unloaded in comparison to the end bearing load. Therefore, upon loading, the toe may actually be supporting a greater load than the load cell, which is zeroed after driving, would indicate. The residual stresses are the least at the top of the pile due to the fact that the top portion of the pile has the least amount of friction to overcome. And conversely the stresses are greatest near the bottom of the pile where the friction the pile has to overcome is greater than the elastic potential of the pile material. Randolph *et al.* (1994) stated that residual stresses remain a significant problem in creating a usable formula for determining the bearing capacity of piles in sand.

Kraft (1991) concluded that the end bearing may be as much as 1.25 to 2 times as great as the measured load. As the pile length is increased, the percentage of error in the measured frictional resistance is reduced due to the increasing portion of the load taken by the pile in this manner. The reduction in percentage of error reduces the overestimation of the shear friction resistance. This reduction in overestimation will lead to an apparent decrease in the rate of increase in shear friction. This will appear to be a leveling out of the shear friction and thus misleading researchers to accept the limiting value theory for shaft resistance. This will have little effect on reasonably similar piles that have been scaled off the original. However, for a piles of significantly different length this could amount to a significant error in the calculated bearing capacity.

This leads to the observation that residual stresses can be reduced if the stiffness of the driven piles is increased. Sparrow (1988) measured the residual stresses, in straight piles similar to those used in this investigation, and concluded that the residual stresses were insignificant due to the short length and high stiffness of the model piles.

2.4 Tapered Piles

2.4.1 General

Though tapered piles are not commonly used in modern construction this has not always been the case. The original tapered piles were constructed out of wood due to the fact that a tree stripped of its branches forms a natural tapered shape. However, wood doesn't have the strength of concrete or steel, nor does it have the long term durability that may be

required in many cases. Finally the length of a monolithic wooden pile is limited by the height of the tree. Modern piles benefit from the advantages provided by new materials, but are usually cylindrical or prismatic in nature. The requirements placed on foundations by modern structures have created an interest in the potential advantages provided by tapered piles manufactured with new construction materials.

Lindqvist and Petaja (1981) concluded that piles provide greater resistance in shear as the angle of the taper is increased. This follows conventional shear resistance theory as shown in Figure 2.6 and described by Equation (15).

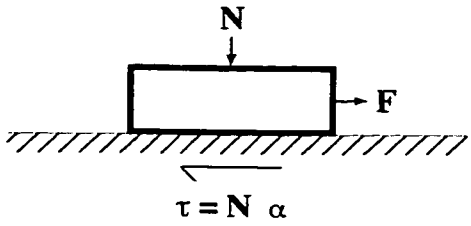

Figure 2.6 - Basic Shear Theory

$$\tau = N \cdot \alpha \tag{15}$$

where, τ = Maximum developed shear stress resisting movement

N = Force normal to shearing plane

α = Coefficient of friction, is equal to $K_s \cdot \tan \delta$

As a pile penetrates through the ground, either by driving or by settlement, the surrounding soil densifies and approaches the Rankine passive state. Thus, the surrounding soil provides greater resistance and therefore a greater normal force is developed. The result of which is the development of a greater resisting shear stress.

Lindqvist and Petaja (1981), and Kodikara (1993) both state that the benefits due to

tapering are the greatest in dense frictional soils. Figure 2.7 shows the effect of taper on K_s as proposed by Nordlund (1963) for various combinations of pile taper, ω, and soil friction angle. This figure shows the diminishing effect of taper on soils of low internal friction and the need for greater taper angles for the soil to reach limiting shear values. Upon analysis of several sites where tapered piles have been used, Lindqvist and Petaja (1981) suggest that large amounts of silt, clay or artesian ground water will hinder the benefits provided by tapered piles.

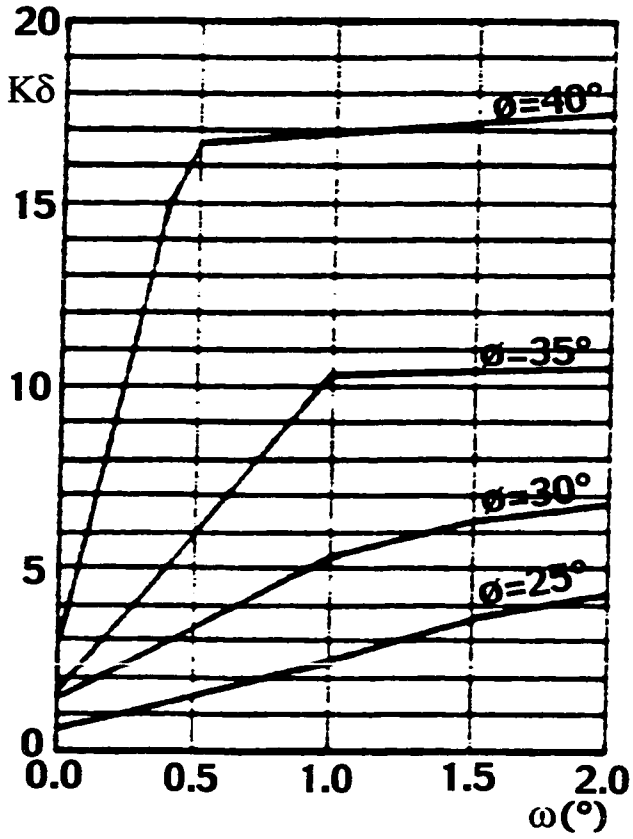

Figure 2.7 - Effects of Pile Taper on K
(Lindqvist and Petaja, 1981)

In Finland, where many soil strata consist of a loose to medium-dense sand layer overlain by a clay layer, partially tapered piles are being made use of more frequently, according to Lindqvist and Petaja (1981). This allows the tapered portion to extend into the sand layer where it becomes most useful, and allows a less expensive straight portion to be present in the clay layer.

Saha and Ghosh (1986) concluded that tapered piles have a different response to vibration and dynamic loading than prismatic piles do. The tapered shape induces an increased stiffness in the soil during driving. The densified soil is beneficial for bearing capacity, however it causes a decrease in the dampening ability of the soil.

Gregersen *et al.* (1973) concluded that taper is somewhat beneficial for both the compressive and tensile capacities of piles in sand. It was also noted that the residual stresses are greater in tapered piles than in straight piles.

2.4.2 Step Tapered Piles (Case Studies)

D'Appolonia *et al.* (1963) conducted a test using an instrumented Raymond step-tapered pile. The pile was driven through layers of compact clayey-sand and gravel coming to rest in a shale bedrock. At the design load of 100 tons only 10% of the load reached the pile tip, and at twice the design load of 200 tons the load at the tip increased to approximately 20% of the total load. D'Appolonia stated three different factors which enhance the bearing characteristics of the step tapered piles. The first was the displacement of soil which increases the lateral soil pressure and thus the shear resistance of the soil. The second factor is the annular area at each step, and finally the corrugated surface of Raymond step-taper piles causes the shear failure plane to occur in the soil vs. at the soil-pile interface.

2.4.3 Continuously Tapered Piles (Case Studies)

Peck (1958) performed a comprehensive analysis on in situ driven piles in both sands and clays. Part of this analysis compared tapered and untapered piles. Peck concluded that tapered piles have a beneficial effect on pile capacity, with the benefits being more apparent in dense soils and with piles that have a greater taper. The results of the analysis demonstrated that a pile with a 1° taper provides a bearing capacity that is 1.5 to 2.5 times that of an untapered pile.

Robinsky and Morrison (1964) conducted testing with both straight and tapered piles. The sand bed used for testing had lead shot added at regular intervals to the sand bed. Using x-ray spectography it was possible to track the movement of the lead as the pile was driven into the sand. Tracking the shot allowed the authors to observe movements of the soil in the region of the pile. The testing involved two different straight piles and one tapered pile with both smooth and rough surfaces. From the x-ray spectography it was observed that the majority of the soil compaction occurs in the region of the tip where a noticeable cone develops. Figure 2.8 illustrates the displacement of the surrounding soil was in the form of a bulb around the pile. The size of this bulb would increase with increased pile diameter, pile taper, surface roughness and sand density, with the largest bulb existing around the tapered pile. Robinsky and Morrison observed that as the pile tip passes by, the soil undergoes vertical expansion. This creates a thin sleeve of soil with a lower ϕ' than exists under the pile point. This sleeve of loose sand, approximately 1/4 of the pile diameter in thickness, is surrounded by a ring of dense sand which prevents much of the

lateral soil pressure from reaching the pile wall. Straight piles have little to no ability to recompact this loose soil, but tapered piles are able to recompact the sand further up the pile wall. The testing also showed that with an equivalent volumetric displacement tapered piles provide 40% greater bearing capacity.

Figure 2.8 - Stress Bulb Around Pile (Robinsky and Morrison, 1964)

It is possible to install continuously tapered piles not only through driving, but also by a cast-in-place method. Rybnikov (1990) described field tests comparing two cast-in-place uniform diameter piles to five cast-in-place tapered piles, all of which were 4.5 m long. For the five tapered piles, tapers ranged from 1°20' to 2°40'. The holes for the tapered piles were bored through the use of special augers attached to the end of a drilling rig. The augers are in the form of an endless screw, allowing them to create constant taper over the entire pile length. The site soil strata consisted of sandy loam, loam, and sand. The tapered piles had 20% to 30% greater bearing capacity in comparison to the uniform diameter piles of equal length and equal or greater volumetric displacement. With an increase in the taper angle the

bearing capacity increased, and there was a proportional decrease in the volume of material required to form the pile.

Zil'berberg *et al.* (1990) compared the tapered pile foundation of a new factory to previously installed uniform diameter pile foundations that were typically used in the region. The primary bearing strata was a saturated fine loose sand ($\phi = 28°$) overlain by a sand-loam fill. The piles used were 3 m long pre-cast piles which tapered from 70 x 70 cm to 10 x 10 cm ($\approx 5.7°$). It was determined that the tapered piles provided 2.5 to 3 times the bearing capacity of the 10 to 12 m long piles (30 x 30 cm) that were normally used. It was further determined that the settlement was also less than would be expected using the uniform prismatic piles. The use of the tapered piles provided nearly a 45% reduction in the cost of the foundation resulting from savings not only in materials, but also in labour and machine hours.

Sterin *et al.* (1984) described a variation of the tapered piles called pyramidal piles. Figure 2.9 illustrates how these piles are similar to other tapered piles except that only two of the four faces are tapered. Figure 2.10 demonstrates how the piles are installed in groups of 4, this essentially creates a large tapered foundation beneath the columns. These piles were found to be inexpensive to produce, and provide high bearing capacity with little settlement.

Monotube® piles are fluted steel tapered or partially tapered piles. The fluted shape

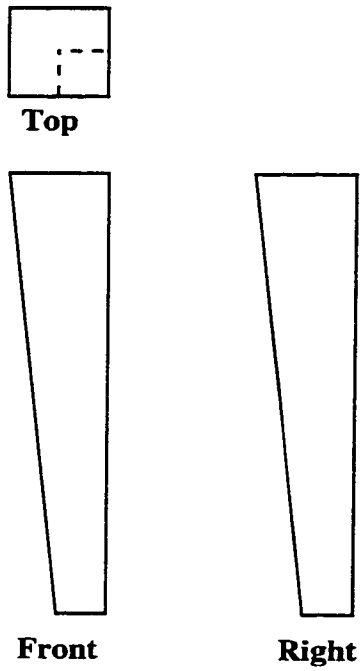

Figure 2.9 - Pyramidal Pile Cross Section

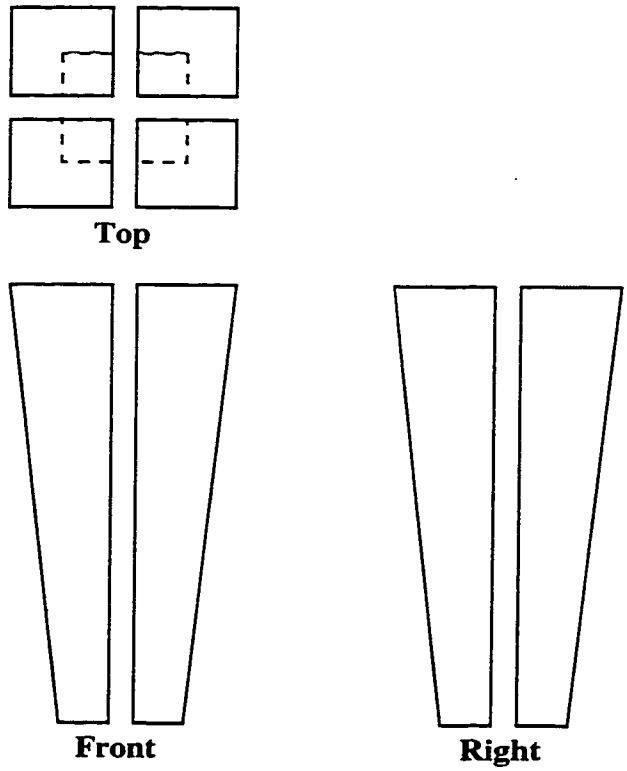

Figure 2.10 - Group of Pyramidal Piles

provides the piles with greater rigidity such that they are less likely to become damaged during transportation and driving. After driving the piles are generally filled with concrete to increase the pile strength and stiffness. The Monotube piles come in tapers of approximately 0.334° to 0.955°. Several tests have been conducted to determine the effectiveness of Monotube piles. The most demonstrative compared driving test piles for a 16 story building. It was determined that for the 60 ton design load, H-piles would have to be driven 198 ft through a weak sand to bedrock. An on site tapered test pile driven to a depth of only 56 ft provided sufficient capacity for the design load of the piles to be changed from 60 tons to 80 tons. Each pile was thus 70% shorter in length, and the site required 400 fewer piles than would otherwise have been necessary.

Monotube also recorded several comparative uplift field tests. From these tests it was concluded that the uniformly tapered piles provide greater uplift capacity than similar untapered piles in sands. This increased uplift capacity was attributed to increased densification of the soil, uniform taper, and the fluted configuration.

Jain *et al.* (1978) conducted tests with driven wooden timber piles 3.5 m in length. The piles had a square cross-section with the top of the tapered piles being 20 x 20 cm and the toe varying from between 8 x 8 cm to 16 x 16 cm. The results were compared with straight piles with cross-sections of 18 x 18 cm and 16 x 16 cm. It was concluded that tapered piles do provide greater capacity than untapered piles. It was also noted that the capacity of the piles tends to decrease with an increase in taper.

Dutta (1985) conducted bearing and uplift tests on six differently shaped concrete model piles. The different pile shapes tested were uniform in diameter, square and triangle cross-sections as well as step taper, conically tapered, and pyramidally tapered. Each pile was designed such that all piles possessed a length to diameter ratio of approximately 10 and the volume, length and tip area were constant. The piles were tested in a 70 x 70 x 110 cm wooden vessel containing sand with a $\phi \approx 39°$. The piles were placed freely on the surface of a thin layer of sand on the bottom of the tank, then the remainder of the tank was filled using the pluviation method. Both bearing and uplift tests were performed by incrementally loading the pile through the use of a screw jack centered above the pile. The results from these series of tests showed that the uniform triangle pile provided the greatest bearing capacity, followed by the uniform square, step tapered, pyramidally tapered, conically tapered, with the uniform diameter pile having the lowest bearing capacity. In terms of uplift capacity the uniform triangle pile once again had the greatest bearing capacity followed by the uniform square, step tapered, uniform diameter, pyramidally tapered, and finally the conically tapered pile.

Tests using model timber piles were conducted by Kurian and Srinivas (1995). The piles tested involve uniform diameter, square and triangle shapes as well as their respective tapered equivalents. All piles had a length of 700 mm, a top cross-sectional area of 2500 mm^2, a tip area of 100 mm^2 and a volume of 72,333 mm^3. The previous constraints result in the tapered piles having tapers of 1.63° for the prismatic, 1.83° for the circular and 2.48° for the triangular pile. The piles were tested in a tank 800 x 800 x 800 mm filled

with sand ($\phi \approx 37°$, $\gamma \approx 15.5$ kN/m^3). In an attempt to simulate the conditions of the piles being used as replacement piles beneath an existing structure, the piles were placed in the tank at the appropriate height then a consistent sand layer was pluviated into the tank. On average the tapered piles provided approximately 10% greater bearing capacity than did the equivalently shaped straight pile. The testing further showed that for an equivalent load the tapered piles settled approximately 25% less than their uniform counterparts. It was estimated that the stress on sides of the tapered piles was approximately five times greater than on the untapered piles. A finite element analysis program developed in conjunction with the testing showed a rotation of the planes of principal stresses as shown in Figure 2.11. According to this program the failure of the tapered piles occurs in the region of the pile tip. Finally the optimal cross-section was determined to be the triangular, followed by the square, with the circular being the least efficient.

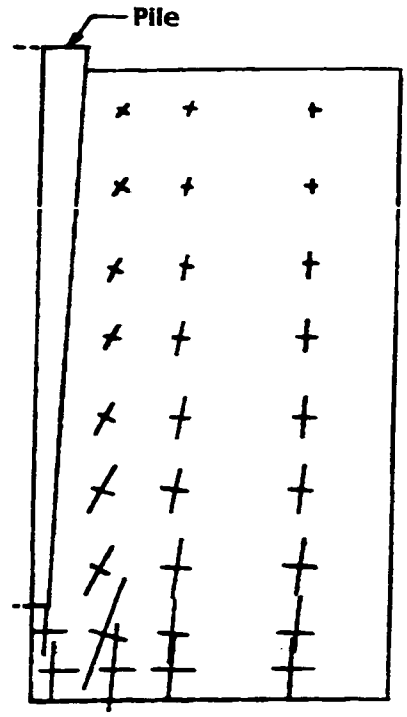

Figure 2.11 - Principal Stress Planes (Kurina and Srinivas, 1995)

El Naggar and Wei (1998) conducted a series of compression and tension tests on both straight and tapered piles. All piles tested were 1,524 mm long, with the straight piles having a diameter of 168.3 mm, the first tapered pile having a top diameter of 203.2 mm and a bottom diameter of 152.4 mm, and the second tapered pile having a top diameter of

196.8 mm and a bottom diameter of 165.1 mm. The piles were tested in a tank, 1,445 mm tall with a diameter of 1,500 mm, which provided a confining pressures up to 100 kPa, but without an applied surcharge pressure. Similar to the procedure of Kurian and Srinivas (1995), sand was pluviated into the tank to a height of 0.4 m. A pile would then be placed slightly into the sand, and the remainder of the sand pluviated around the pile. The piles were loaded in 10 increments of 10% of the predicted bearing capacity and held for 2.5 minutes at each load. The testing procedure involved a compression test followed by a tension test which returned the pile to its original position. The pressure in the tank was then raised to the next pressure and tested. The confining pressures tested were between 0 and 100 kPa in increments of 20 kPa. From these series of tests it was concluded that in compression there was a beneficial effect to tapering the pile, but in tension the tapered piles only achieved similar capacities at confining pressures of 100 kPa. Hence, it was further concluded that the ratio of compressive:tensile capacity for straight piles was less than that of tapered piles.

Olson and Long (1989) collected several thousand pile load tests from various sources in an attempt to determine the effectiveness of present design methods. The analysis of the data demonstrated that there was an average bearing capacity increase of 11% and a small increase in pull out capacity for tapered piles as compared to untapered piles in clay. Olson and Long noted that the increased capacity in clays was not conclusive due to the small amount of data available. In sands, the average bearing capacity of tapered piles was 2.2 times that of untapered piles. Based on a small number of tests available, the uplift

capacity of tapered piles appeared to be 2.1 times that of untapered piles. It was concluded that the bearing capacity of piles in layered soils increased in proportion to the percentage of the driving depth occupied by sandy soils.

Olson and Long assumed that the effect of taper varied with radial strain. This assumption agreed with the observation that the increase in capacity with tapered piles was a result of increased radial stresses in the soil. These stresses depend on the radial strain developed in the soil after the pile tip passes through the soil. The proposed method of calculating the frictional capacity developed along the sides of the pile was:

$$Q_{side_{factored}} = Q_{side}(1 + F_t \cdot R_s) \tag{16}$$

where, F_t = an empirical factor likely to decrease with an increase in strain (0.1 for clay and 10 for sand)

The radial strain R_s is defined as $R_s = \dfrac{(D - D_p)}{D_p}$ (17)

D = diameter at the top of the pile

D_p = diameter at the pile toe

The empirical modifiers of Dennis and Olson (1985) were also used in the calculation of the piles.

$$F_{point} = \frac{1.0}{0.15 + 0.008L} \tag{18}$$

$$F_{side} = \frac{1.0}{0.6^{(L/(60D))}} \tag{19}$$

These correlations were the result of the API RP 2A underestimating the bearing capacity of short piles, those typically less than 50 feet in length. Using all of the proposed modifiers, the ratio of calculated bearing capacity to actual capacity was an average of 1.0 over the 573 tests analyzed using this method. The majority of the samples fall within a safety factor of 2 but a safety factor of 3 provides a reliability of 99%.

2.4.4 Methods of Estimating Tapered Pile Bearing Capacity

The methods for calculating the bearing capacity of tapered piles are limited. Nordlund (1963) made one of the first attempts to determine the bearing capacity of driven tapered piles. Figure 2.12 illustrates the basis for Nordlund's model which is represented by the following equation:

$$Q_u = N_q \cdot A \cdot \sigma_v + \sum_{d=0}^{d=D} K_s \cdot \sigma_d \cdot \sin(\omega + \delta) \cdot \sec\omega \cdot C_d \cdot \Delta d \qquad (20)$$

where N_q = bearing capacity factor

A = pile toe area

σ_v = effective overburden pressure at the pile toe

K_s = coefficient of lateral earth pressure

σ_d = effective overburden pressure at depth d

ω = pile taper angle

δ = soil-pile interface friction angle.

C_d = perimeter of pile at depth d

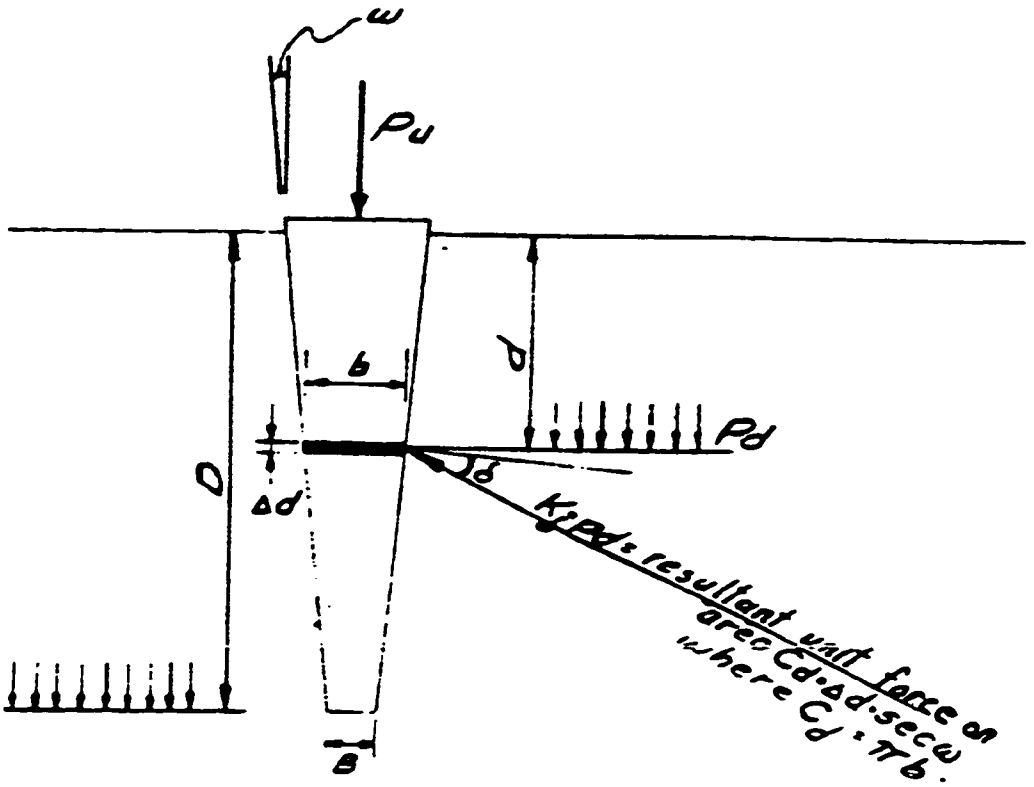

Figure 2.12 - Nordlund Tapered Pile Model (Nordlund, 1963)

Δd = small incremental change along the length of pile

The model was based on a an infinitely long wall being pushed into the soil. As previously proposed the sides of this wall interact with the soil via a friction angle of δ. As the sides of this wall are rotated outwards the pressure on the sides of the wall increase due to the development of passive pressure. At some limiting taper angle the ultimate passive pressure of the soil will be achieved and therefore there will be no further increase along the shaft beyond this point. Nordlund proceeded to create a series of figures relating the taper angle, ω, to K_s for $\phi=\delta$ values of 25°, 30°, 35° and 40°. These figures corrected the development of K_s depending on the volumetric displacement per unit length of the pile.

These figure indicated that the lower the friction angle of the soil the more effective a larger taper becomes. Figure 2.13 indicates that the upper limit of the effective taper angle is in the region of 2° for a full displacement pile with $\delta = \phi =$ 30°. Figure 2.14 is used to correct the value of K_s depending on the value of δ/ϕ.

Kodikara and Moore (1993) proposed another method that makes the assumption that the pile is preformed in

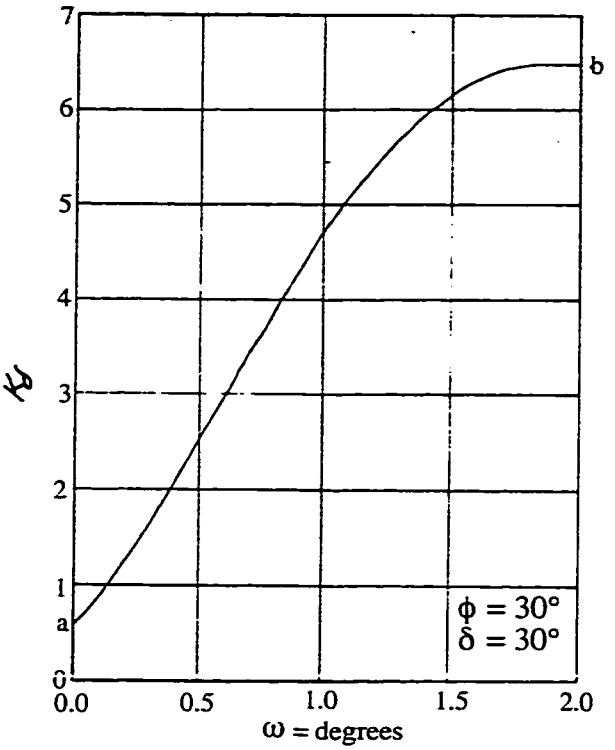

Figure 2.13 - Effect of Pile Taper on K (Norlund, 1963)

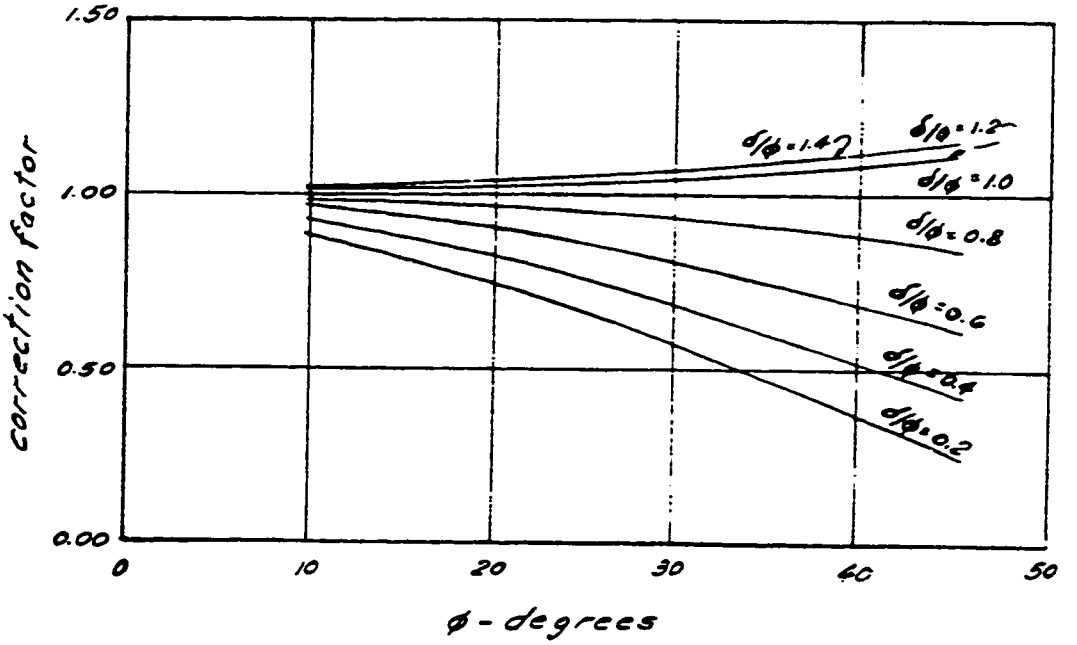

Figure 2.14 - Correction factor for K (Norlund, 1963)

an ideal elastic-plastic soil. The model divides the soil into three distinct phases. The first phase describes the soil and the pile in a state where the two are basically bonded together, and therefore both deform elastically. Phase two involves slip occurring between the pile and the soil, yet the soil is still in an elastic state. In phase three slip is still occurring along the pile-soil interface, but the soil in this region acts as a perfectly plastic solid. As shown in Figure 2.15 one of the major factors in the bearing capacity of the pile is G, the shear modulus of the elastic soil. The experimental line in this figure resulted from the values taken from Rybnikov (1990), since there was no information available on G the authors estimated that the value ranged between 10-16 MPa due to ϕ of the soil. Figure 2.16 illustrates that this method shows a continually increasing

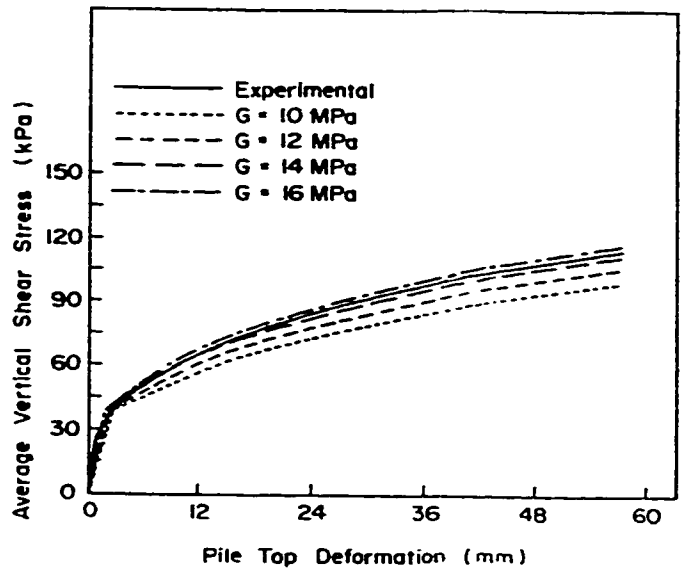

Figure 2.15 - Effect of Shear Modulus on Shear Stress (Kodikara and Moore, 1993)

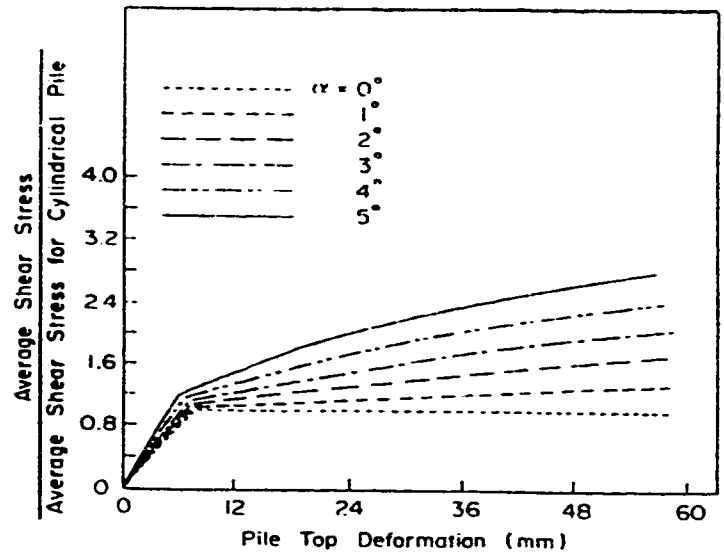

Figure 2.16 - Effect of Taper Angle on Shear Stress (Kodikara and Moore, 1993)

shear resistance in accordance to an increased taper angle. The difference in bearing capacity caused by varying ϕ, c, and G in comparison to each other can be seen in Figure 2.17.

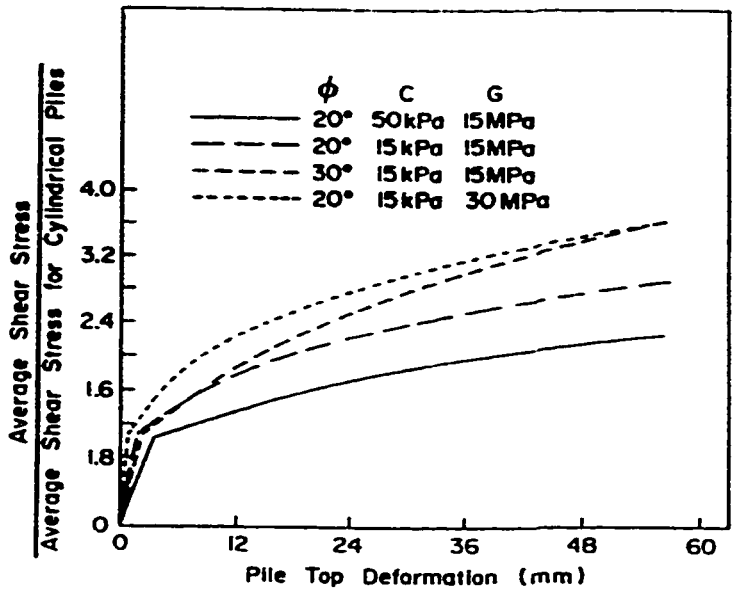

Figure 2.17 - Effect of Modifying ø, c, and G (Kodikara and Moore, 1993)

The Monotube Pile Corporation uses an in house method of determining the bearing capacity of tapered piles. While the company does not endorse the use of any particular formula or method they do suggest that wave equation analysis programs (WEAP) or other methods that take residual stresses into account may be appropriate for use. Wave equation programs are evolutions of the method proposed by Smith (1960). As per Figure 2.18 the pile is broken up into a series of springs and dashpots. As the hammer hits the pile an energy wave travels through the pile beginning at the top and traveling downward. A certain amount of energy is transferred along to the next pile increment and a certain amount is absorbed by the dashpot. When the wave reaches the base of the pile it rebounds back up towards the top. The maximum displacement in the last segment is the penetration of the pile due to a hammer fall. Obviously wave equation programs are only used for driven piles.

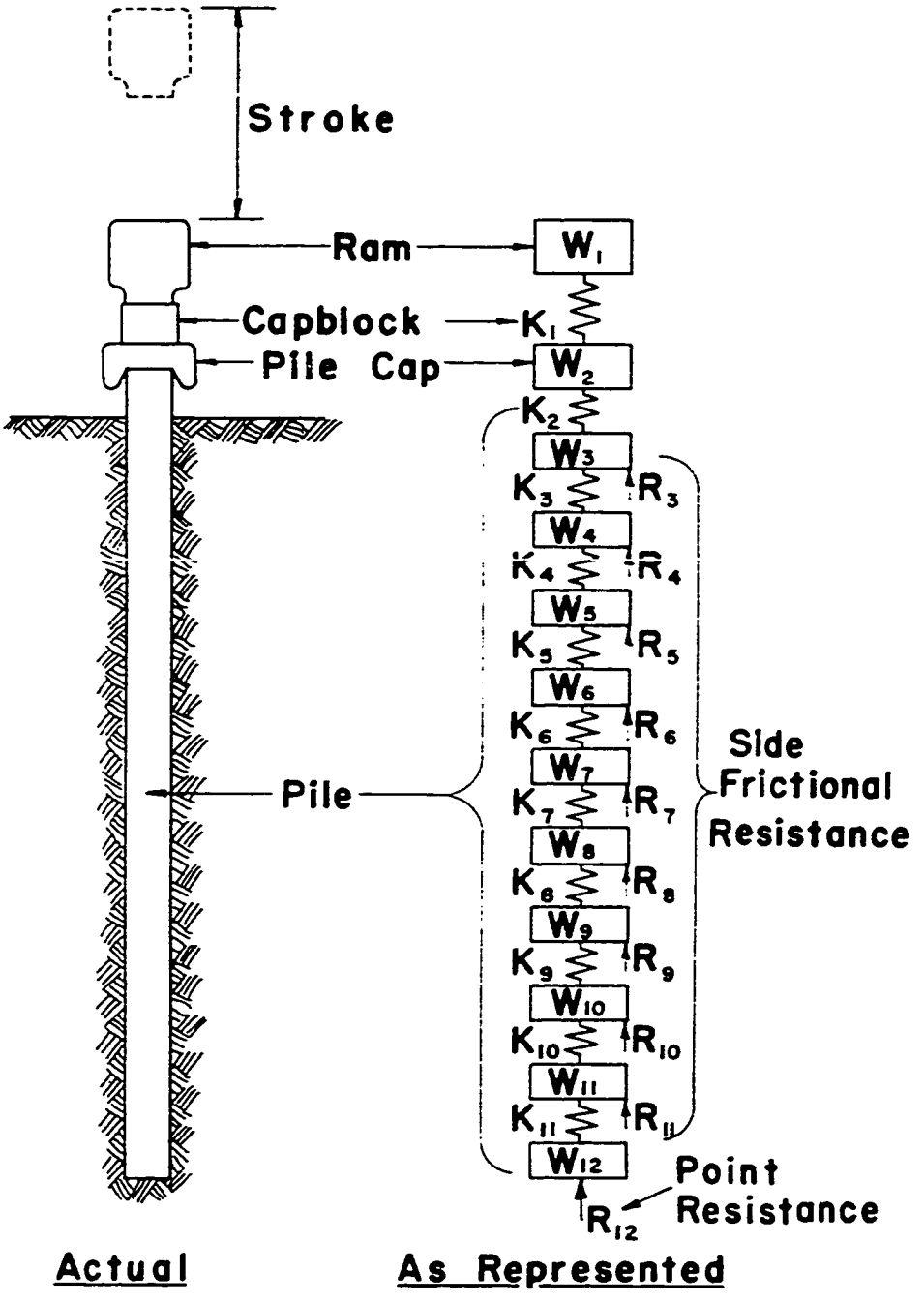

Figure 2.18 - Wave Equation Model (Smith, 1960)

Another proposed method is to use a dynamic pile driving formulas such as the following one published by the Engineering News Record:

$$P = \frac{2 \cdot W_h \cdot H}{s + 0.1 \cdot \left(\frac{W_p}{W_h}\right)} = \frac{2 \cdot E}{s + 0.1 \cdot \left(\frac{W_p}{W_h}\right)} \quad \text{where } \frac{W_p}{W_h} \geq 1 \tag{21}$$

where P = allowable load in pounds

W_p = total weight being driven (pile, pile cap, etc...)

W_h = weight of hammer

H = height of hammer drop

s = penetration of pile into ground at the depth where successive blows give similar penetration

E = energy delivered by the falling hammer

However, there has been much debate over the usefulness of such formulas. Tavenas and Audy (1972) analyzed a large number of field data and concluded that driving equations did not accurately predict the bearing capacity of the driven piles. It was concluded that driving formulas may become more accurate if the amount of energy actually transferred to the piles could be accurately determined. Vijayvergiya (1980) came to a similar conclusion about the ineffectiveness of dynamic driving formulas to reliably predict static bearing capacity.

Kurian *et al.* (1995) modeled a finite element program based on the results of laboratory testing. The elements used were three dimensional 8-node cubes or 6-node wedges. Few

specifics were available on the modeling used since it has become a commercial product.

New methods such as the use of neural network programs are being developed. Chan *et al.* (1995) created a neural network based on current driving formulas. Teh *et al.* (1997) worked on neural networks to estimate pile capacities according to data received from CAPWAP field testing. There are also newer equations being created similar to those already in use, but with minor modifications (Kay, 1997).

2.5 Soil Arch

The soil arch is analogous to the arch that is used in construction, particularly in ancient Roman structures. Just as a structural arch is kept completely in compression, the soil arch is also a fully compressed form. Handy (1985) noted that the natural soil arch is in the form of a catenary and not a semi-circle seen in classical structures. The catenary is a form seen elsewhere in engineering due to its natural ability to evenly distribute loads. The main cable on a suspension bridge is a catenary from which cables that connect to the deck are attached.

Terzaghi (1936) conducted one of the earliest tests on soil arching in sand. The testing involved lowering a trap door in the base of a tank filled with sand. As the trap door was lowered the pressure on the trap door was reduced. This indicated the presence of a soil arch due to other portions of the sand taking the load. As the trap door yielded further the soil underwent further expansion and the arch disintegrated. Terzaghi also determined that

the flow of water through the sand has no effect on the development or effectiveness of the arch. Furthermore, vibrations will aid in the disintegration of the arch, but the amplitude of these vibrations must be significant. From observations, Terzaghi concluded that minor vibrations like the kind that would be created by a travelling subway car are insufficient to break the friction bonds of the arch forming the subway tunnel.

2.6 Model Testing

2.6.1 General

Much of the testing on piles is conducted in the laboratory due to the high costs associated with full scale pile testing conducted in the field. Not only does model testing reduce the costs by using smaller piles, which are usually one fifth to one twentieth the size of actual piles, but more of the materials are reusable for future testing. In the laboratory it is relatively easy to control and determine the soil properties, but in the field it is difficult to obtain an undisturbed sample of the soil for purposes of analysis (Meyerhoff 1956). Model testing provides greater control of the various specific parametric differences allowing for easier and more controlled comparisons. Ghionna *et al.* (1991) pointed out that deficiencies with laboratory simulations include scale effects and the difficulty of accurately recreating field conditions such as cementation, non-uniformity of layers, etc...

2.6.2 Calibration Chambers

Calibration chambers have become an established method for modeling in-situ conditions of cohesionless soils (Schnaid *et al.*, 1991). Calibration chambers are vessels, usually in

the form of a box or cylinder, which contain soil to be used for testing purposes. Calibration chambers can be either fixed walled or flexible walled, also referred to as double walled. Fixed walled calibration chambers impose the lateral boundary condition of zero strain on the soil. This type of chamber is simpler to build and maintain, and has been used for experimentation in several cases (Mattes and Poulos, 1971; Hanna and Tan, 1973; Cooper, 1976; Last, 1979; Smits, 1982; Dutta, 1986; Sparrow, 1989; Anderson and Pyrah, 1991; Kulhawy, 1991; Achari, 1991; Kurian and Srinivas, 1995).

Flexible walled chambers are created through the use of an inner flexible membrane. The first chamber of this type was built in 1969 by Holden and Lilley in order to study the performance of full sized cone penetrometers under laboratory conditions. It is most common for the walls of large chambers to be flexible with the base and the top either rigid or have pressure applied by a cushion. Veismanis (1974) noted that the flexible walled chambers more accurately reflect field conditions. Table 2.1 illustrates the boundary conditions that can be imposed on the soil through the use of a calibration

Table 2.1: Flexible Walled Chamber Boundary Conditions

Boundary Condition	σ_v = constant	σ_h = constant	$\Delta\varepsilon_v = 0$	$\Delta\varepsilon_h = 0$
B1	✓	✓		
B2			✓	✓
B3	✓			✓
B4		✓	✓	

chamber. Boundary condition B1 indicates that both vertical and horizontal pressures are being applied to the soil sample, thus the soil is able to move in all directions, but the stresses remain constant. Boundary condition B2 represents an inability of the soil to move in either direction, but the stresses along the walls may change. Finally, B3 and B4 represent the case where the sides are pressurized and the top and bottom are fixed or vice-versa.

Chambers that lack a flexible top or base are only able to create boundary condition B2 and B4. Holden (1971) concluded that the lateral pressure has a greater influence on the performance of piles and penetrometers, and therefore calibration chambers that are flexible only on the walls generate acceptable results.

2.6.3 Scale and Boundary Effects on Calibration Chambers

There has been much debate over the required size of a calibration chamber such that the boundary effects are minimized. In chambers where the walls are rigid, such as in the B2 and B3 conditions, the soil may not be able to expand laterally as it would in the field. For flexible walled chambers the applied lateral pressure is designed to simulate the far field stress in the soil. However, the distance at which the far field stress is located may be further out than is being simulated by the chamber. A surcharge load may be partially transferred to the walls of the tank instead of straight down through the soil. These effects can lead to erroneous bearing capacity values.

Meyerhof (1959) was the first to propose an acceptable pile to chamber diameter. Since that time, particularly in the eighties and nineties, many further studies have been performed in order to determine an acceptable pile/chamber diameter ratio. Table 2.2 shows a compilation of the proposed values.

Table 2.2: Proposed Chamber Sizing Restrictions

Author	Year	Chamber to Pile Diameter	Pile Diameters From Chamber Base	Limitations on Sand Parameters
Meyerhof	1959	10	-	-
Schmertmann	1976	34	-	-
Baldi *et al.*	1982	-	-	Medium-Dense
Parkin and Lunne	1982	21.4	-	D_r = 15-30%
		50	-	NC Dense Sand
		100	-	OC Dense Sand (OCR > 8)
Robertson and Campanella	1984	10 - 20	-	-
Williams *et al.*	1988	3-4	6	-
Ghionna and Jamiolkowski	1991	30-35	-	Loose Sand
		60	-	Dense Sand
Kraft	1991	20	-	Loose Sand
		50 - 100	-	D_r = 90%
O'Neal	1991	60	5	-

D_r = Relative Density

NC = Normally Consolidated

OC = Over Consolidated

OCR = Over Consolidation ratio

Schnaid and Houlsby (1991) concluded that for low density sands there is general agreement that chamber tests are reasonably accurate. However, it was also noted that as the density of the sand increases the effects of the chamber diameter to the pile diameter become more pronounced. Foray (1991) noted that the conditions that exist in the field may fall somewhere in between the B1 and B3 boundary conditions making the present models inaccurate. This may account for some of the problems being encountered in determining an appropriate chamber size.

A decrease of 15% in the end bearing capacity in rigid walled chambers was noted by Parkin (1988). Fiovante *et al.* (1991) noted a similar decrease in total bearing capacity as the chamber to pile ratio dropped from 60 to 33 and 35.7 to 20 for fixed and flexible walled chambers, respectively.

2.6.4 Preparation of Soil

Calibration chamber testing relies heavily upon the ability to deposit a uniform and reproducible soil layer within the chamber. For this reason the majority of the calibration chambers have been designed for use with sands. The pluviation method (Rad, 1984) is widely used to create sand bends of uniform density. The pluviation method has become such a standard that virtually every paper dealing with sand calibration chambers from the *Proceedings of the First International Symposium on Calibration Chamber Testing/ ISOCCTI* (1991) mentioned using this method.

The application of the pluviation method is quite simple. A sand filled tank of equal diameter to the calibration chamber is placed directly above the chamber. A diffuser sieve, which usually consists of two sieves at 45° to each other, is placed several centimeters from the bottom of the calibration chamber and is attached to a heavy plate which resides on the surface of the upper tank. Sand released from the upper tank falls at a constant rate into the chamber where it contacts the sieve and loses its momentum. Since the height of the sand in the tank is decreasing at the same rate that the sand in the chamber is increasing, the sieve is always a constant height from the top of the sand in the chamber.

Rad and Tumay (1987) conducted tests on the variables in the pluviation method in order to determine the effects on the pluviated sand bed. An increase in the size of the holes in the shutter, and therefore an increase in the speed of deposition decreased the density of the soil bed. An evenly spaced hole pattern in the shutter provides greater bearing capacity than a shutter with randomly placed holes. The consistency of the sand bed is greatest when sieves at 45° to each other are used, but there is no benefit to using more than 2 sieves arranged in this fashion.

2.7 Test Parameters

There are various related aspects of the soil-pile interaction that can affect the resulting bearing capacity. Kraft (1991) proposed four parameters that affect the bearing capacity of piles: soil attributes, pile characteristics, method of pile installation, and the method in

which the pile is loaded.

2.7.1 Soil Attributes

The bearing capacity of piles is affected by various soil parameters such as the internal angle of friction, crushability, compressibility, lateral earth pressure coefficient, stiffness modulus, and the soil-pile friction angle

Internal angle of friction ϕ' - The magnitude of the internal angle of friction is affected by the mineralogical composition and the density of the soil. The internal angle of friction is a key factor affecting the bearing capacity of piles due to its large influence on both the end bearing and shear friction developed by the pile.

The end bearing of piles increases with an increase in ϕ' due to the logarithmic relation between N_q and ϕ'. The angle ϕ' is the primary factor in determining the lateral earth pressure coefficient, K, and the soil-pile friction angle, δ. These two factors are the most significant factors when determining the developed shear friction in granular soils. Bishop (1972) and Bolton (1986) determined that an increase in confining pressure will lead to a reduction in ϕ'. These conclusions lead Randolph *et al.* (1994) to conclude that N_q should be reduced with an increase in overburden stress and hence depth.

Compressibility and Crushability - Kraft (1991) observed that a decrease in soil

compressibility will result in an increase in lateral stress on the pile surface. The compressibility of a soil is affected by the elastic deformation of the material, rearrangement of the grains, crushing of the grains and breaking of the cementation bonds (Nauroy and LeTirant, 1983). As such, the effects of compressibility are only applicable to granular materials such as sands. Several studies (Touma and Reese, 1974; Meyerhoff, 1976; Randolph, 1988) have concluded that the lateral pressure acting on the periphery of the pile is a function of the soil's compressibility. Testing performed by Nauroy and LeTirant (1983) reinforce this premise by showing that the skin friction varies logarithmically with the compressibility index of the soil. This testing showed that an increase of ten fold in the soil's compressibility index resulted in a 30 fold decrease in shaft resistance.

Sands are classified as being either calcareous or siliceous in nature, depending on the chemical composition of the grains. Calcareous sands are composed of at least 10% carbonate, whereas siliceous sands are composed of at least 80% silica. Kraft (1991) noted that loose calcareous sands often have greater values of ϕ' than medium-dense siliceous sands, but develop only a fraction of the shaft resistance. Lu (1988) attributed this to a lateral reduction in stress due to a volumetric contraction in the soil.

Elastic deformation of the soil and rearrangement of the grains occur in both calcareous and siliceous sands. Crushing and cementation occur easier in, and are more characteristic of calcareous sands (Nauroy and Le Tirant, 1983). The amount of crushing is not only

dependent upon the chemical composition of the sand particles, but is also affected by the physical dimensions of the particles. Smaller and rounded particles are less susceptible to crushing regardless of the chemical composition. Lu (1988) observed that calcareous sands are generally softer, more angular and have more interparticle voids, thus increasing their susceptibility to grain crushing. The crushing was greatest in the area immediately adjacent to the pile and occurred during both driving and loading. Beyond 25 mm (1 inch) away from the pile surface (ϕ = 1.5 inches) there was little to no crushing present in the soil. Leung *et al.* (1996) concluded that grain crushing increases with an increase in both stress and duration. Grain crushing has the benefit of increasing the uniformity coefficient of the soil due to the smaller crushed grains filling in the space between larger grains. The increase in the uniformity coefficient of the soil increases the ϕ' of the soil.

Lateral earth pressure coefficient - As previously discussed in Section 2.2.2, the ratio of the lateral pressure to the vertical pressure is described by the lateral earth pressure coefficient, K. The higher the value of K the greater the normal force along the pile shaft and therefore the greater the developed shear force.

Soil-pile friction angle δ - The conditions that exist in the region of the interface between the soil and the pile are critical to the shear friction that can be developed along the pile shaft. As mentioned in Section 2.2.2 an increase in surface roughness of the pile or an increase in ϕ' will increase the value of δ, resulting in improved pile shear resistance.

2.7.2 Pile Characteristics

Piles differ from one another in both the type of material used as well as the dimensions. Piles are most commonly constructed out of three materials: wood, concrete and steel. In some cases piles are constructed from more than one of the above materials.

Timber - The simplest timber piles are created by removing the branches and bark from a felled tree. This type of pile was the sole source of piling prior to the twentieth century and continues to be used today. Due to natural limits on size and strength, these pile have the lowest material strength and also have length restrictions. Another disadvantage to using timber piles is the potential shorter life span due to the rotting that may occur under fluctuating ground water conditions.

Concrete - Concrete piles form a large percentage of the piling used during the twentieth century. Concrete piles can be either cast-in-place or precast, thus allowing for the greatest variation in shape of all three type of piles. Some of the precast piles are prestressed thus allowing them to be used in situations where tensile or bending loads are present. The major drawback to using concrete piles is that, unlike wood and steel, they are costly to lengthen or shorten after casting.

Steel - Steel piles are also very common in modern engineering design and can be either high displacement or low displacement piles. Closed ended pipe piles are the most

commonly used high displacement steel piles. H-section and open ended pipe piles are the most common low displacement steel piles used. H-sections are often used in locations where weak soils necessitate driving to bedrock or a denser layer of soil.

Diameter - In general, a larger pile diameter will result in an increase in both the end bearing and the shear resistance of the pile. Meyerhof (1983) proposed that for piles with diameters greater than 0.5 m that a reduction factor should be used when calculating the end bearing capacity of piles. This reduction is more predominant in dense soils than in loose soils. However, it was also noted that the unit skin friction resistance of the pile is unaffected by the pile diameter.

Length - Increasing the pile length results in greater end bearing and shaft resistance. As discussed in Sections 2.2.1 and 2.2.2 unit end bearing and shear resistances may reach constant values or increase, but at decreased rates past D/B ratios of 10 to 30.

Compressibility - The importance of the relationship between the compressibility of the soil and that of the pile is questionable. The relative compressibility of the pile is affected by the pile length, diameter, wall thickness in steel piles, and Young's modulus with respect to the piles and the stiffness modulus of the soil. Hanna and Tan (1973) noted a decrease in the shaft resistance when the pile stiffness was reduced by a factor of 6. The reduced steel area decreased the pile stiffness increasing the residual stress in the pile and soil. Hettler (1982) conducted tests using several different materials, with a wide range of

Young's moduli, and found no difference in the shear friction developed during tension tests.

Displacement - Low displacement piles are piles that disturb the surrounding soil to a very small degree when installed. These pile include bored cast-in-place, H-section and open ended steel tubular piles. High displacement piles are generally considered to be driven precast or closed ended steel piles. These piles generally cause densification of the soil surrounding the pile resulting in an increase in the shear resistance due to the increase in lateral pressure on the pile walls. Vesic (1964) reported a 40% increase in the shear resistance of a driven displacement pile versus a similar low displacement pile.

2.7.3 Pile Installation

The determination of the method of installation plays a critical role in the final bearing capacity of a pile. The type of pile and the method of installation are based upon the most economical means of providing suitable support for the superstructure. Piles are installed in one of three methods: bored cast-in-place, pre-drilled or jetted, and driven.

Bored cast-in-place piles - Holes are created through the use of an auger and filled with concrete. Depending on the loading that will be applied to the pile, a mesh of reinforcing steel may be inserted into the hole before the concrete is poured. In certain situations a casing is inserted into the hole as it is being augered in order to prevent the walls from caving in. If greater end bearing is required, belled or Franki piles can be created.

Pre-drilled or Jetted - Pre-drilling and jetting are used to form holes into which a prefabricated pile is placed. These methods are used to ease the penetration of driven piles into the soil when refusal is reached at an unacceptably low penetration into the soil (Kraft 1991). The soils most often subject to these methods are the dense cohesionless soils.

Jetting is performed while the pile is being driven into the soil. High pressure water and/ or air is injected into the soil ahead of the pile tip. The injection loosens the soil and creates excess pore water pressure, thus reducing the effective stress making it easier to advance the pile through the soil. Hunter and Davisson (1969) determined that jetted piles have a bearing capacity that is 2/3 that of driven piles. Mansur and Hunter (1970) and McClelland (1974) have shown that jetting can have a significantly negative effect on the shear resistance of the piles. A pile fully jetted 14.6 m into a medium-dense sand had only 10% the uplift capacity of a similar pile driven into the soil.

Driving - Pile driving can take place in one of two methods: vibratory driving or impact driving. A vibratory pile driver applies an oscillating axial load in order to drive the pile into the soil. The frequency of the oscillating load varies depending on the application. Low frequencies are often used to install sheet piling and light cross-section low displacement piles. At these low frequencies, the entire pile is pushed into and lifted out of the ground on each cycle. At higher frequencies, resonance between the pile and the surrounding soil can be achieved. Gendron (1970) reported that, through the use of

resonant frequencies, high displacement piles had been driven in excess of 100 feet with vibratory pile drivers. Gendron (1970) observed the advantages of vibratory pile drivers in relation to impact drivers include: an improved ability to drive lighter cross-sections to greater depths, quicker installation, reduced amplitude of the vibrations conveyed to nearby structures and lower installation noise.

Impact driving is the oldest and most common method of pile installation. It involves the transfer of energy from the downward moving hammer onto the pile cap. The hammer may be acting solely under the influence of gravity or may have additional downward acceleration provided through mechanical means. The dense soils and piles with larger diameters require greater energy for driving, thus heavier hammers and/or greater drop heights become necessary. Toolan *et al.* (1990) observed that driving resistance increases with depth then the resistance reaches a fairly constant value after approximately 10 pile diameters for loose soils and 25 for dense soils.

2.7.4 Pile loading

Aging - Aging refers to the change in bearing capacity of the piles when tested at a later date rather than immediately after installation. Kraft (1991) used the common assumption that there was no setup time involved with sands due to the immediate release of pore water pressure. However, Tavenas and Audy (1972) performed testing in order to determine the potential effects of aging on soils. Concrete piles driven into a wet uniform medium-dense calcareous sand bed, tested after 20 days as opposed to 12 hours exhibited

50% to 90% increase in bearing capacity. The increase in the bearing capacity was due to increased interlocking of and cementation between the sand particles.

Mitchell and Solymar (1984) stated that a freshly deposited bed of clean washed sands may be considerably weaker and have a lower modulus than an older sand bed. It was determined that the freshly deposited sand beds undergo a seasoning process for several months, during which time there is an increase in the strength and modulus of the sand bed.

Chow *et al.* (1997) observed that the shear resistance of piles in sand can increase with long term loading. This increase in shear friction was attributed to long term changes in the stress regime surrounding the pile leading to an increase in σ'_h. Chow *et al.* concluded that the stress increase along the pile was due to the dense ring of soil, proposed by Robinsky and Morrison (1964), breaking down and releasing stress slowly over time. It may, therefore, be permissible to design for higher than original design loads on existing aged piles (Chow *et al.*, 1997).

Loading Method - There have been several different loading methods developed in order to simulate field conditions in the laboratory. The three loading methods described in the American Society for Testing and Materials D1143-81 (1981) are the Slow Maintained-Load (Slow-ML) test, the Quick Maintained-Load (Quick-ML) test, and the Constant Rate of Penetration (CRP) method.

The ASTM D1143-81 (1981) recommends the Slow-ML testing method for performing load tests. This method involves loading the pile to 200% of the design load in increments of 25% of the design load. The increment loads are held constant until the rate of settlement decreases to 0.5 mm in 10 minutes or after the load has been sustained for two hours, whichever comes first.

The Quick-ML test, developed by the Texas Highway department, dates back to 1962. The pile is loaded until 200% to 300% of the expected failure load in 20 even load increments. ASTM 1143-81 (1981) suggests that the time increment between load increments should be 2.5 minutes or as otherwise specified.

Unlike the previous two testing methods, the CRP test pushes the pile into the ground at a constant rate and records the resulting applied load. Whitaker (1957) developed the test while attempting to determine the settlement required to fully mobilize the soil resistance. Whittaker and Cooke (1961) later performed full scale testing and suggested a loading rate of 0.5 mm/min. ASTM 1143-81 (1981) proposed rates of 0.25 to 2.5 mm/min depending on the soil being tested.

After comparing the Slow-ML, Quick-ML and CRP methods, Joshi *et al.* (1989) concluded that CRP is an acceptable loading method if used only to verify the capacity of the pile. The most significant difference between these tests is the time required for testing. Sparrow (1989) concluded that the three testing methods yield similar results.

The CRP test is not only the fastest of the test methods, but it also delivers a curve that is the simplest to read and interpret.

2.8 Analysis Methods of Load-Settlement Data

Various methods for the determination of the ultimate load of a pile from the load-settlement plots have been proposed. These methods vary from mathematical models based on theoretical idealization of a hyperbolic shape to empirical methods developed over time. There are many different methods available from literature, however only the analysis methods used are presented here. These methods of analysis were determined to be the most reliable methods by previous studies on the equipment used (Sparrow,1989; Achari, 1991; Smith, 1995).

2.8.1 10% Criteria

This method was developed by Vesic (1977) and is based on empirical experience. When the settlement reaches 10% of the pile diameter the maximum load is estimated to have been reached.

2.8.2 Single Tangent Method

As shown in Figure 2.19 the ultimate load is defined as the regression back to the load axis of a line tangent to the plastic range of the curve.

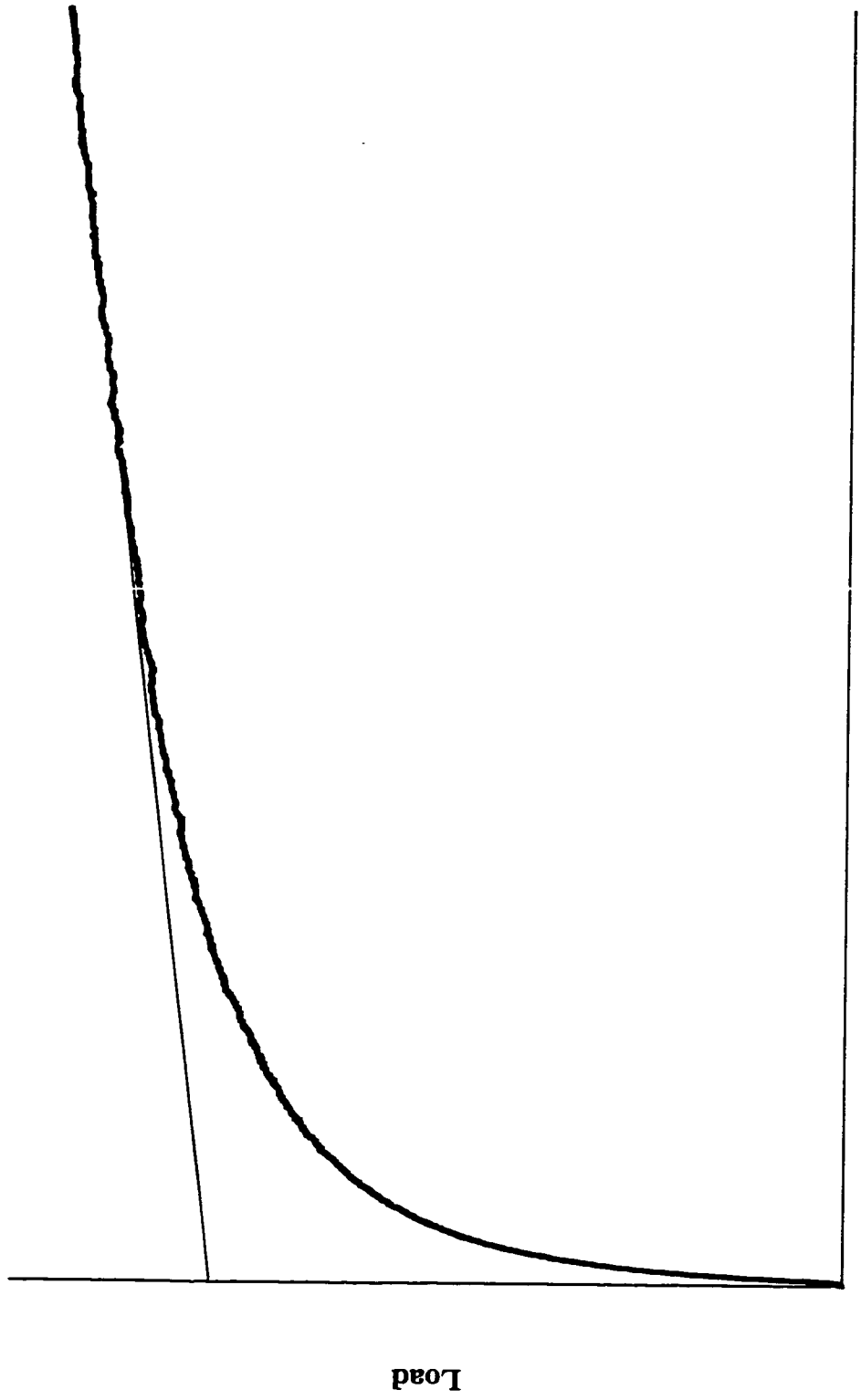

Figure 2.19 - Single Tangent Method

2.8.3 Double Tangent Method

In Figure 2.20 tangents are drawn to both the elastic and plastic portions of the load-settlement curves. The intersection of the two tangents describes the ultimate load of the pile.

2.8.4 Brinch-Hansen 80% Criteria

This method plots the square root of settlement/load versus settlement. The slope of this line provides a constant C_1 and the intersection on the y axis a second constant C_2. The ultimate load is given by the equation:

$$Q_{max} = \frac{1}{2\sqrt{C_1 C_2}} \tag{22}$$

2.8.5 Brinch-Hansen 90% Criteria

Brinch-Hansen (1963) proposed this method for CRP testing. As shown in Figure 2.22 Q_{max} is defined as the load at which the settlement is twice as great as the settlement at 90% of Q_{max}. The determination of Q_{max} by this method is completed through a trial and error method.

2.8.6 Chin Method

Chin (1970) proposed a method which assumes a hyperbolic load-displacement curve. As illustrated in Figure 2.23, the inverse of the slope of the line produced by a displacement/ load versus displacement plot estimates the ultimate bearing capacity of the pile.

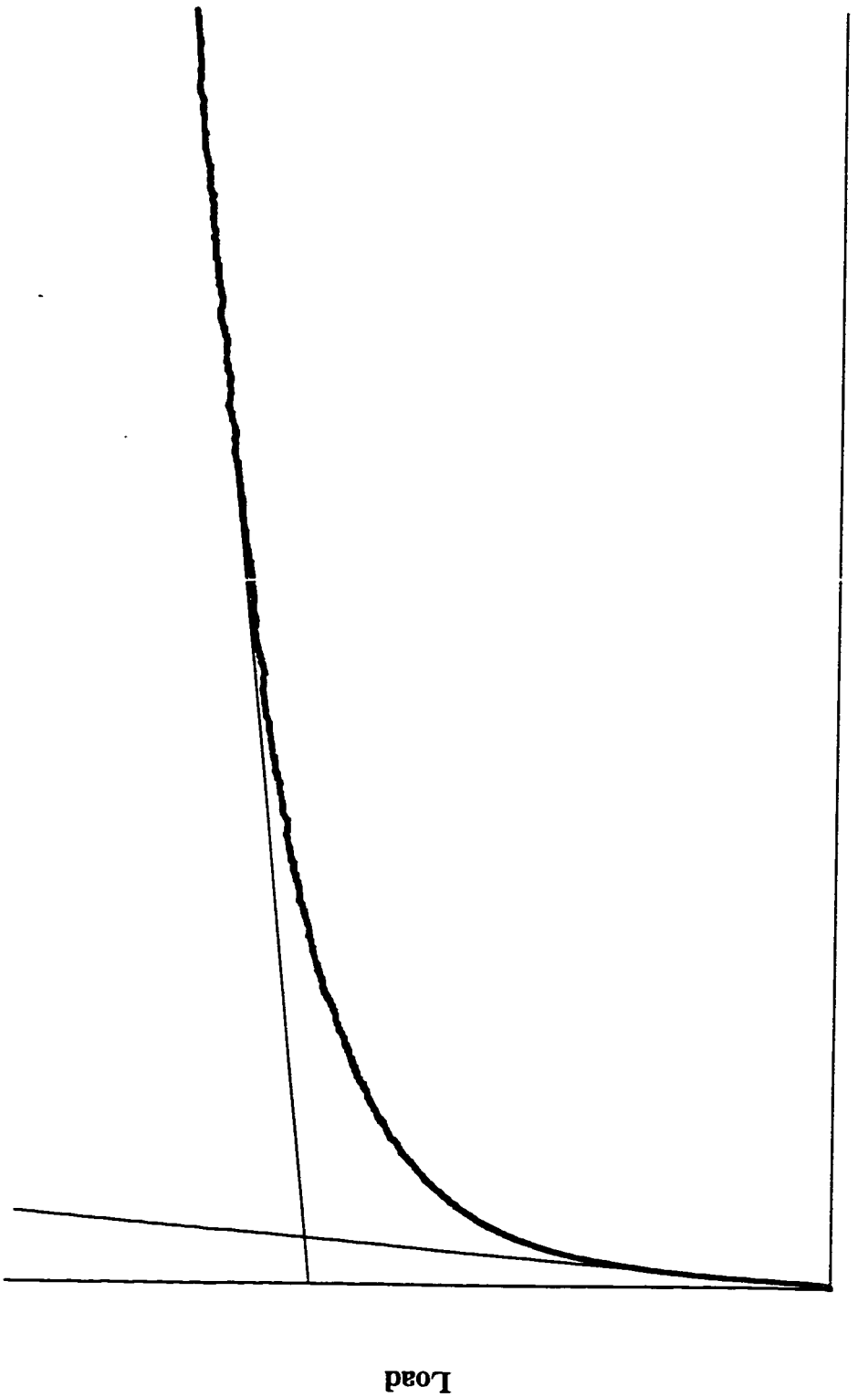

Figure 2.20 - Double Tangent Method

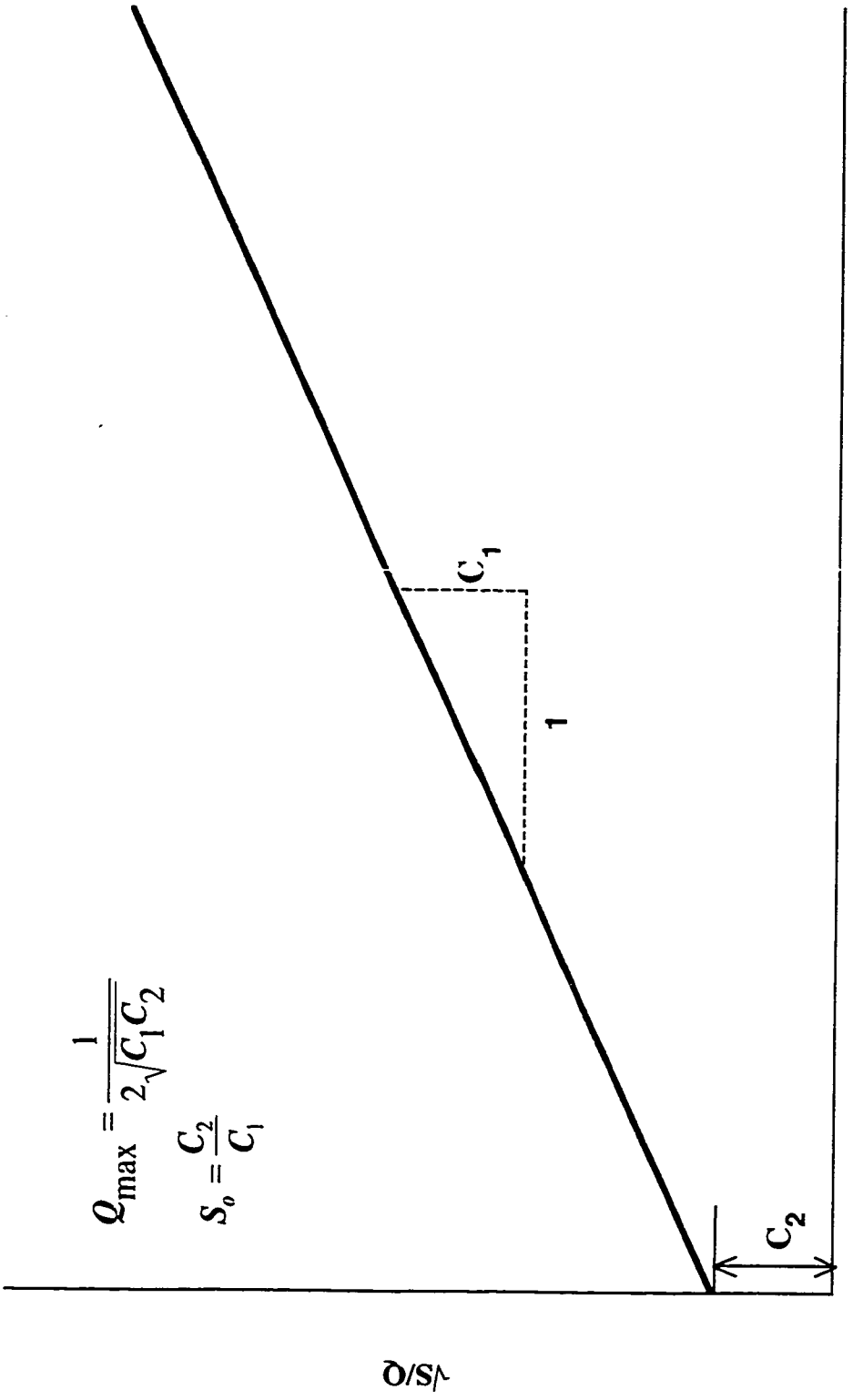

Figure 2.21 - Brinch-Hansen 80% Criteria

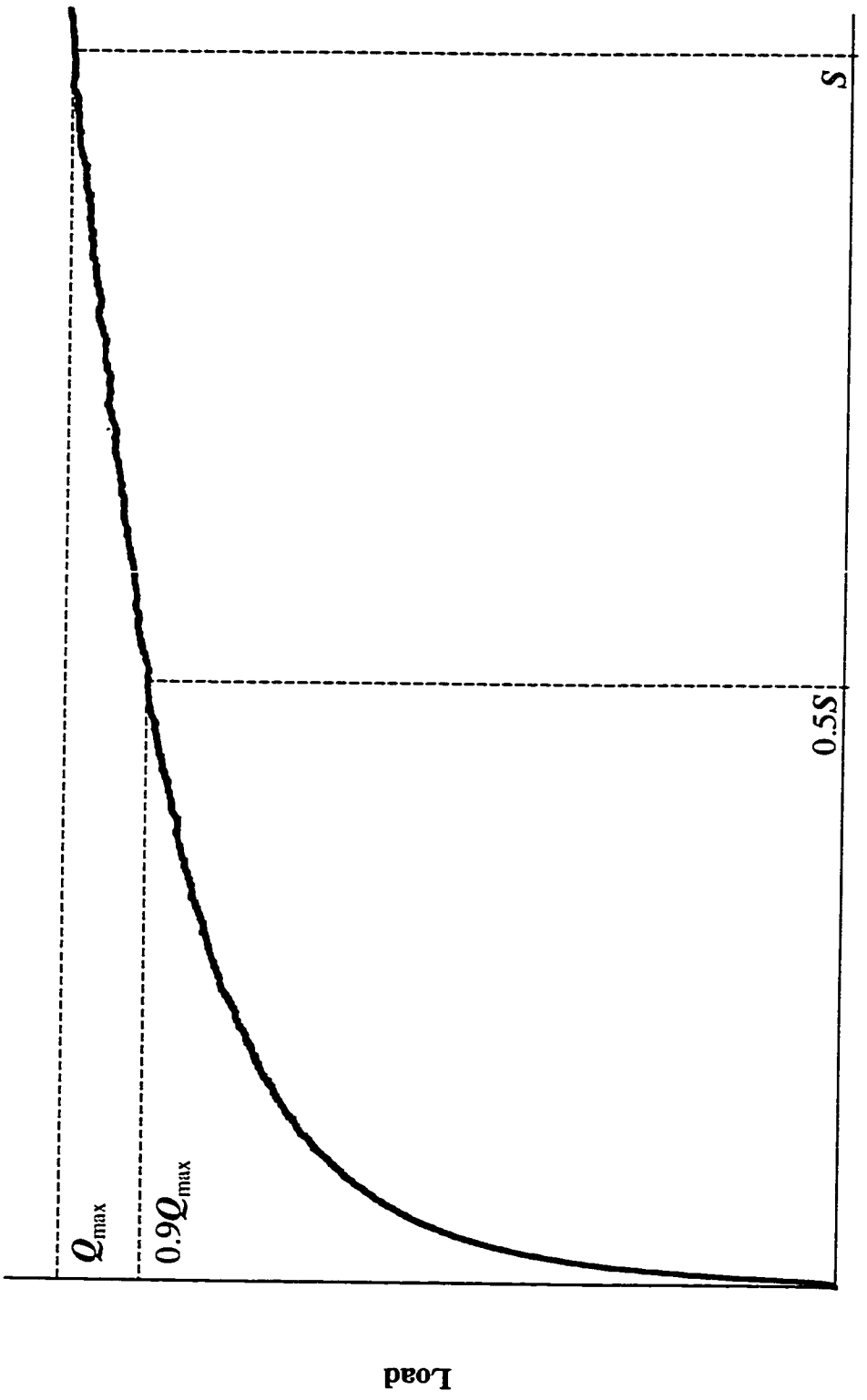

Figure 2.22 - Brinch-Hansen 90% Criteria

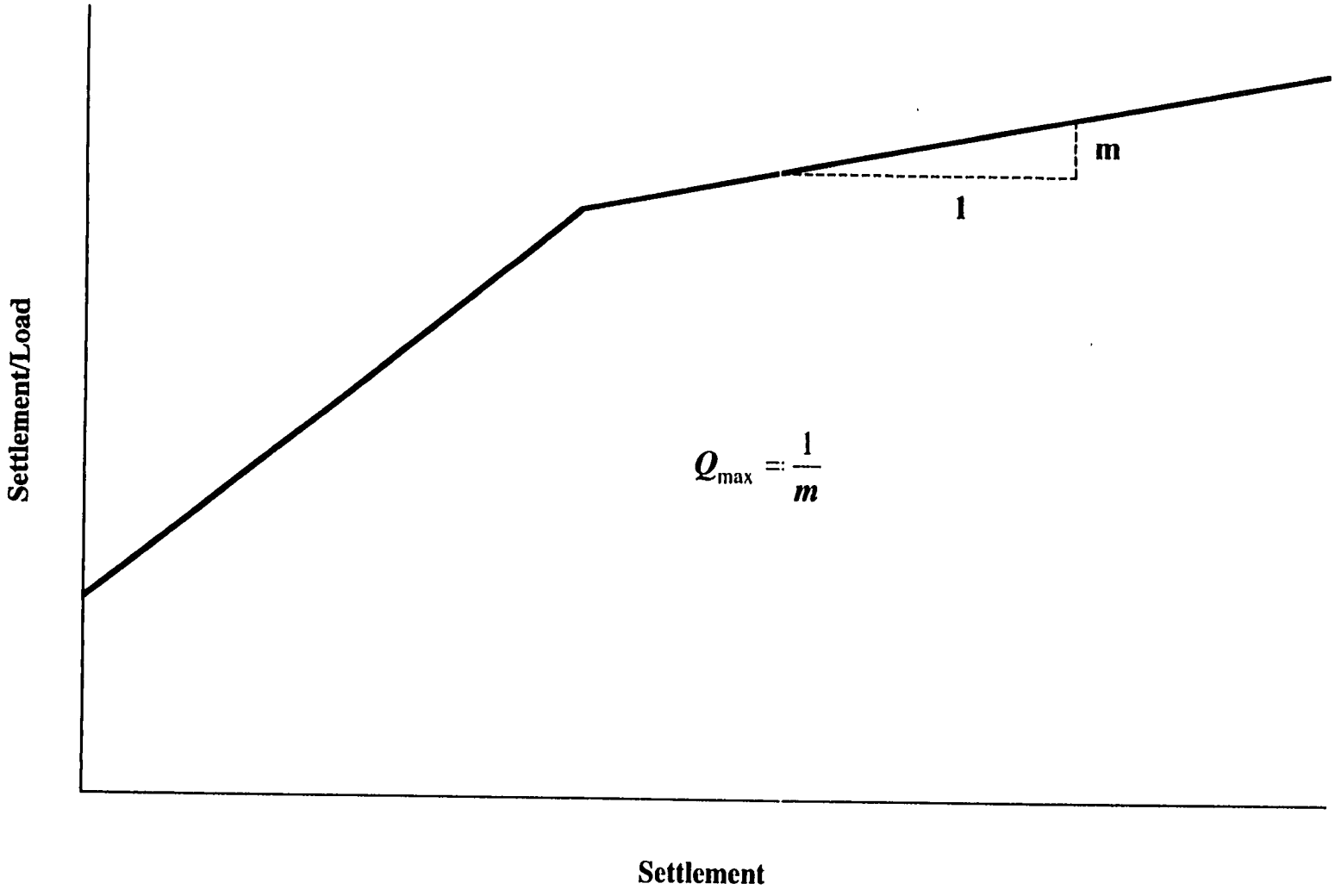

Figure 2.23 - Chin Method

2.8.7 Mazurkeiwicz Method

Mazurkeiwicz (1972) proposed a method in which 4 equally spaced vertical lines, in the region of transition between elastic and plastic behaviour, are drawn on a load versus displacement plot as in Figure 2.24. Then horizontal lines, connecting the y-axis to the intersection of the vertical lines and the load displacement curve, are added. Lines drawn at 45° from lower loads to the next highest loads are then drawn. A straight line between these 3 intersection points crosses the y-axis at the point of maximum bearing capacity.

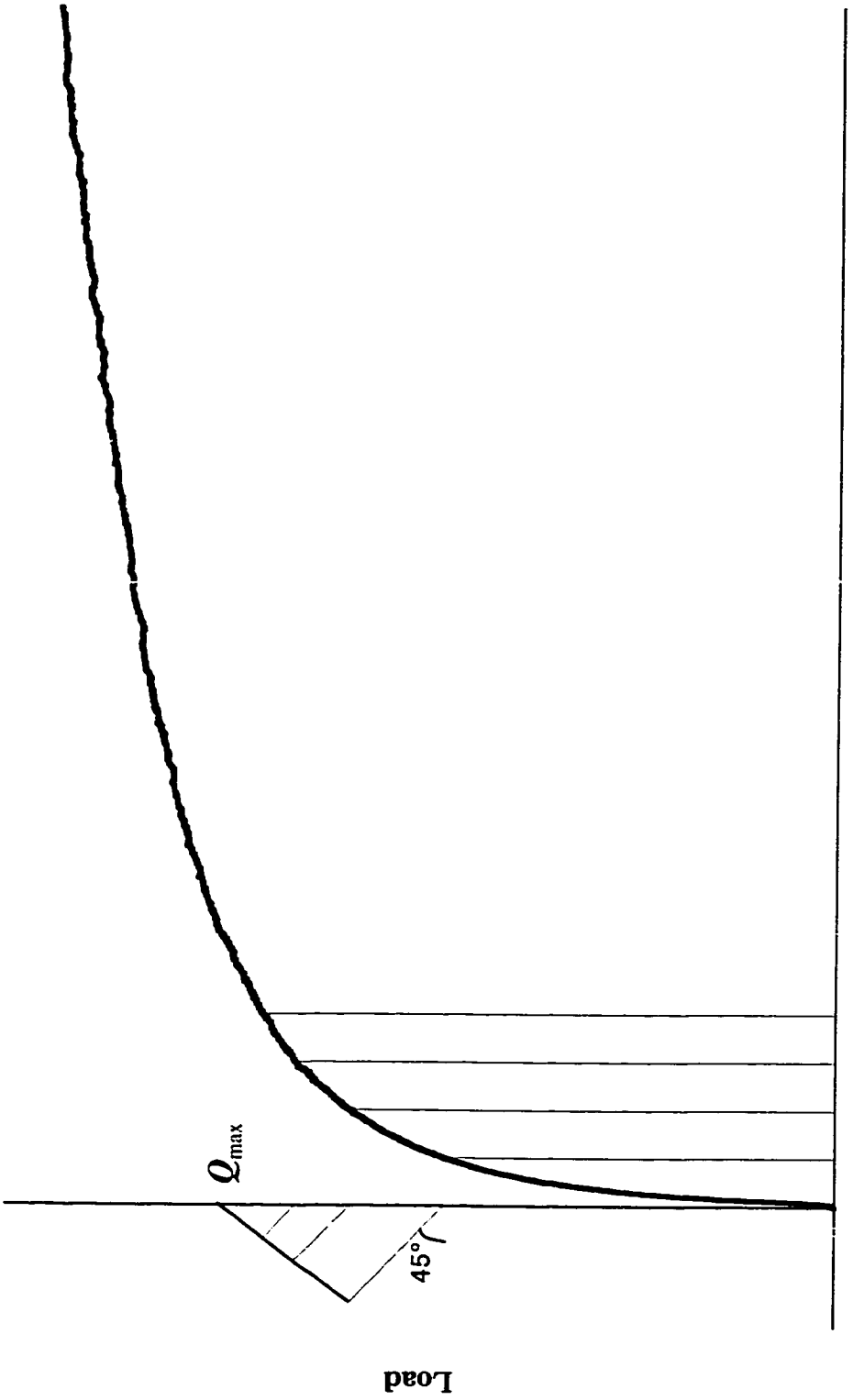

Figure 2.24 - Mazurkeiwicz Method

Chapter 3

Apparatus and Test Procedure

The apparatus for model testing was originally designed and assembled as a rigid walled calibration chamber by Sparrow (1989). It has since been modified twice, once by Achari (1991) and again by Smith (1995) to allow application of vertical and horizontal stresses, thus making the test apparatus a flexible walled chamber. For the series of tests presented herein, there were no major modifications made to the equipment, and only minor modifications to the test procedure and pile types.

3.1 Apparatus

3.1.1 Test Tank

Sparrow (1989) originally formed the test tank by bolting two 16 gauge 900 mm diameter cylindrical steel sections one atop the other. These bolted cylinders were welded to a 9.5 mm thick base plate. Unidirectional wheels were added under the corners of the base plate in order to roll the apparatus into place for testing.

Achari (1991) performed several modifications to the tank in order to apply surcharge loading to the sand. The tank itself was modified by welding horizontal rings onto the tank in order to stiffen the walls enough to resist the additional horizontal loads resulting from the application of surcharge loading. An inflatable rubber doughnut shaped bag encased in a flexible nylon housing was designed in order to apply a surcharge load to the

top of the sand bed. In the middle of the surcharge bag there was a 76 mm (3 inch) opening for the pile to move through. Additionally, a steel lid which can be bolted on to the top of the tank was manufactured. This 12.7 mm (1/2 inch) thick steel plate was reinforced with several 12.7 mm thick stirrups. Like the surcharge bag, the lid also had a 76 mm diameter opening. A perspex cylinder with a 76 mm outer diameter was placed inside the surcharge bag's opening in order to prevent the bag from expanding and adding friction onto the surface of the pile which passed through the hole after driving.

The tank was most recently modified by Smith (1995) in order to apply a horizontal confining stress to the sand. Angles were welded to the outside face of the tank in order to further stiffen the walls against the increased loads that would need to be restrained. The inside of the tank was covered with a bitumen backed plastic sheet in order to cover any holes that may have been created in the walls when the stiffening members were welded in place. A perforated 840 mm diameter aluminum cylinder was placed inside the tank, this cylinder supported a 20 mil polyvinylchloride (PVC) membrane which formed the flexible lining. The membrane was attached to the side and the base of the tank by metal rings. The cylinder was instrumented with nine strain gauges in order to determine the horizontal stress in the soil at various points. The aluminum cylinder was held in place by inflated rubber tubes to ensure it was stationary throughout the testing procedure. This allowed air to be pumped between the membrane and the tank wall in order to apply a confining stress to the soil. A wooden buffer to go between the surcharge bag and the soil was added to prevent the surcharge bag from crushing the aluminum cylinder. The buffer had the added

benefit of ensuring a consistent stress across the top surface of the sand bed.

3.1.2 Pluviation Tank

In order to create a uniform sand bed by pluviation a second tank is required. Sparrow (1989) designed the pluviation tank as per the recommendations presented by Rad and Toumay (1987). The pluviation tank is 2.13 m high, 0.89 m in diameter and rests upon four metal legs. At the base of the pluviation tank is a shutter through which the sand is transferred from the pluviation tank into the testing tank. The shutter is composed of two 9.5 mm thick plates. One plate is fixed to the tank while the other can be moved via a lever on the outside of the tank. Both plates contain an identical pattern of 12.7 mm (1/2 in) holes with a centre to centre spacing of 63.5 mm (2 1/2 in). When the lever is raised the holes are aligned and the sand is free to flow out from the pluviation tank. When the lever is lowered again, the holes no longer line up and the flow of sand out of the tank ceases.

The diffuser sieve is comprised of 2 horizontal sieves with a nominal opening of 6.35 mm. The sieves are spaced 80 mm apart and are rotated at 45° with respect to each other. The diffuser sieve was reduced from 0.84 m in the original tank to 0.75 m due to the modification made by Smith (1995). Small wheels were added to the side of the diffuser sieve due to concern that the sieve would puncture the PVC liner during the pluviation process. The diffuser is suspended by four steel ropes such that before sand transfer begins the sieve is 0.54 m from the bottom of the test tank. These ropes go through several

pulleys and attach to a heavy metal plate critical for the pluviation process.

The transfer of sand between the two tanks resulted in an undesirable amount of fine particles being released into the air. Sparrow (1989) attached a fabric shroud between both tanks, but the finest sand particles were still able to make their way through the fine mesh of the fabric. Smith (1991) modified this setup with a plastic shroud and a location for a vacuum to be attached. The plastic is impermeable and thus it is impossible for the fines to escape from this closed system. A vacuum was attached to provide the air leaving the test tank with an escape route, without letting any fine particles into the air. Figure 3.1 illustrates the interaction of all the components in the pluviation process.

3.1.3 Piles

The piles as pictured in Figure 3.2 were constructed of 0.362 m (14 1/4 in) lengths of steel pipe. The diameter of the straight piles was 50.8 mm (2 in), and the tapered piles ranged from a top diameter of 50.8 mm (2 in) down to 25.4 mm (1 in) at the tip. The straight piles have a wall thickness of 3.18 mm (1/8 in) and the tapered piles are step tapered on the inside resulting in a wall thicknesses of 3.18 mm (1/8 in) to 6.35 mm (1/4 in).

The pile sections joined together to form piles of 0.72 m (28 1/2 in), 1.09 m (42 3/4 in), and 1.45 m (57 in). A top section 0.457 m (18 in) was added to the top of the piles in order to extend the pile above the tank lid so to apply load during testing. The piles were driven to depths of 0.72 m (28 1/2 in), 1.09 m (42 3/4 in), and 1.32 m (52 in) as illustrated in

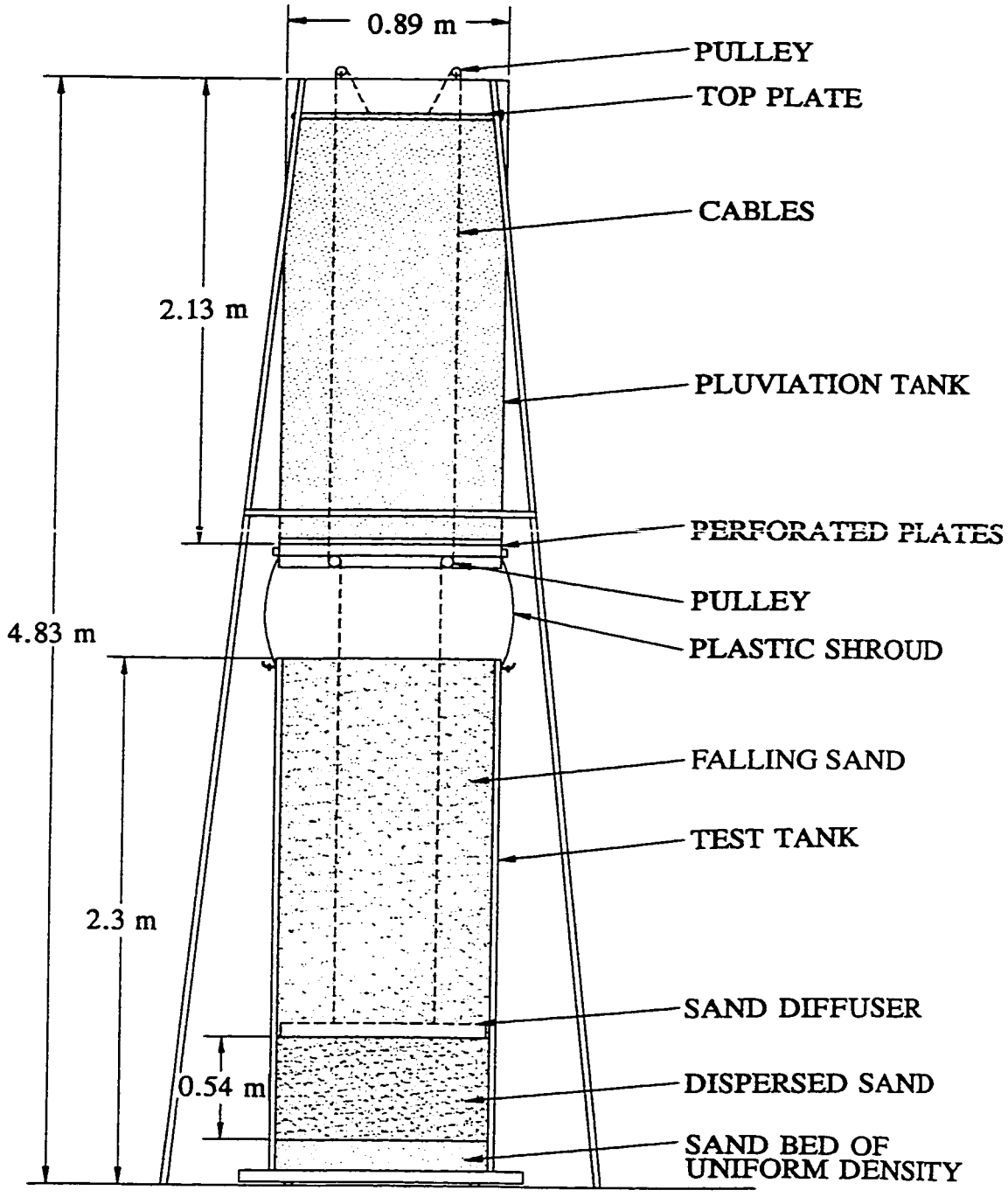

Figure 3.1 - Pluviation Schematic (Smith, 1995)

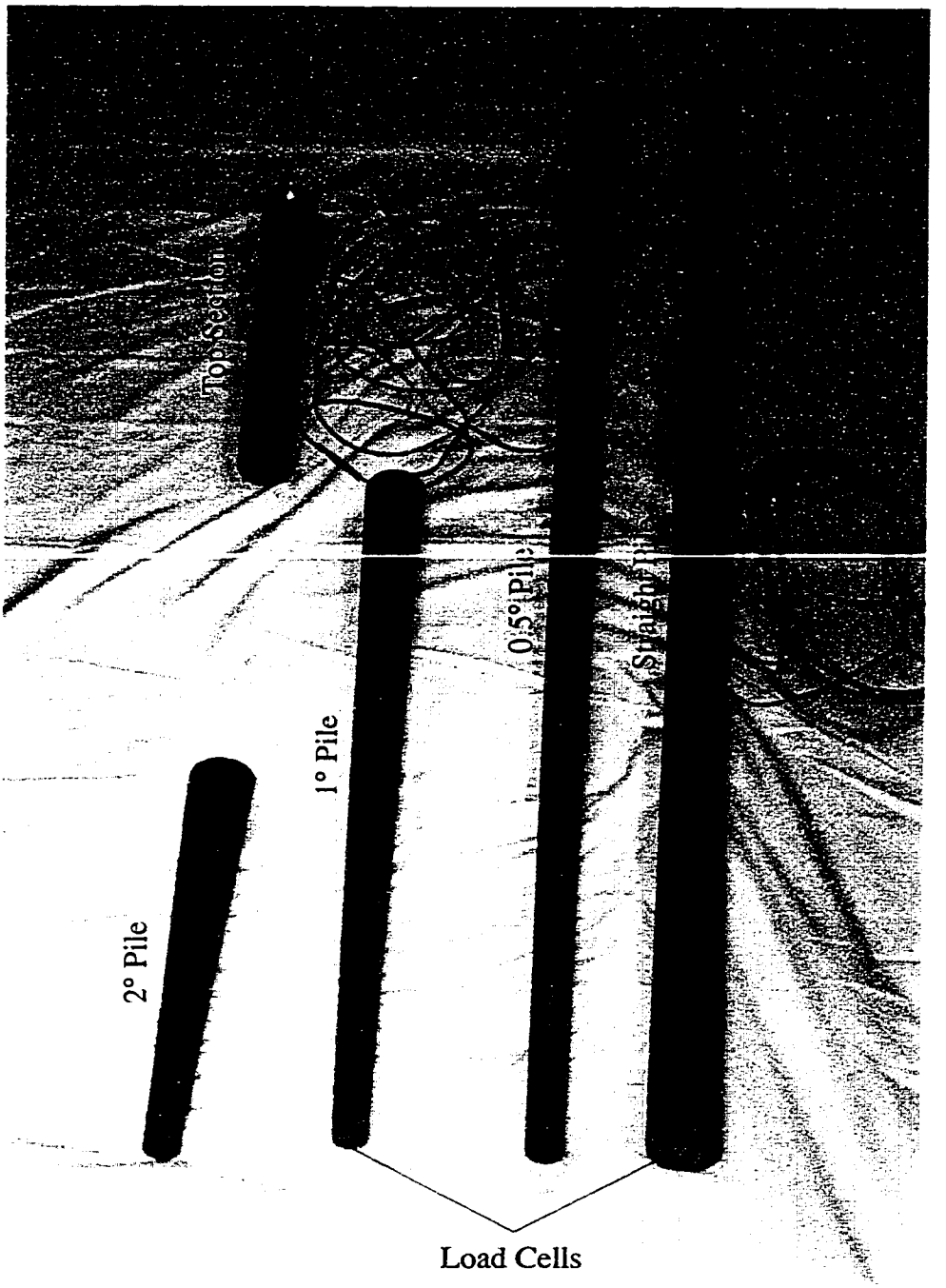

Figure 3.2 - Piles

Figure 3.3. The maximum driving distance was limited to 1.32 m to allow 0.6 m of distance between the pile tip and the bottom of the test tank as per Hanna and Tan (1973). In the case of the 1° and 2° tapered piles, straight sections made up the remainder of the height after the tapered section reached 50.8 mm (2 in) diameter.

3.1.4 Driving Apparatus

The drop hammer driving device designed by Sparrow (1989) was used to drive the piles into the pluviated sand bed. The drop hammer consisted of a cylindrical driving hammer with a mass of approximately 10 kg. The hammer was attached to the shaft of the driving apparatus such that it was only free to move in the vertical direction. The top of the hammer was attached to a rope and pulley system for ease of driving. The pile was driven to the appropriate depth through a consistent drop height of 0.8 m.

The pile was held in place during driving by either one or two of the restraints or leads seen in Figure 3.4. These restraints were also fixed to the shaft of the driving apparatus, they allow the pile to move vertically, but not horizontally, during driving by the two wheels, one on either side of the pile.

3.1.5 Sand

The sand used in this experiment was the same sand used by Smith (1995) and is classified as an SP using the Unified Soil Classification System, as seen in Figure 3.5. The sand had a uniformity coefficient of 2.7 and a coefficient of gradation of 1.2. According to ASTM

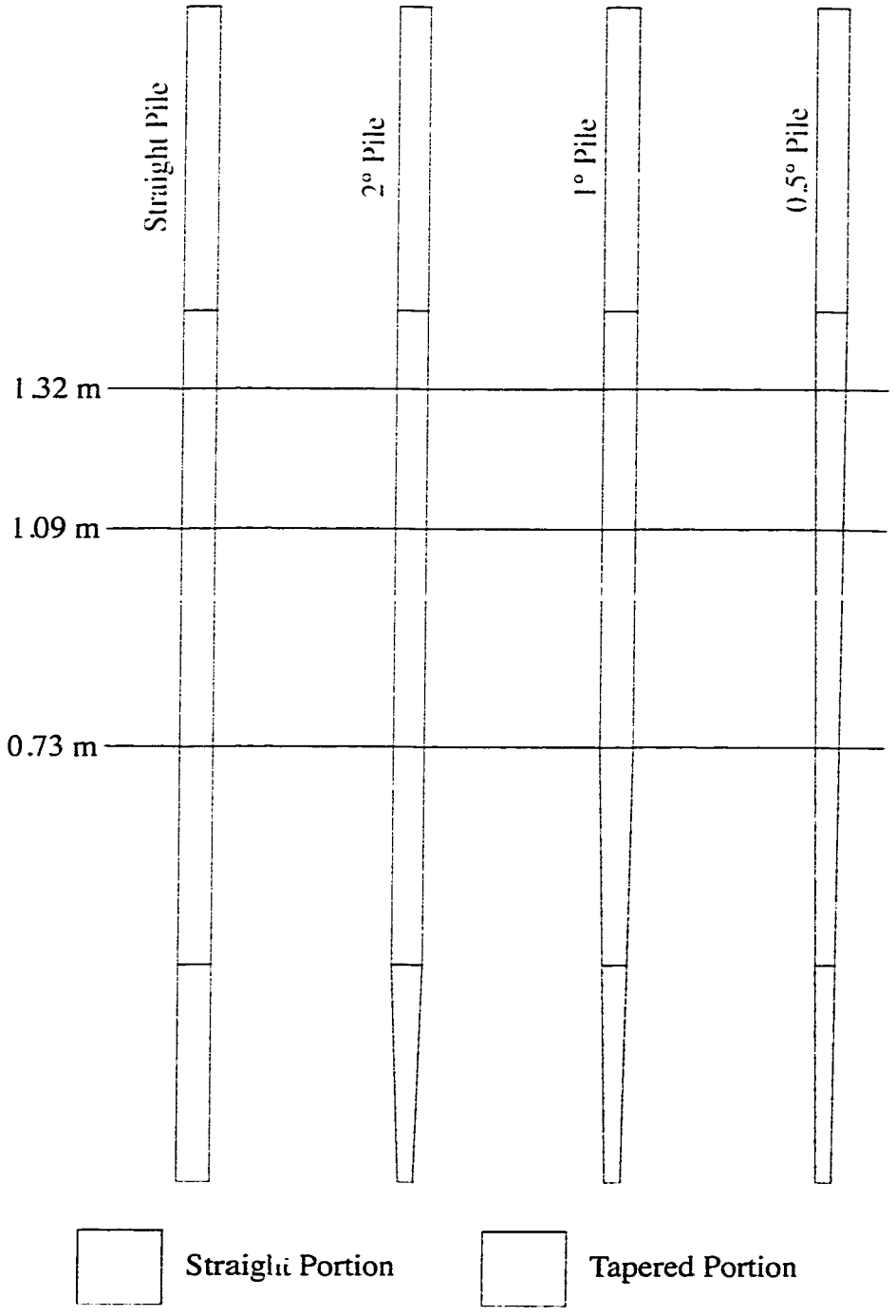

Figure 3.3 - Driving Depths

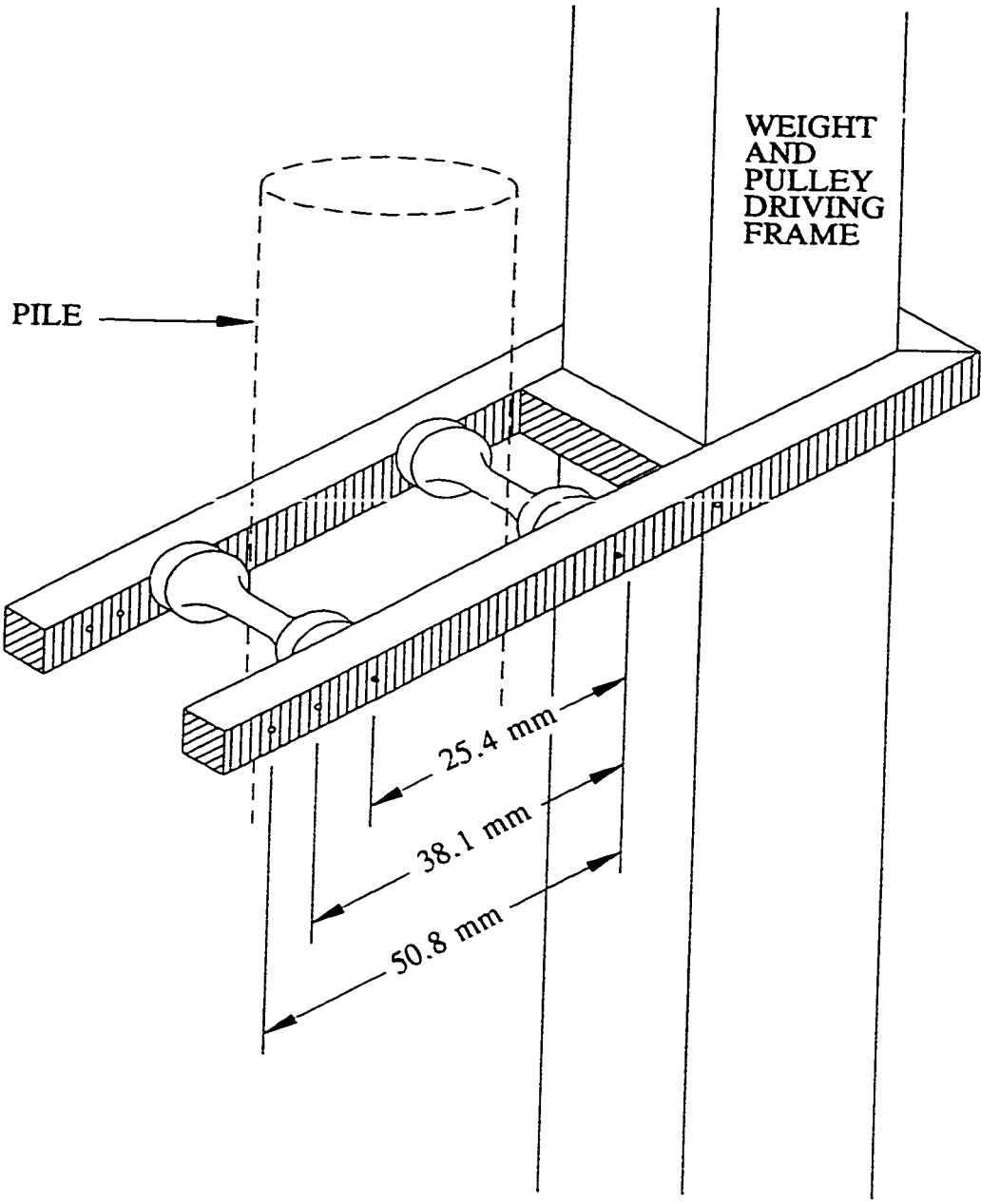

Figure 3.4 - Driving Restraint (Smith, 1995)

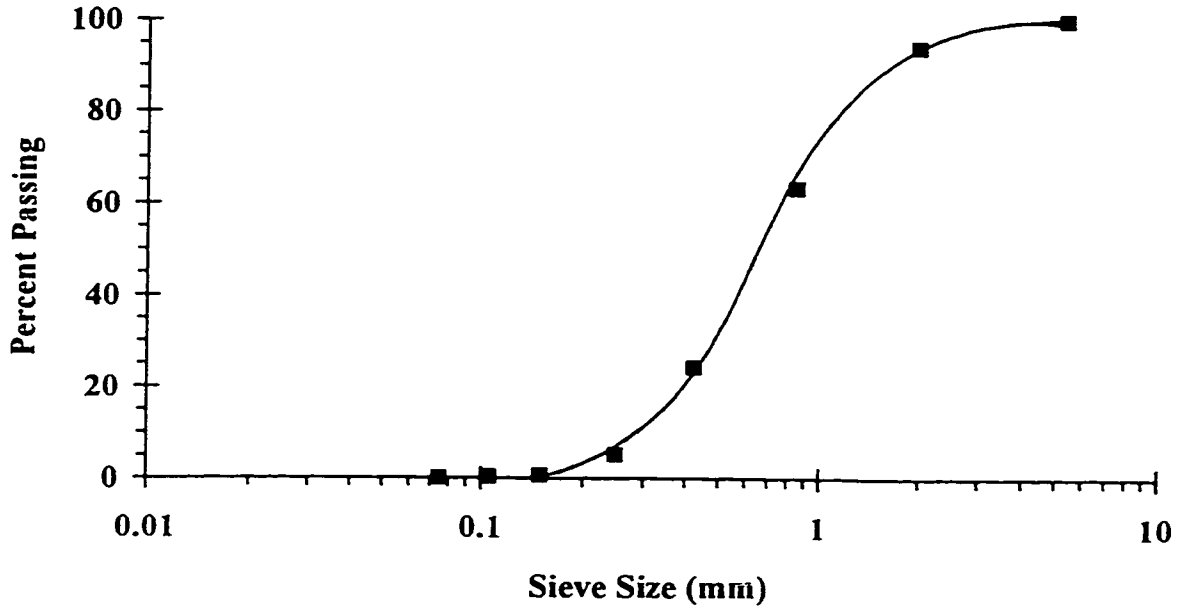

Figure 3.5 - Sieve Analysis of Sand (Smith, 1995)

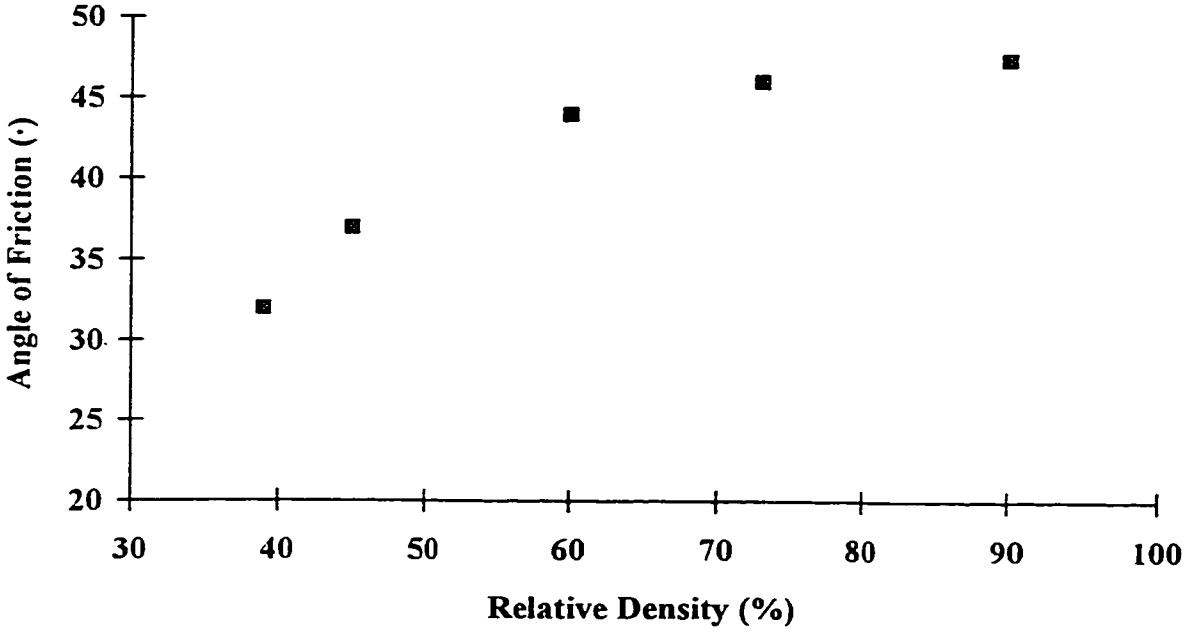

Figure 3.6 - Angle of Friction versus Relative Density (Smith, 1995)

standards the maximum and minimum densities were determined to be 17.72 kN/m^3 and 15.35 kN/m^3 respectively. These densities relate the soil friction angle via the chart shown in Figure 3.6.

3.2 Test Procedure

3.2.1 Setup Procedure

The setup and testing of the piles are a multi-step process that requires 24 hours to complete. Figures 3.7 to 3.11 show the main steps involved in preparing and testing the soil.

The Following is a summary of the steps required for each test

Step 1 - Empty the sand from the test tank into the pluviation tank by placing the test tank above the pluviation tank and opening the drainage slot in the bottom of the test tank.

Step 2 - Remove the remainder of the sand from the base of the tank using a specially designed long pole. This is required since the drainage slot in the base of the test tank is much smaller than the base itself.

Step 3 - Position the test tank under the pluvial tank for the creation of the test sand bed.

Step 4 - Lower the diffuser sieve down into the tank and attach to the heavy steel plate placed on top of the sand and perform the pluviation process.

Step 5 - Move pluviation tank away.

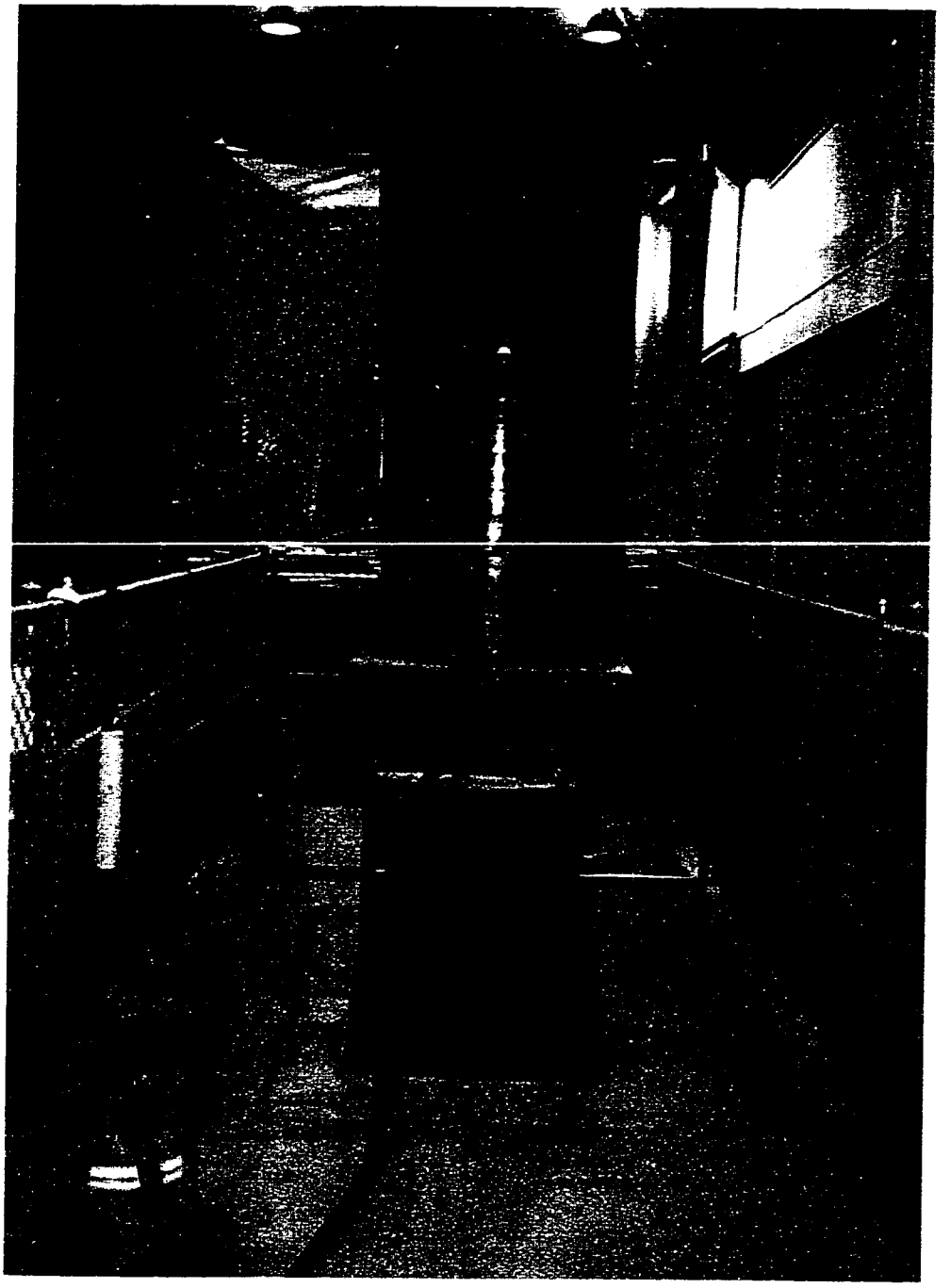

Figure 3.7 - Removal of Sand from Test Tank into Pluviation Tank

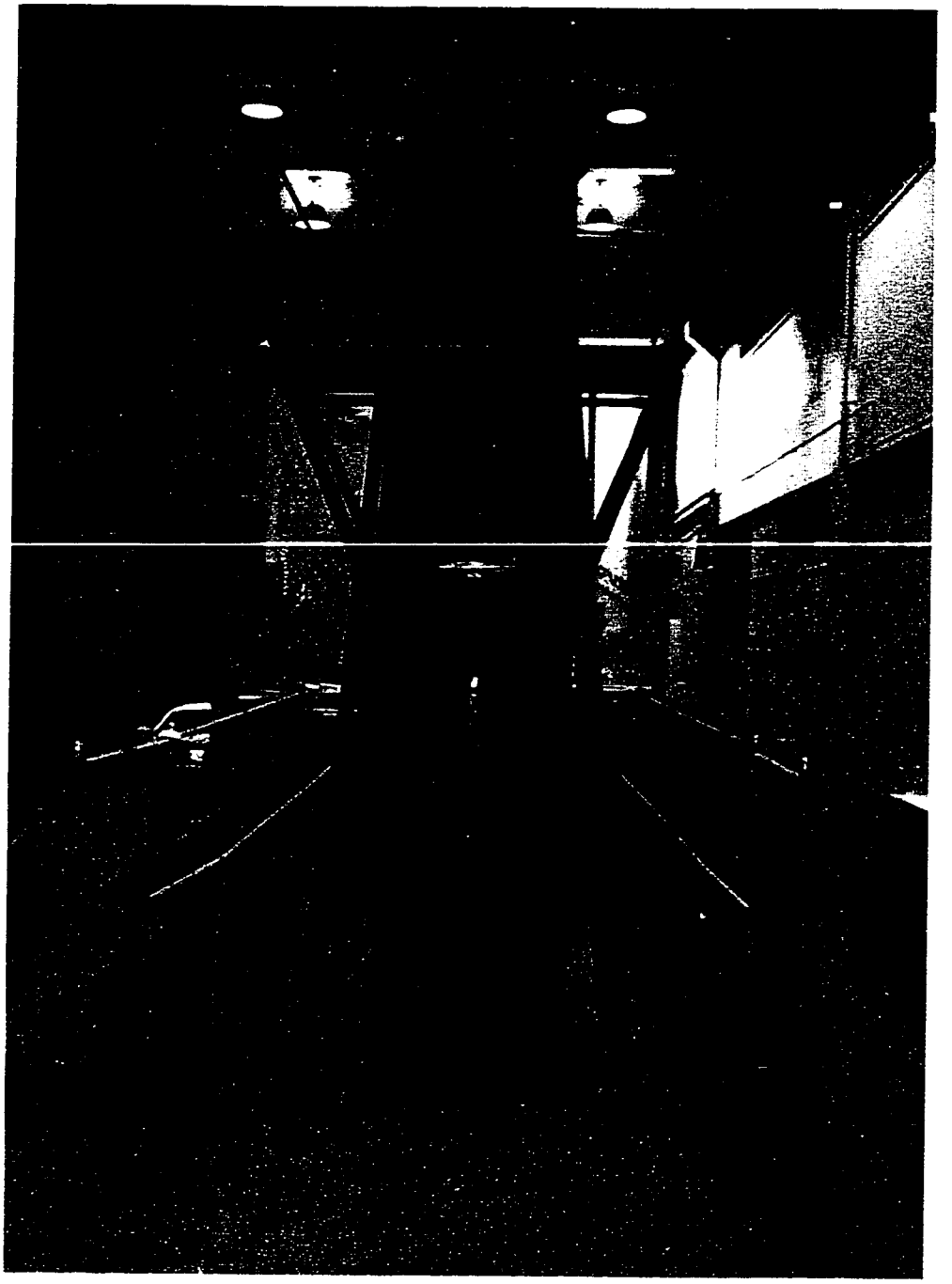

Figure 3.8 - Test Tank in Place for Pluviation

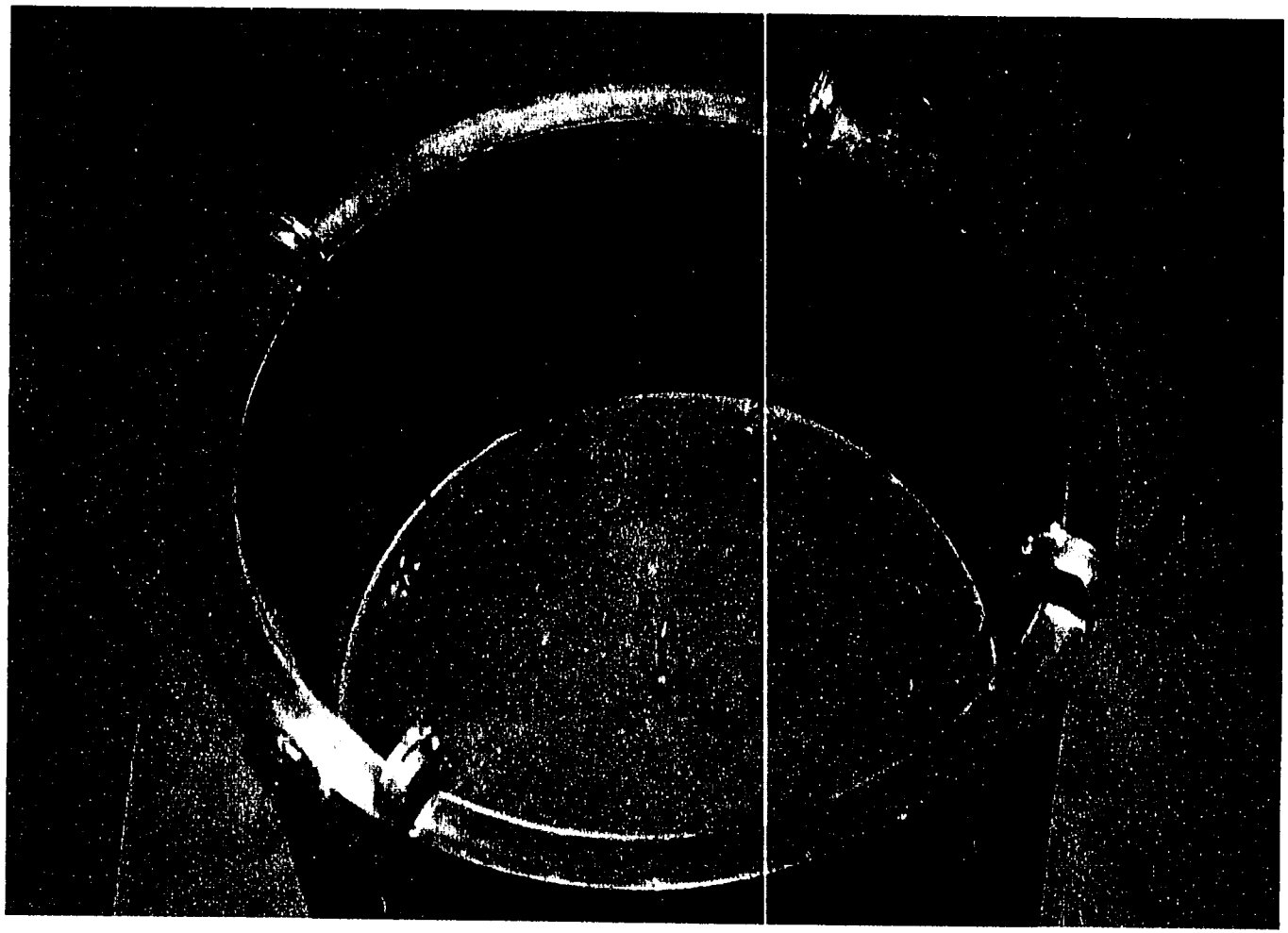

Figure 3.9 - Top Plate Resting on Sand in Pluviation Tank

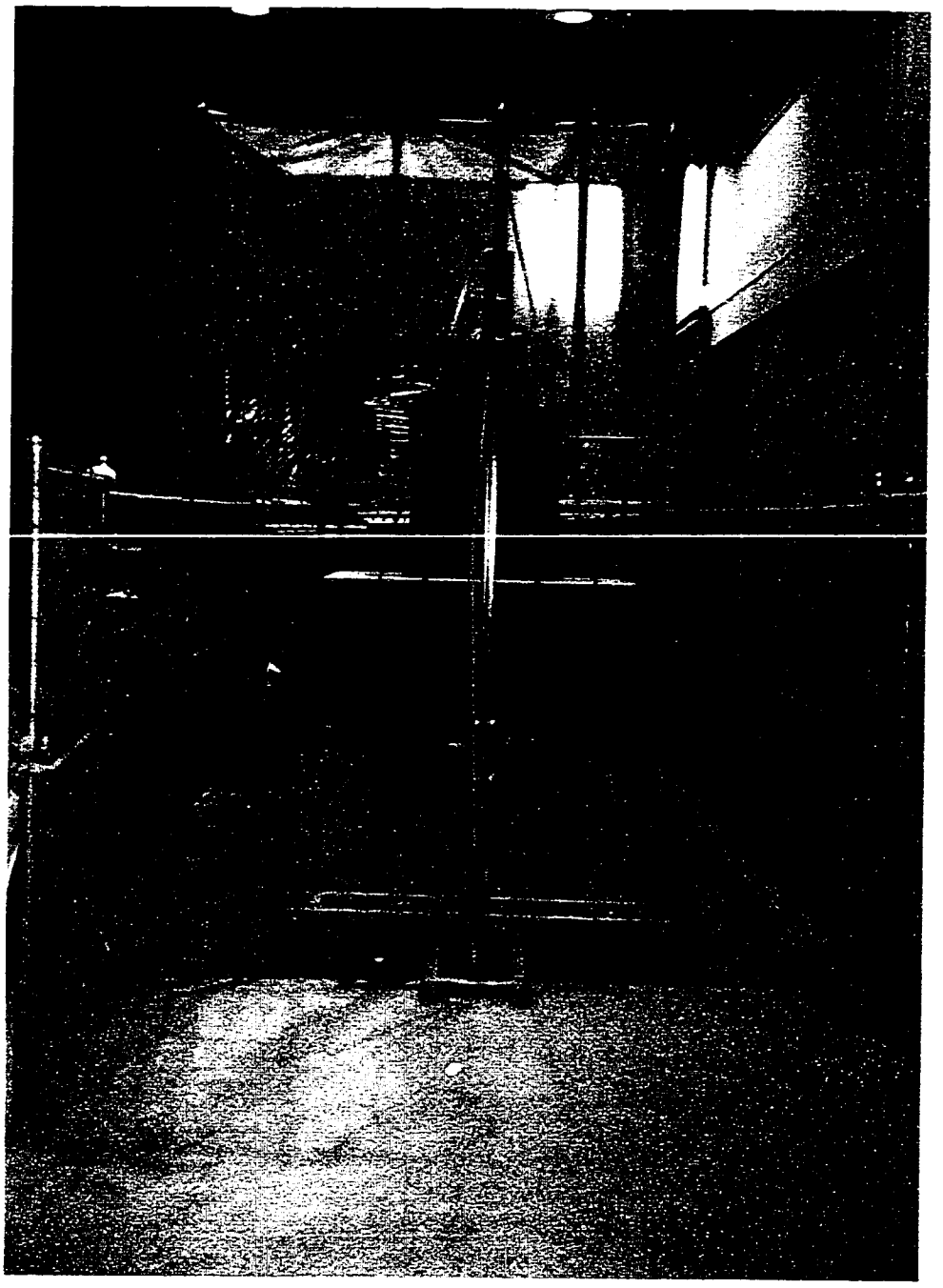

Figure 3.10 - Driving Apparatus Positioned Above Test Tank

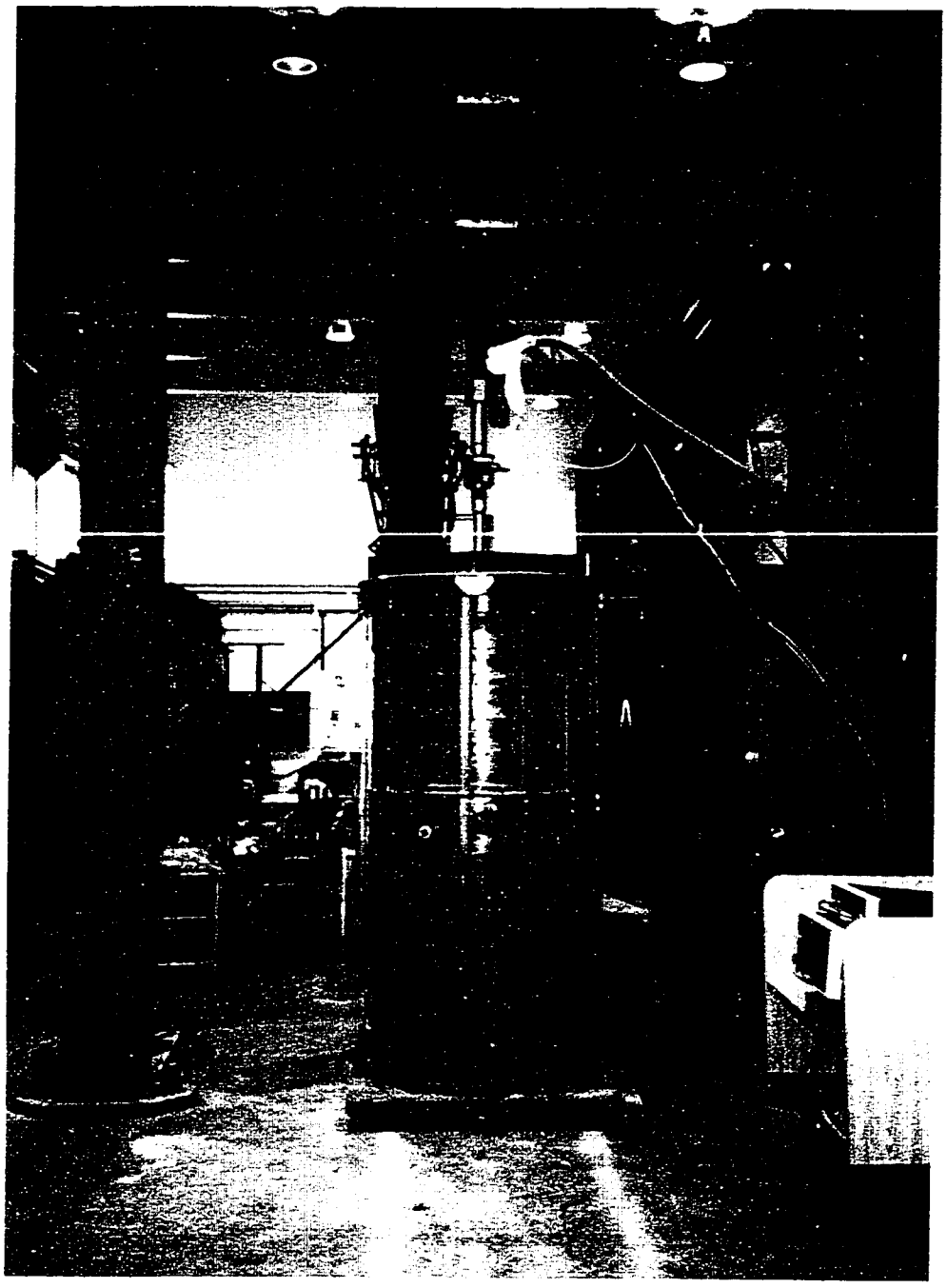

Figure 3.11 - Test Tank Beneath Loading Frame

Step 6 - Place the surcharge bag and lid on the tank and pressurize if needed for this test.

Step 7 - After approximately 1 hour drive the pile into place.

Step 8 - After approximately 18 hours test the pile.

3.2.2 Pressure conditions

The sand was subjected to three different pressurization conditions within the test tank. The first condition was a no additional pressure condition where the pile is driven into the sand as was after completion of the pluviation process. The second condition, used by Achari (1991), was a modification of the process. This involved applying a surcharge pressure to the top of the soil, but, unlike Achari, the pressure was applied prior to the driving process. The final condition involved a surcharge pressure on the top of the sand and a confining pressure on the sides. Once again the pressure was applied to the sand prior to the driving as opposed to Smith (1995) who applied the pressure upon completion of the driving. The applied pressures were 50 kPa in surcharge and 25 kPa in confining stress. A confining stress of 25 kPa was chosen due to limitations of the test tank.

3.2.3 Testing and Data Acquisition Process

A Material Test System (MTS) was used to load the piles at a constant rate of 0.5 mm/min. The pile was loaded evenly by using a spherical seat between the MTS ram and the top of the pile. The load applied to the top of the pile, the resulting load at the pile toe, and the pile displacement were recorded using a PC running Datascan and Labtech Notebook.

Readings were recorded every second for approximately 50 minutes or 25 mm (1 in) of settlement. Blow count data was also recorded for every 0.36 m section during the driving process.

Chapter 4

Test Results and Discussion

More than 80 tests were conducted from which the data for 42 different tests is presented in 4 different sections: straight piles, tapered piles, comparison of straight and tapered piles, and numerical analysis of the data. These sections will compare the effects of changing the pile lengths and the soil stress regime upon the resulting total, side, and end bearing stresses. The bearing capacity of each of the piles was determined from the collected data by the methods presented in Section 2.8.

4.1 Straight Piles

4.1.1 No Additional Pressure

Figure 4.1 shows the results from the testing of the straight piles with no additional surcharge or confining pressure applied to the soil.. All curves are very similar in nature and show the importance of the load carried in end bearing upon the total pile capacity. Table 4.1 compares the bearing capacity of the piles as calculated via the various methods presented in Section 2.8. The Brinch Hansen (1963) 90% method was excluded from the calculations due to the inability of some piles to meet the failure criteria. The piles reached their ultimate capacity after approximately 10.5 mm to 11 mm of settlement.

The large settlements are a result of the Brinch Hansen 80% and Chin methods in which settlements exceeded the average value by as much as 31%. A modified mean of the total

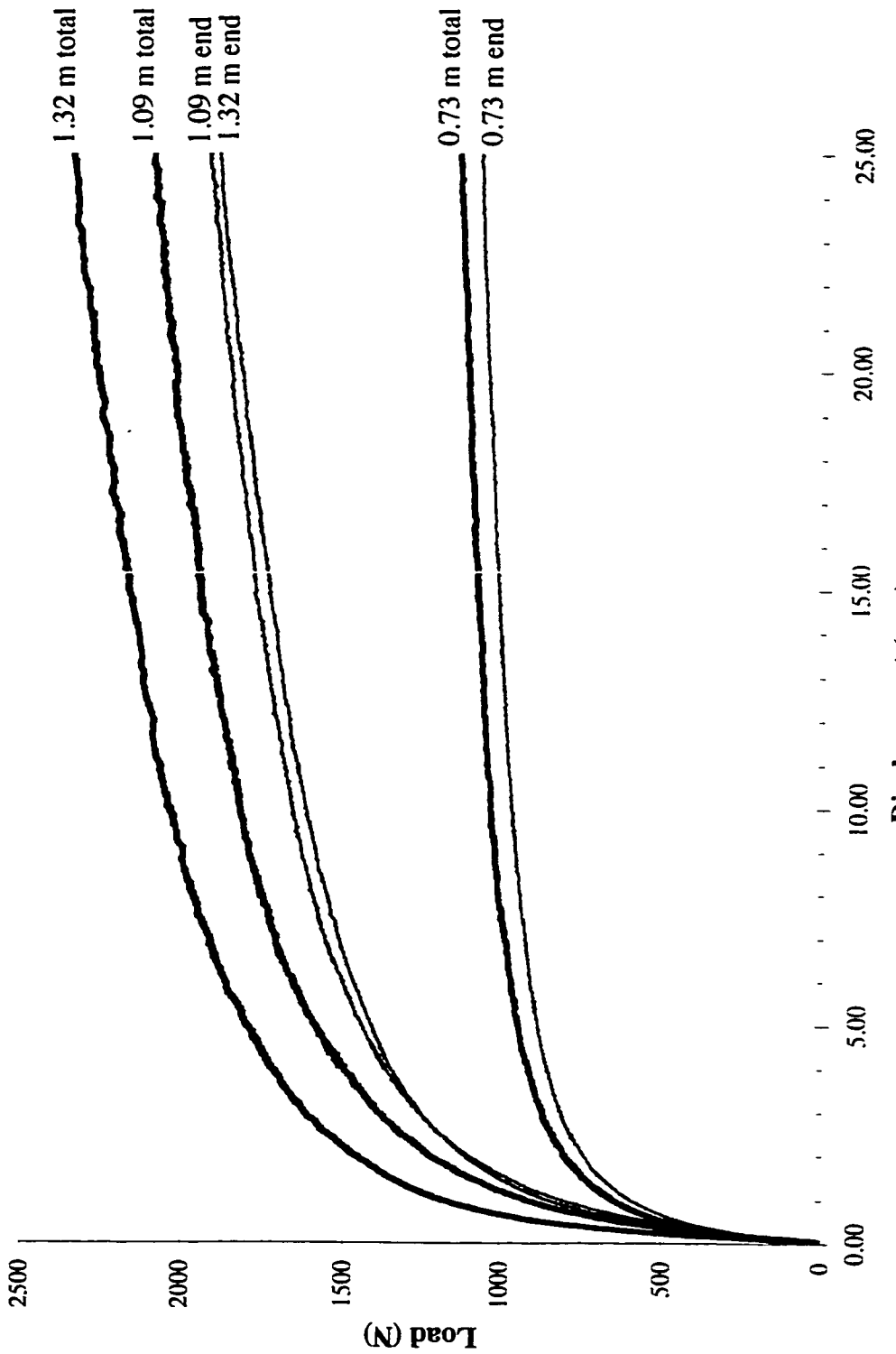

Figure 4.1 - Straight Piles with No Additional Pressure

Table 4.1: Bearing Capacity of Straight Piles - No Additional Pressure

Method	Bearing Capacity (N)		
	1.32 m	**1.09 m**	**0.73 m**
10 %	1,805	1,599	942
Single Tangent	1,890	1,717	986
Double Tangent	1,912	1,739	993
Brinch Hansen 80 %	2,254	2,025	1,112
Chin	2,714	2,390	1,251
Mazurkeiwicz	1,854	1,644	948
Mean	2,071	1,852	1,038
Displacement (mm)	10.9 mm	11.0 mm	10.6 mm
End Bearing	1,648	1,688	972
Percentage of Total	79.6 %	91.1 %	93.6 %
Modified Mean	1,978	1,781	1,009
Mod. Displ. (mm)	8.2	8.6	7.9
Mod. End Bearing	1,564	1,620	938
Mod. %age of Total	79.1 %	91.0 %	93.0 %

load which removes the highest and lowest values is presented in order to eliminate any single value which may skew the results. This leads to lower settlements and therefore lower total bearing capacities.

As expected, the deeper the pile penetration into the soil the greater the bearing capacity of the pile. Also, the deeper the depth of driving, the greater the percentage of the load taken in shear resistance. As seen in Table 4.1, the end bearing of the 1.32 m long pile was approximately 80% of the total load supported by the pile. In comparison, previous

testing of 50.8 mm (2 in) piles by Sparrow (1989), Achari (1991), and Smith (1995) found the ratio of end bearing to total load to be in the region of 60 % to 70 %. Sparrow and Achari used a different sand than was used by Smith and these series of tests. These current tests resulted in shear resistance 35 % to 40 % lower than the results obtained by Smith. The magnitude of the impact force transmitted to the pile was significantly greater than that used by the previous testers. A drop height of 0.8 m instead of the 0.3 m used during previous testing regimes may have had an effect on both the end bearing and the shear friction of the pile.

Using the same criteria as used to calculate the modified values, the tests from Smith showed a bearing capacity of 1,858 N, an end bearing of 1,252 N, and a shear friction of 606 N versus values of 1,978 N, 1,564 N, and 414 N, respectively. This discrepancy can be explained by an increase in residual forces. Longer hammer drops will drive the pile in further with each blow than will smaller hammer drops. The smaller incremental movement provided by the smaller drop induce more residual stresses into the pile. This is due to the fact that the shear resistance of the pile absorbs a larger percentage of energy delivered by the shorter hammer drops than the long drops. Thus the amount of energy reaching the toe is reduced causing smaller pile movement and creating residual stresses.

The L/D ratios of the piles are 26.0, 21.5, and 14.4 for the 1.32 m, 1.09 m, and 0.73 m piles respectively. Comparing the percentage of load taken through end bearing at the various driving lengths, it becomes obvious that the shear resistance continues to increase

at an increasing rate. This would indicate that the L/D ratio of 26 is not sufficient in this soil to develop the ultimate shear friction along the pile shaft. According to Vesic (1967) and Meyerhoff (1983) the looser the soil the greater the L/D ratio must be in order to maximize the potential shear friction of the soil.

4.1.2 Surcharge Pressure

Figure 4.2 shows the same piles driven into the soil, but with a surcharge pressure of 50 kPa applied to the soil. The bearing capacity of the piles obtained by the various methods for these tests are shown in Table 4.2 and are similar to, but proportionally larger than, the values of the tests with no additional surcharge pressure on the soil. Unfortunately the sand in the tank for the testing of 1.09 m long pile appears to have been loose making it difficult to draw trends from the data. Comparing Tables 4.1 and 4.2 shows that the required settlement to achieve the ultimate bearing capacity is nominally greater with the surcharge loading than without.

The total load was approximately three times as large as that of the no pressure situation. The maximum end bearing capacity appeared not to have been attained either. Once again it was difficult to determine this precisely due to one test occurring in a sand bed that was not deposited to the expected density, despite use of the pluviation process.

It was not possible to correlate the data with previous testing by Achari (1991) and Smith (1995). This was due to significant changes in the testing procedure during this series of

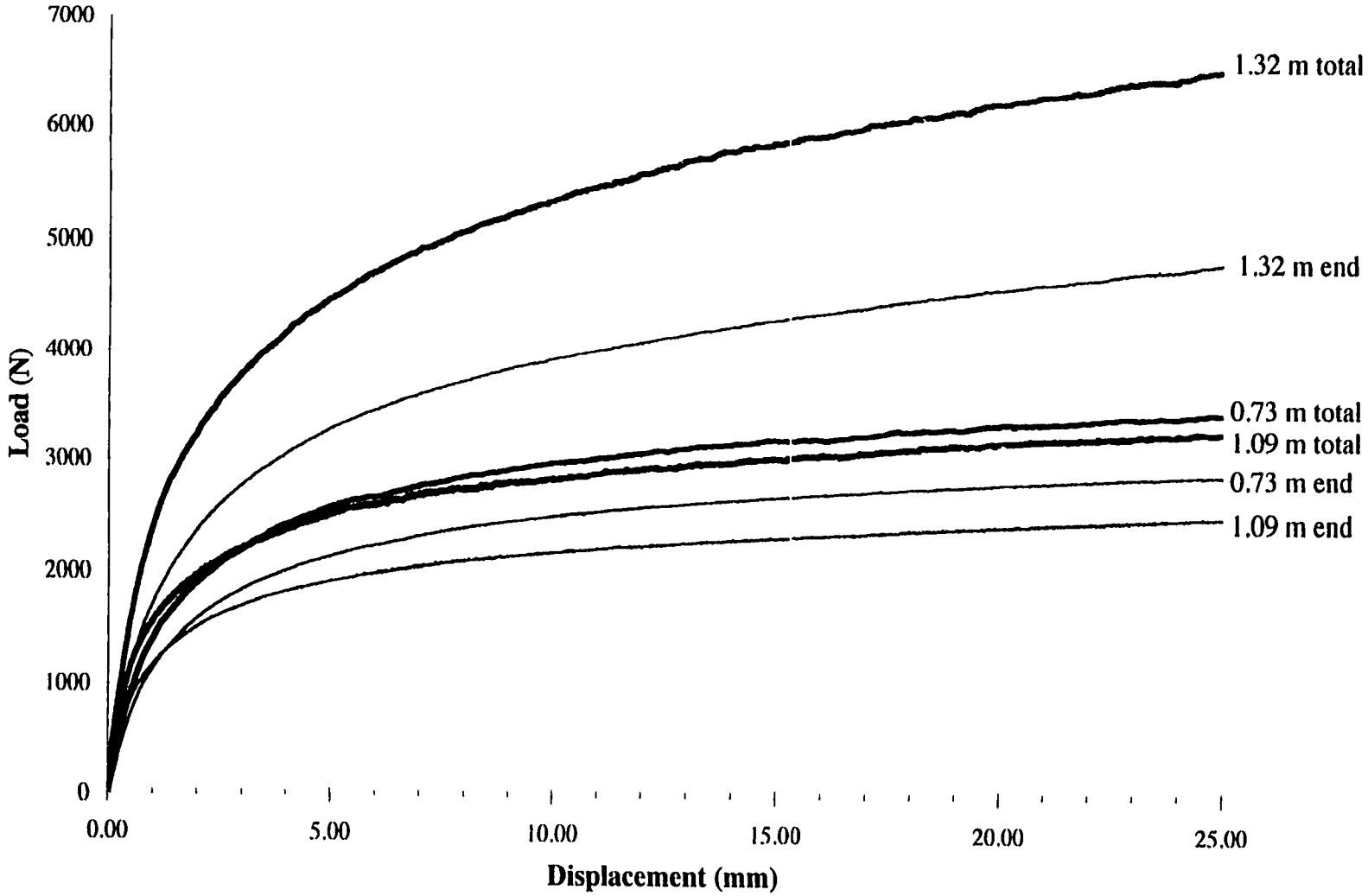

Figure 4.2 - Straight Piles with Surcharge Pressure

Table 4.2: Bearing Capacity of Straight Piles - Surcharge Pressure

Method	Bearing Capacity (N)		
	1.32 m	**1.09 m**	**0.73 m**
10 %	4498	2510	2572
Single Tangent	4894	2659	2802
Double Tangent	5002	2689	2844
Brinch Hansen 80 %	6321	3141	3325
Chin	7850	3736	3919
Mazurkeiwicz	4961	2587	2723
Mean	5588	2887	3031
Displacement (mm)	11.9	11.1	11.1
End Bearing	4086	2216	2538
Percentage of Total	73.1 %	76.8 %	83.7 %
Modified Mean	5294	2769	2924
Mod. Displ. (mm)	9.5	8.4	9.1
Mod. End Bearing	3886	2122	2452
Mod. %age of Total	73.4 %	76.6 %	83.9 %

tests as compared to the previous tests.

4.1.3 Surcharge and Confining Pressure

Figure 4.3 illustrates the load-displacement curves from the testing in which a surcharge of 50 kPa and a confining stress of 25 kPa was applied to the soil. A perusal of the data in Table 4.3 indicates that, while not as great as the increase between the no pressure and the surcharge pressure cases, there was a significant increase in the bearing capacity of the piles in comparison to the surcharge pressure only case.

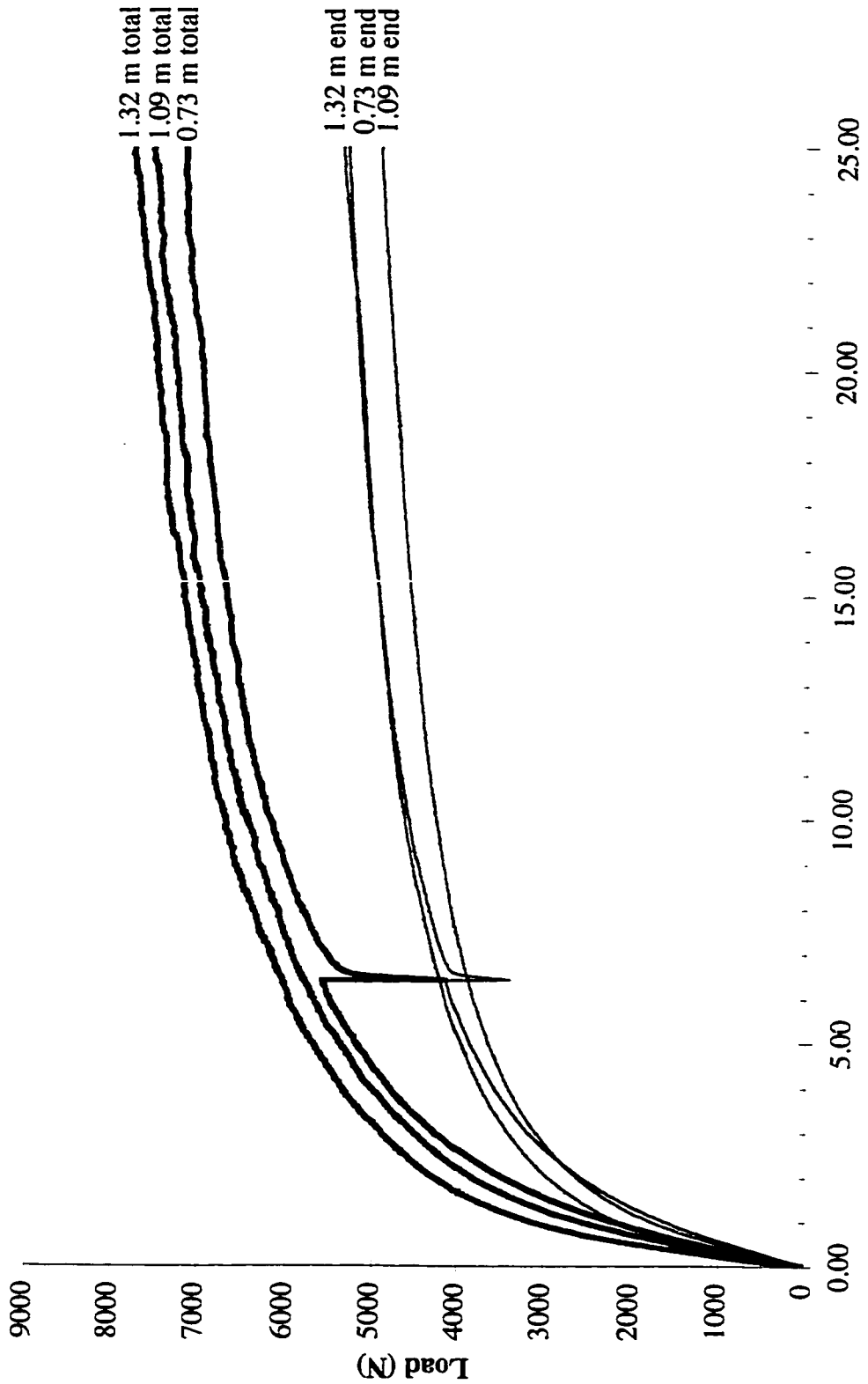

Figure 4.3 - Straight Piles with Surcharge and Confining Pressure

Table 4.3: Bearing Capacity of Straight Piles - Surcharge and Confining Pressure

Method	Bearing Capacity (N)		
	1.32 m	**1.09 m**	**0.73 m**
10 %	5,724	5,401	5,213
Single Tangent	6,345	6,161	5,945
Double Tangent	6,444	6,284	6,075
Brinch Hansen 80 %	7,522	7,422	7,167
Chin	8,844	8,608	8,178
Mazurkeiwicz	5,896	5,656	5,732
Mean	6,796	6,588	6,385
Displacement (mm)	10.7	11.0	11.41
End Bearing	4,708	4,354	4,722
Percentage of Total	69.3 %	66.1	74.0 %
Modified Mean	6,552	6,381	6,230
Mod. Displ. (mm)	8.9	9.7	10.2
Mod. End Bearing	4,538	4,248	4,626
Mod. %age of Total	69.2 %	66.6 %	74.3 %

While both the surcharge pressure only and the surcharge with confining pressure conditions attempt to simulate a deeper depth of soil, results showed that the surcharge with confining pressure resulted in a better simulation for straight piles. If the tank diameter was extremely large the lateral pressure that the sand would have exerted on the walls would be in the region of 25 kPa. However, due to the relatively small diameter of the tank, arching effects similar to those described by Terzaghi (1936) affect the resulting pressure. As illustrated in Figure 4.4 the surcharge applied at the top of the tank is

progressively transferred to the walls of the tank and not fully transferred to the subsequent layers of sand. With the application of a confining pressure to the tank the effects of arching are reduced due to the recreation of conditions that would occur naturally in the field. This is in agreement with the conclusions of Smith (1995) who analyzed the presence of arching under the surcharge load state. The effects of arching were determined via strain gauges installed along the perforated aluminum cylinder, located between the tank wall and the inner membrane (see Section 3.1.1)

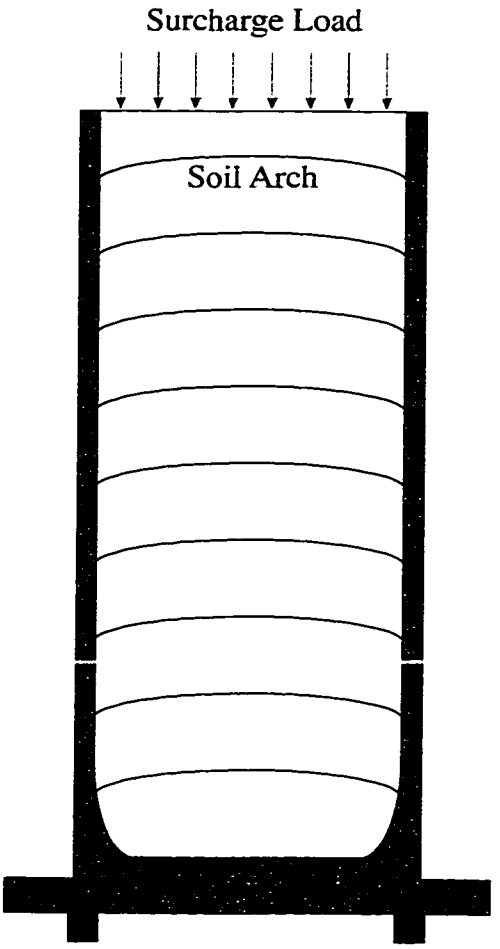

Figure 4.4 - Soil Arches in Test Tank

Unlike the surcharge only condition, the application of a 50 kPa surcharge pressure and a 25 kPa confining pressure simulated a soil depth where the end bearing reached fairly constant values, as per Vesic (1964). Due to the small number of tests, it is also possible that the end bearing continues to increase, but at a decreased rate as proposed by Hanna and Tan (1973).

Compared to the two previous pressure conditions there is a further increase in the percentage of the load carried by shear friction and an increase in the displacement

required for the ultimate bearing capacity of the pile to be reached. The consistent increase across the three stress regimes imply that for straight piles the greater the surrounding stress in the soil, the greater the required pile displacement for ultimate bearing capacity to be achieved.

A similar trend was noted by Vesic (1964) whereby settlements of 14 % and 14.5 % of the pile diameter were required to reach the ultimate bearing capacity of the pile in medium-dense and dense sands respectively. The averages of the mean settlements for the three pressure conditions vary from 16.2% to 18.9% of the pile diameter. It is likely that some scale effects exist between full scale and model piles, and between the simulated and actual field conditions.

4.1.4 Pull Out Resistance

Pull out tests were performed on the 1.32 m long piles following the compression tests. Figures 4.5 through 4.7 compare the shear developed in compression with that in tension. Table 4.4 compares the maximum shear developed in both cases prior to the failure displacements calculated in the previous sections (4.1.1 through 4.1.3).

The shaft resistance under tensile loading is less than under compressive loading due to the introduction of tensile forces into the soil. This tensile action loosens the soil resulting in a lower friction stress along the pile wall, thus reducing the shear which can be developed. The results from the testing show good agreement with Hunter and Davisson

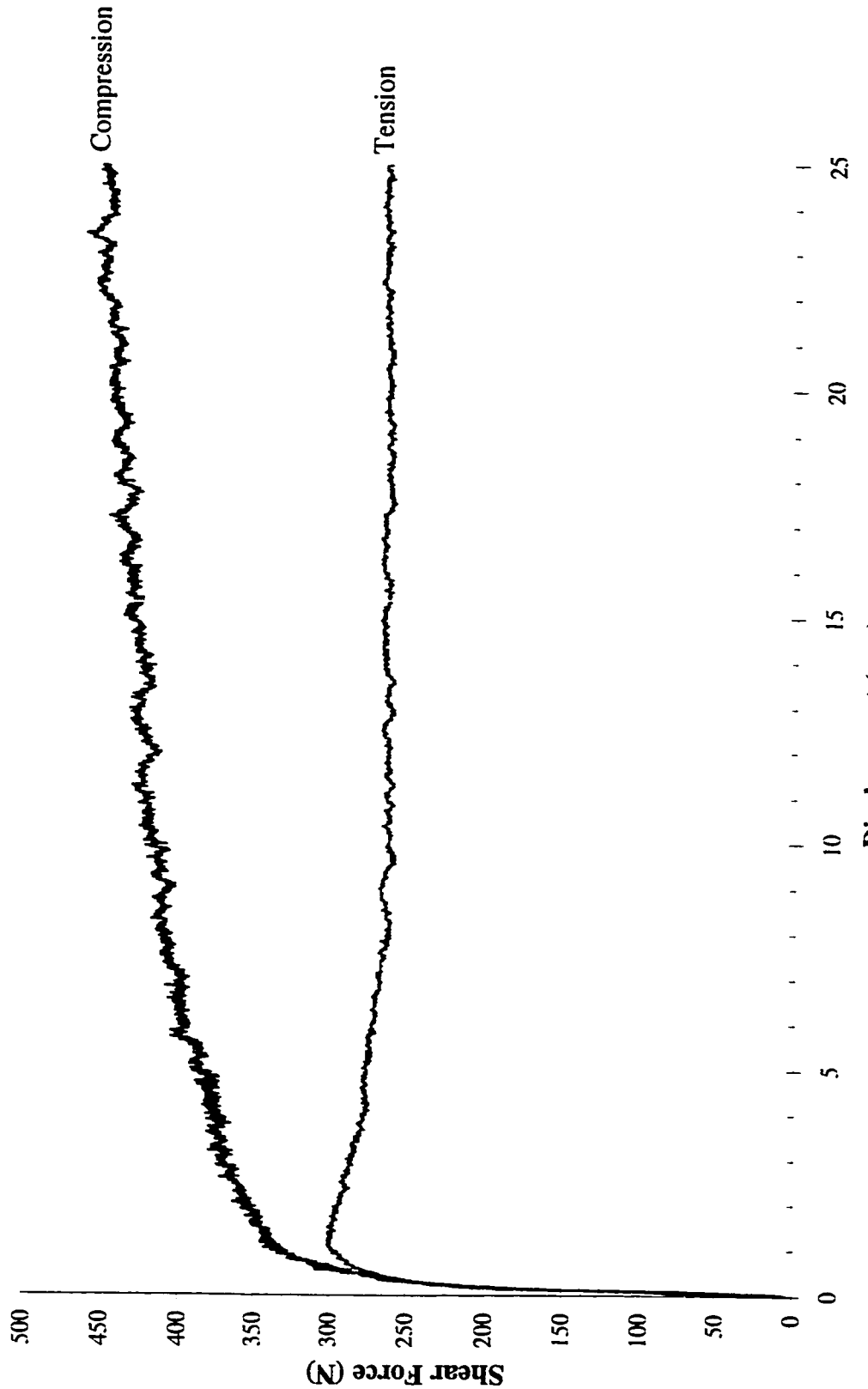

Figure 4.5 - Shear Friction for Straight Piles with No Additional Pressure

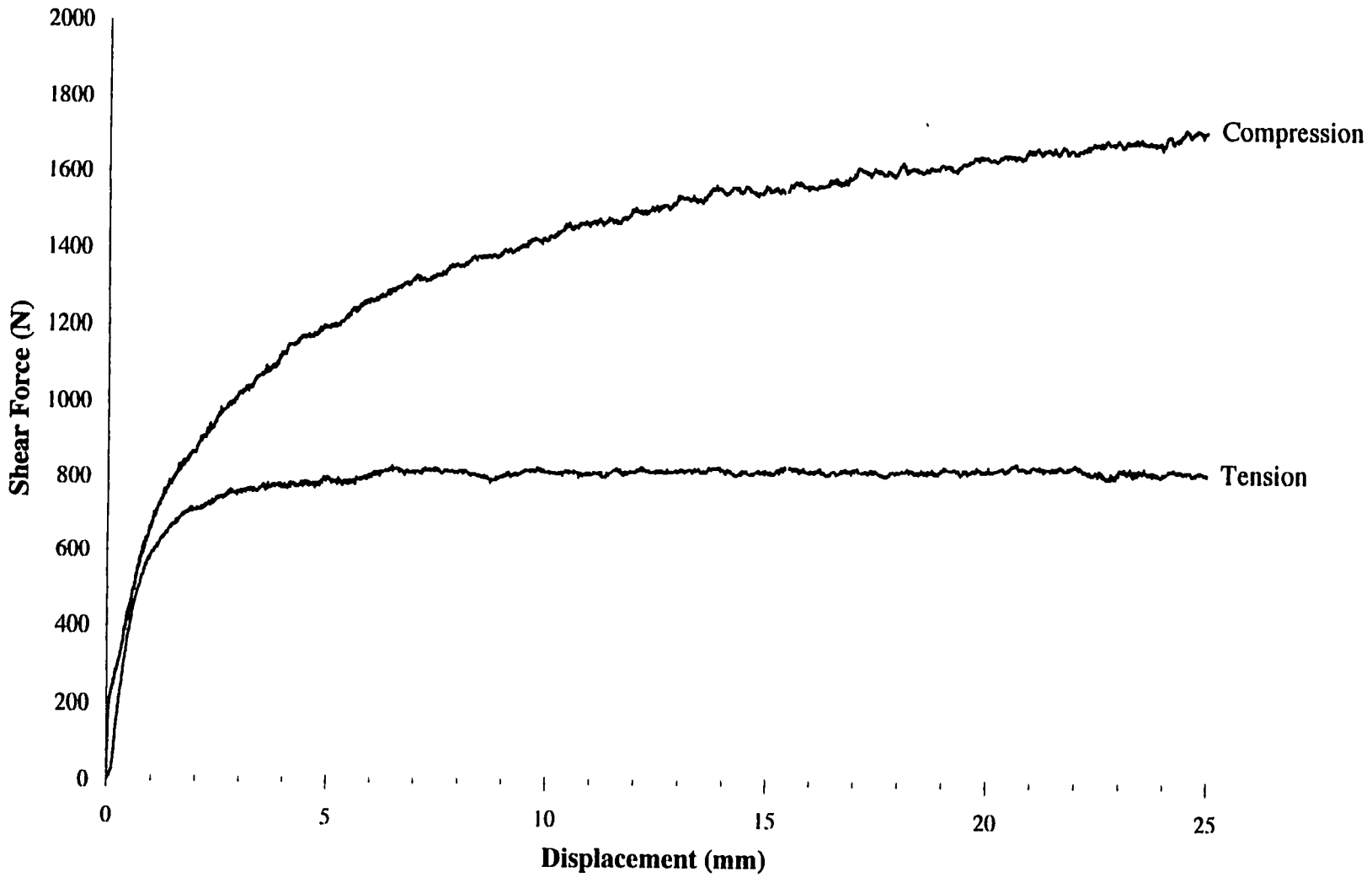

Figure 4.6 - Shear Friction for Straight Piles with Surcharge Pressure

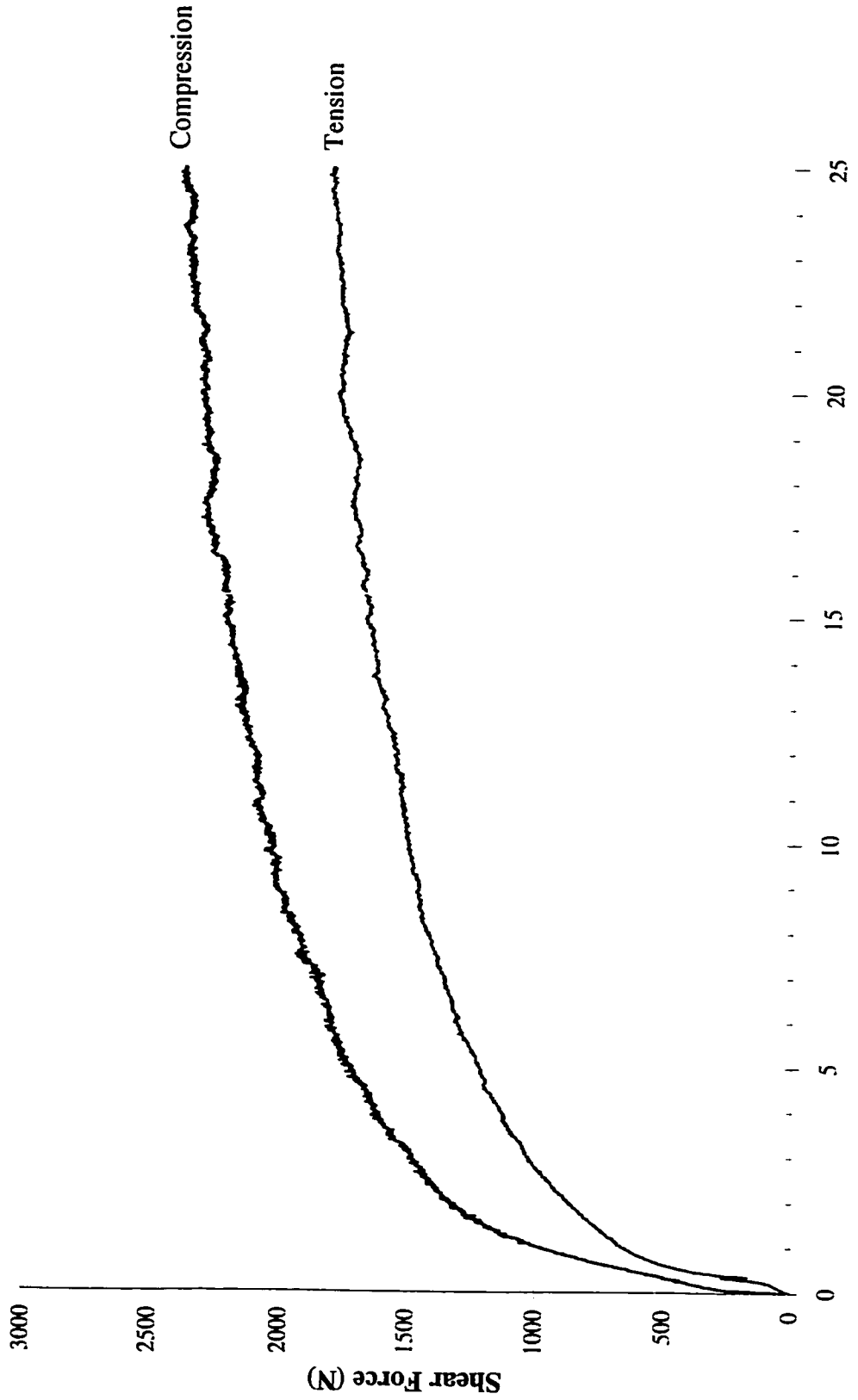

Figure 4.7 - Shear Friction for Straight Piles with Surcharge and Confining Pressure

Table 4.4: Shear Friction in Straight Piles

Location of Pressure	Shear Friction (N)		
	Compression	Tension	Tens:Comp
None	414	301	73 %
Surcharge	1,413	830	59 %
Surcharge & Confining	2,014	1,465	73 %

(1969) and Randolph *et al.* (1994) whose data indicate tension:compression resistance ratios of 70 % and 80 % respectively. It may be noted that, the ratio of compressive to tensile resistance of piles in soils under the vertical surcharge condition was incongruent with the other values due to data being collected from two separate driving tests.

Residual stresses in the compression testing may affect the recorded end bearing values. However, the magnitude of the residual stresses was comparatively small to the total load and less than 8% of the shear in the worst case. This small error results in a maximum of a 2% increase in the ratio of tensile to compressive shear stress.

4.2 Tapered Piles

As previously stated, the piles were tapered at angles of 0.5°, 1°, and 2° and driven to depths of 1.32 m, 1.09 m, and 0.73 m.

4.2.1 No Additional Pressure

Tables 4.5 through 4.7 summarize the data from Figures 4.8 through 4.10. It must be noted that for the Vesic's 10% method the maximum diameter of the driven section was used. To effectively analyze the tapered piles it was necessary to further differentiate the piles into two categories. These categories are identified by the changes in pile cross section with increased length. The increase in length from 0.73 m to 1.09 m and further to 1.32 m resulted in the addition of straight sections onto the tapered portion of the 1° and 2° tapered piles. This allowed for the section to retain the same maximum diameter while

Table 4.5: Bearing Capacity of 0.5° Tapered Piles - No Additional Pressure

Method	Bearing Capacity (N)		
	1.32 m	**1.09 m**	**0.73 m**
10 %	1,957	1,232	828
Single Tangent	1,993	1,289	947
Double Tangent	2,012	1,298	953
Brinch Hansen 80 %	2,369	1,496	1,062
7850	2,842	1,743	1,184
Mazurkeiwicz	1,981	1,286	913
Mean	2,192	1,391	981
Displacement (mm)	11.0	10.9	8.4
End Bearing	541	355	408
Percentage of Total	24.7 %	25.5 %	41.6 %
Modified Mean	2,088	1,342	968
Mod. Displ. (mm)	7.9	7.8	7.7
Mod. End Bearing	509	339	403
Mod. %age of Total	24.4%	25.3 %	41.6 %

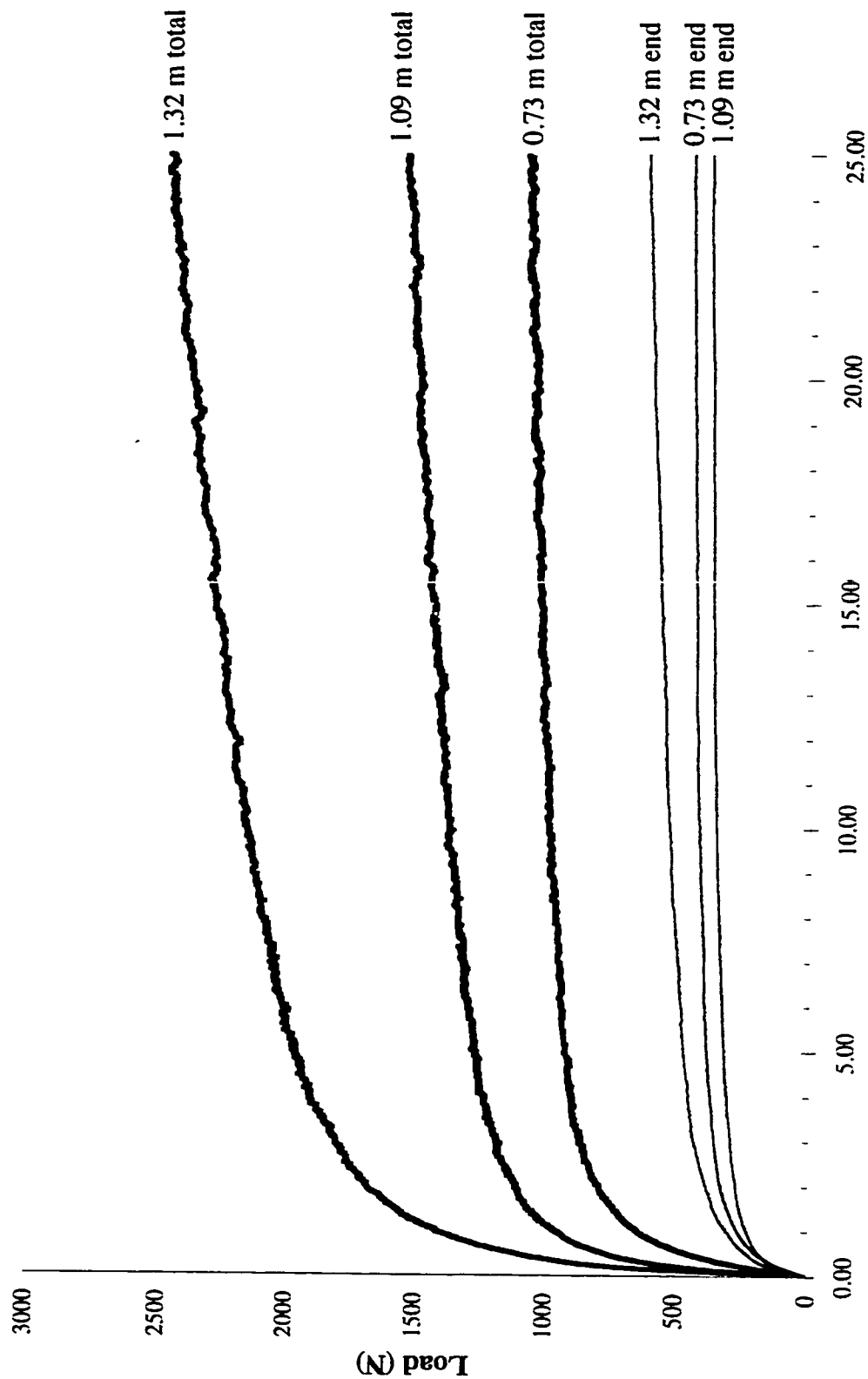

Figure 4.8 - 0.5° Tapered Piles with No Additional Pressure

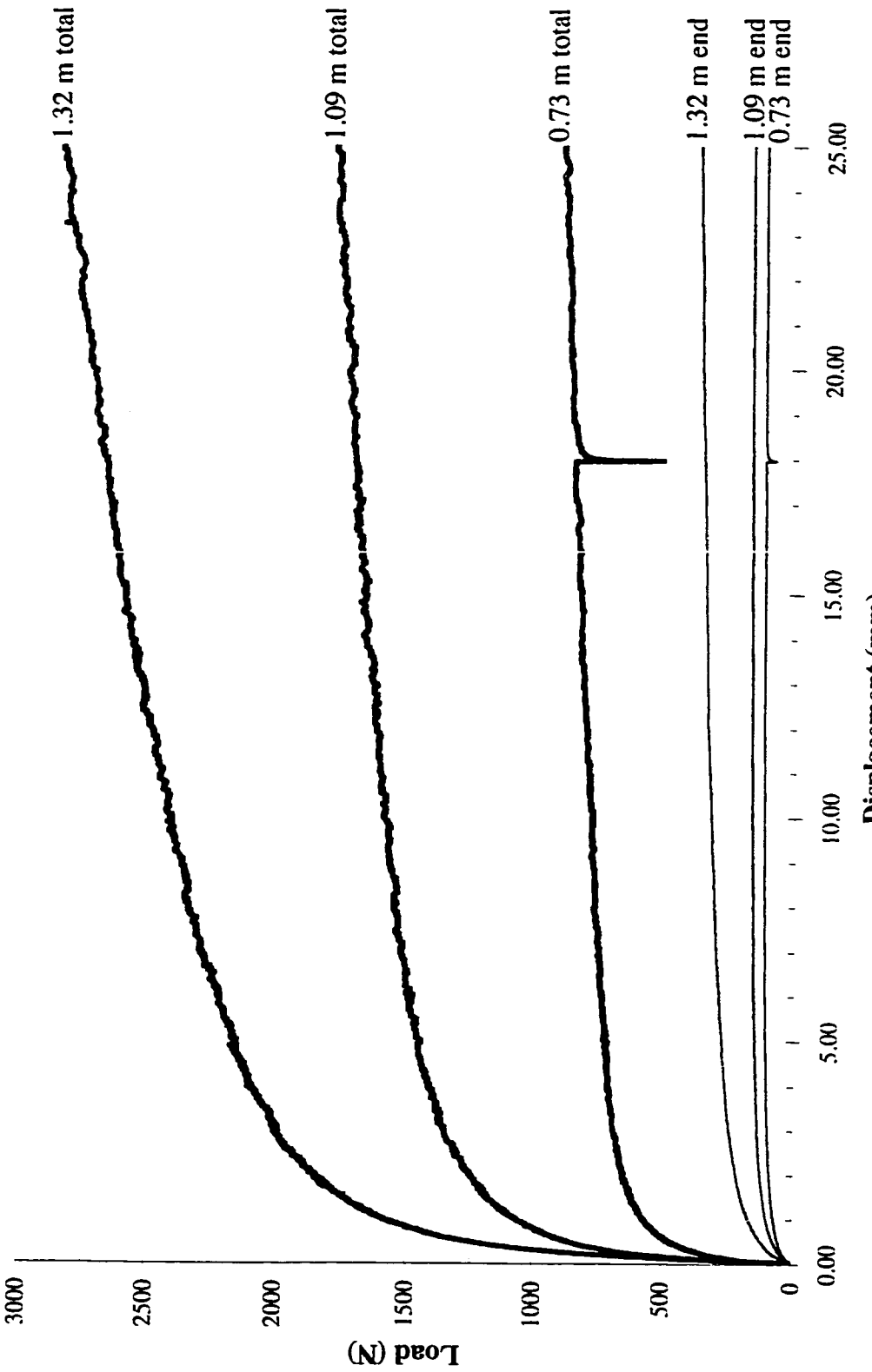

Figure 4.9 - 1° Tapered Piles with No Additional Pressure

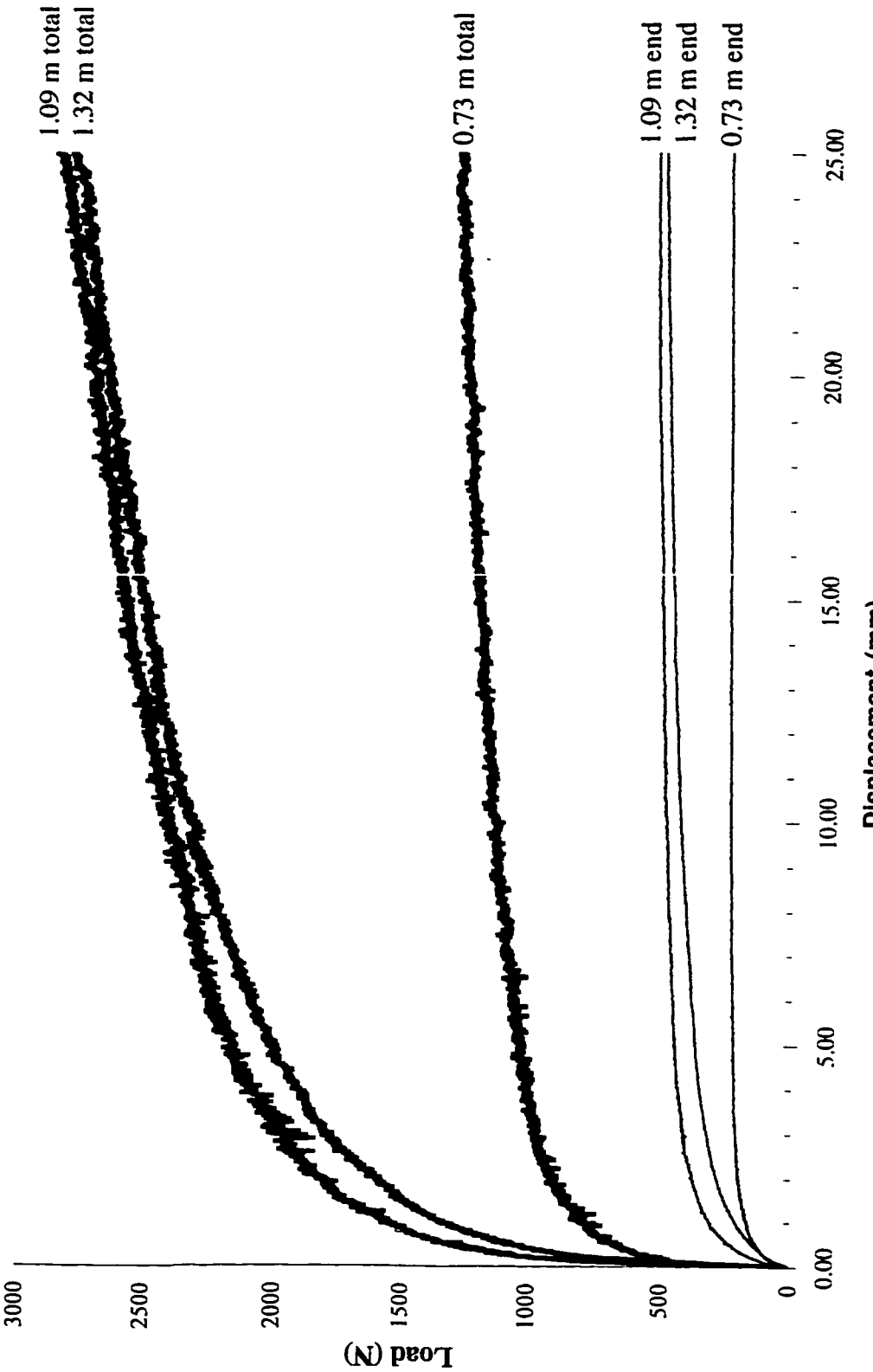

Figure 4.10 - 2° Tapered Piles with No Additional Pressure

Table 4.6: Bearing Capacity of 1° Tapered Piles - No Additional Pressure

Method	Bearing Capacity (N)		
	1.32 m	**1.09 m**	**0.73 m**
10 %	2,161	1,456	723
Single Tangent	2,220	1,497	712
Double Tangent	2,243	1,507	718
Brinch Hansen 80 %	2,695	1,725	857
Chin	3,194	1,941	987
Mazurkeiwicz	2,272	1,487	732
Mean	2,464	1,602	788
Displacement (mm)	11.4	10.6	10.5
End Bearing	323	163	114
Percentage of Total	13.1 %	10.2	14.5
Modified Mean	2,357	1,554	757
Mod. Displ. (mm)	8.9	8.2	7.6
Mod. End Bearing	306	156	111
Mod. %age of Total	13.0 %	10.0 %	14.7 %

changing the percentage of the pile that was tapered. The 0.5° tapered piles were just the opposite, the increase in pile length resulted in the addition of tapered sections resulting in a fully tapered section regardless of the length. Thus, the fully tapered section caused the maximum diameter of the pile to increase with increased depth of driving.

This was evident when comparing the percentage of the applied load that was carried through end bearing, as seen in Table 4.7. The 0.5° tapered piles showed a sizable

Table 4.7: Bearing Capacity of 2° Tapered Piles - No Pressure

Method	Bearing Capacity (N)		
	1.32 m	1.09 m	0.73 m
10 %	2,005	2,164	1,045
Single Tangent	2,107	2,191	1,077
Double Tangent	2,135	2,214	1,084
Brinch Hansen 80 %	2,633	2,680	1,240
Chin	3,143	3,163	1,400
Mazurkeiwicz	1,872	2,.378	1,063
Mean	2,316	2,465	1,152
Displacement (mm)	11.4	10.9	9.7
End Bearing	427	489	236
Percentage of Total	18.4 %	19.8 %	20.5 %
Modified Mean	2,220	2,365	1,116
Mod. Displ. (mm)	7.9	8.6	7.5
Mod. End Bearing	407	476	233
Mod. %age of Total	18.3 %	20.1 %	20.9 %

increase in the percentage of the load taken through end bearing as the length, and therefore diameter, of the pile was decreased. Whereas, the 1° and 2° tapered piles showed a relatively slow increase in the percentage of the load carried by the pile walls with increasing length. This trend appeared to indicate that the primary load bearing region of the partially tapered pile occurred on the tapered portion of the pile.

The end bearing of tapered piles appeared to be a relatively small portion of the overall

load, but as shown in Figure 4.11 there was an additional portion of the end bearing not recorded by the load cell at the pile toe. Along the tapered portion of the pile both end bearing and shear friction are developed. Due to the increasing diameter there was a portion of the soil load that was taken in end bearing. Due to the fact that the end bearing and shear friction developed along the tapered portion of the pile were both directly related to the stress in the adjacent soil, it may be stated that the end bearing and shear friction in this region were directly related. Hence, though the measured end bearing was a relatively small portion of the overall pile load, it was an indicator of the ultimate load.

The end bearing capacity of the 1° piles was recorded to be significantly lower than that of the 0.5° and 2° tapered piles. This is likely due to the failure of the connection between the load cell and the pile tip. This failure was not noticed until the pressurized tests and it was believed to have been confined to said tests.

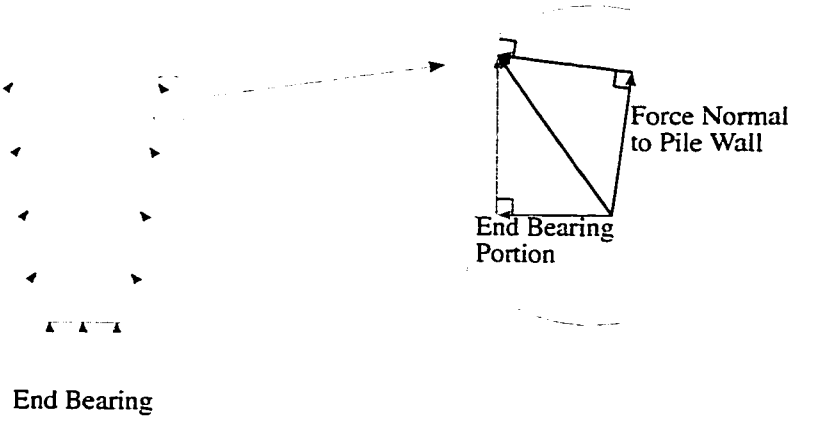

Figure 4.11 - Forces Acting on Tapered Piles

Averaging the settlements required for the mean ultimate bearing capacity for each driving length of tapered piles resulted in very consistent values ranging from 7.8 mm to 8.2 mm. There was some correlation between the ultimate bearing capacity and the settlement required to reach it, such that the greatest bearing capacity of each of the three tapered piles also had the greatest settlement. The test data further indicated that the greater the angle of taper the greater the bearing capacity of the pile under low confining pressure.

There were three major variables which affected the bearing capacity of the tapered piles used during the tests presented herein: the angle of taper, the volumetric displacement of the pile in the soil, and the percentage of the pile that is tapered. The angle of taper has been the most commonly researched aspect of tapered piles and it has been generally agreed that the greater the taper the greater the bearing capacity of the pile (Peck, 1958; Nordlund, 1963; Robinsky and Morrison, 1964; Rybnikov, 1990; Zil'berberg *et al.*, 1990; Monotube® Pile Corporation).

Testing by Jain *et al.* (1978), however came to the conclusions that the increase in taper had the effect of decreasing the bearing capacity of the piles. As previously mentioned, the tests were conducted by driving differently tapered wooden model piles into a loose sand. The taper was formed by maintaining a constant square cross section of 20x20 cm at the top of the pile and tapering down to 8x8 cm to 16x16 cm size. This increase in taper results in a decrease in soil displaced by the installation of the pile. Being a loose soil, the volumetric displacement becomes critical to the densification of the soil. Hence, the

benefits provided by the increase in taper is more than offset by the decrease in the volumetric displacement. The Russian text *Recommendations of Use of Pyramidal-Pile Foundations* noted that the increase in bearing capacity of pyramidal piles over straight piles may be 50% to 100% at equal volumetric displacements. Kodikara and Moore (1993) also made note of the increase in bearing capacity of tapered piles when compared to straight piles of similar volumetric displacement. While this does not directly relate to the differentiation between piles of various tapers it does indicate the known importance of volumetric displacement when dealing with tapered piles.

Partially tapered piles have been discussed by Lindqvist and Petaja (1981) and by the Monotube® pile corporation. Lindqvist and Petaja (1981) note that partially tapered piles are used to extend the pile such that the tapered portion of the pile is driven into sand beneath a clay layer. Monotube® manufactures and sells tapered piles which are extended deeper into the soil by the addition of straight sections. However, neither of these sources contained any records of testing which compared partially tapered piles to fully tapered piles.

Under the low stress conditions, simulated by these series of tests, the greater taper angle and volumetric displacement appeared to be more influential upon the ultimate bearing capacity than the percentage of the pile that was tapered. The 2° tapered piles generally had greater bearing capacity than the 1° piles which in turn was greater than the 0.5° piles. The bearing capacity of the 0.5° piles was further impacted from the reduction of the

maximum diameter, particularly at the shortest length.

4.2.2 Surcharge Pressure

The data from tests with a surcharge pressure of 50 kPa applied to the soil are presented in Figures 4.12 though 4.14 and summarized in Tables 4.8 through 4.10. The data showed signs of being somewhat unreliable in nature. It was likely that the bearing capacity of the piles was affected by arching effects within the tank. These effects were most apparent on the 0.5° piles, but were also evident on the 1° and 2° piles. The 0.5° piles showed a

Table 4.8: Bearing Capacity of 0.5° Tapered Piles - Surcharge Pressure

Method	Bearing Capacity (N)		
	1.32 m	1.09 m	0.73 m
10 %	3,054	2,880	2,669
Single Tangent	3,201	3,056	3,122
Double Tangent	3,293	3,091	3,177
Brinch Hansen 80 %	4,542	3,740	4,142
Chin	6,021	4,635	5,491
Mazurkeiwicz	3,176	3,060	2,884
Mean	3,881	3,410	3,580
Displacement (mm)	12.4	10.8	10.8
End Bearing	243	392	539
Percentage of Total	6.3 %	11.5 %	15.1 %
Modified Mean	3,553	3,237	3,331
Mod. Displ. (mm)	9.0	7.8	7.4
Mod. End Bearing	227	369	501
Mod. %age of Total	6.4 %	11.4 %	15.0 %

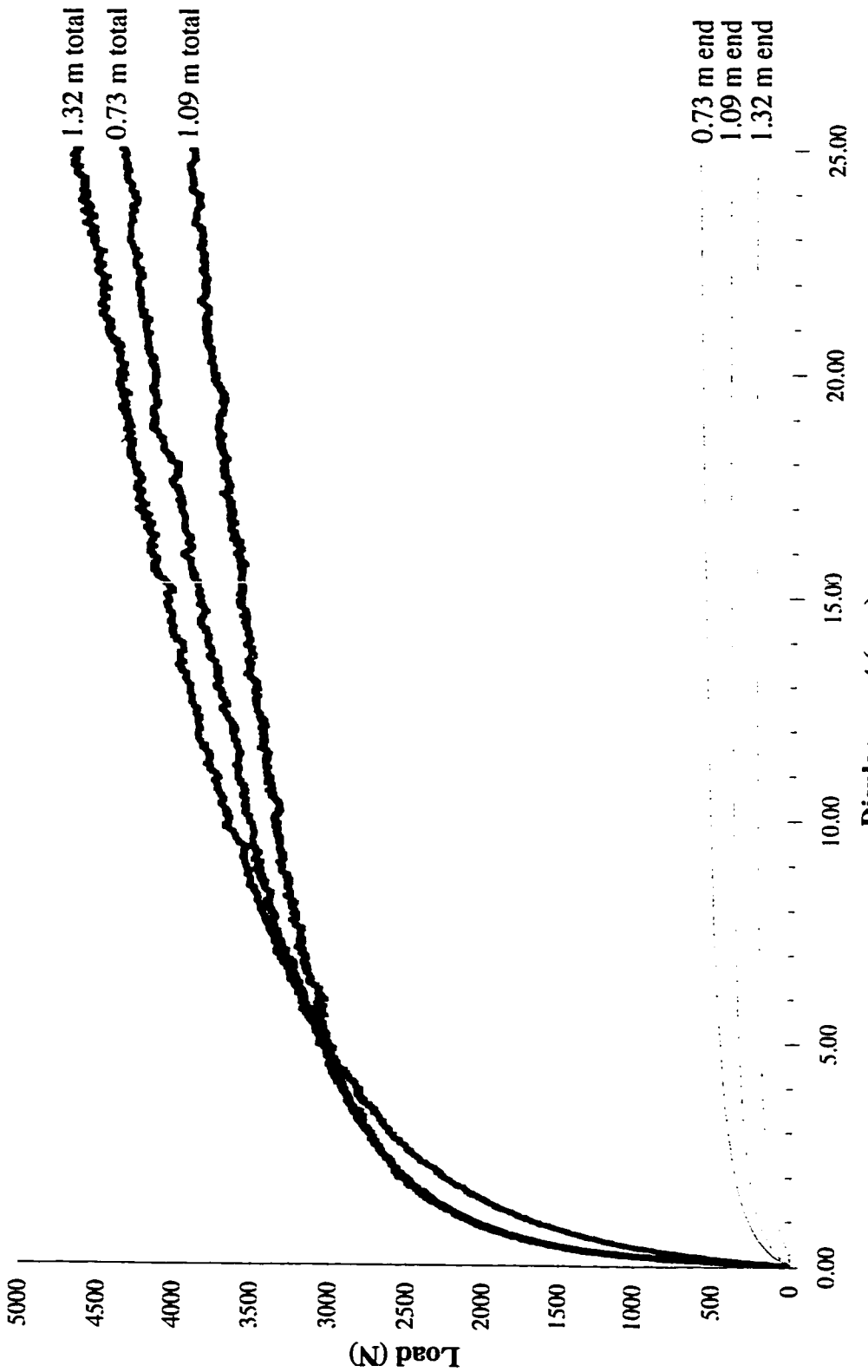

Figure 4.12 - 0.5° Tapered Pile with Surcharge Pressure

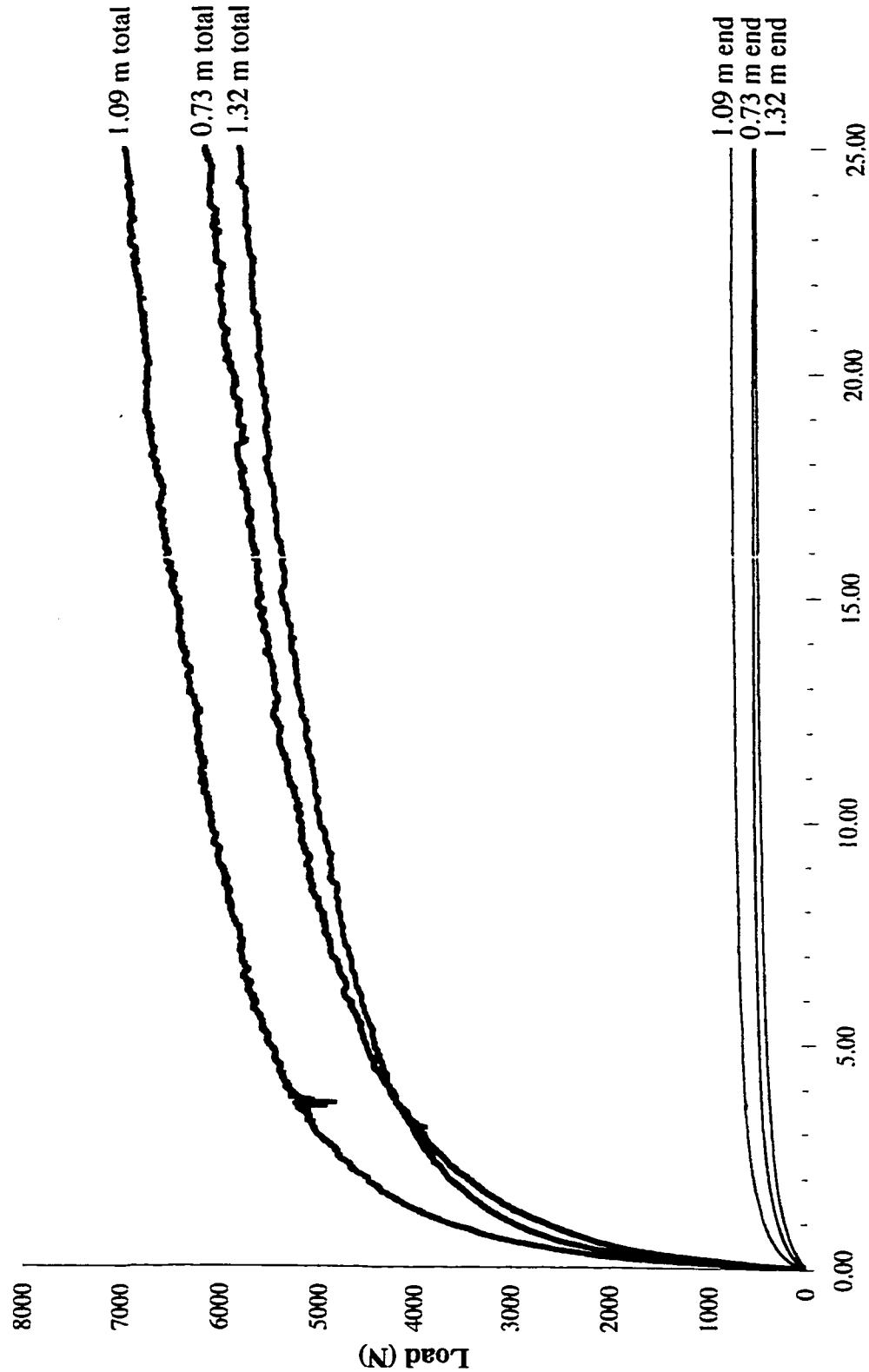

Figure 4.13 - 1° Tapered Piles with Surcharge Pressure

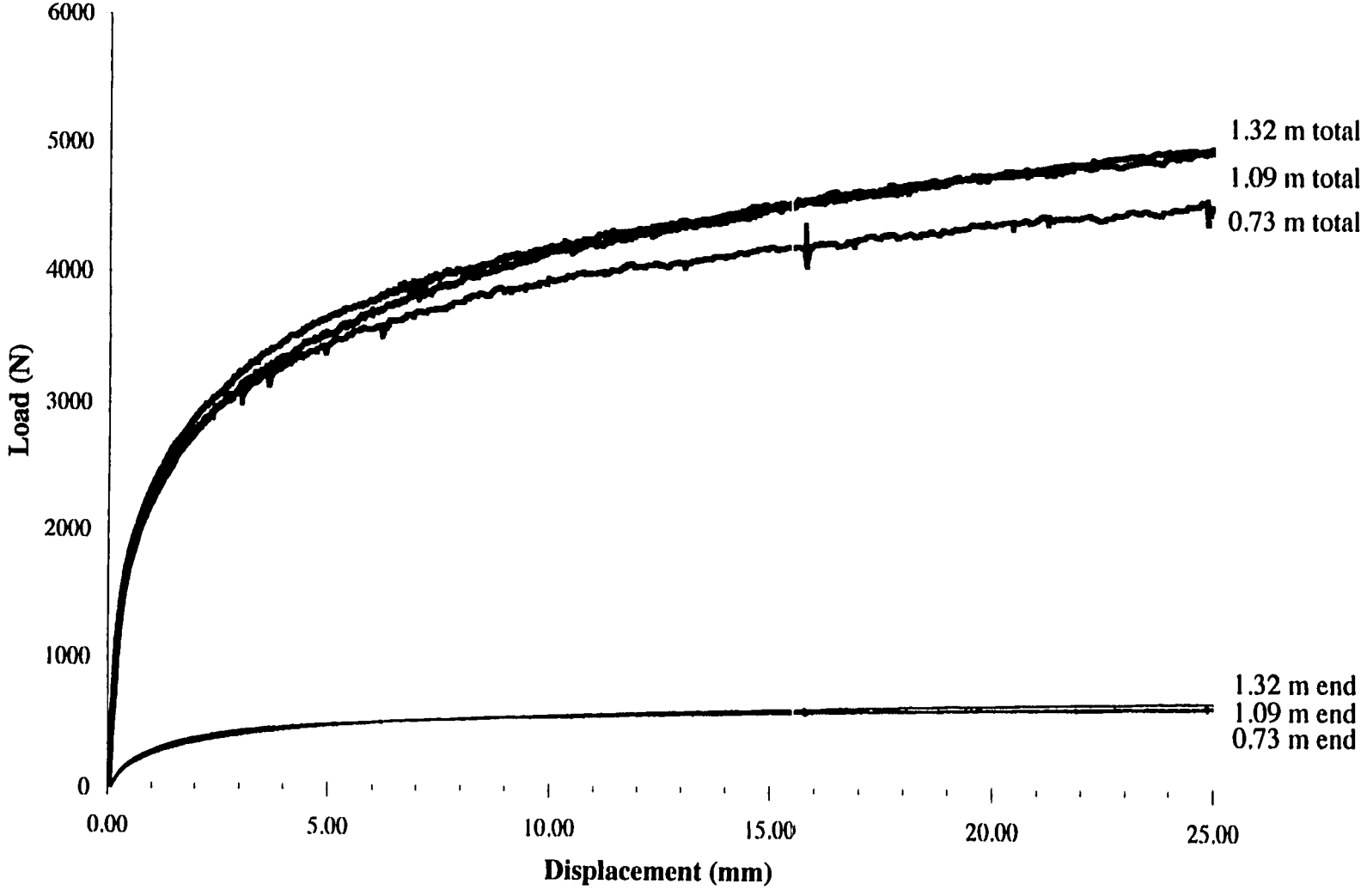

Figure 4.14 - 2° Tapered Piles with Surcharge Pressure

Table 4.9: Bearing Capacity of 1° Tapered Piles - Surcharge Pressure

Method	Bearing Capacity (N)		
	1.32 m	**1.09 m**	**0.73 m**
10 %	4,436	5,544	4,540
Single Tangent	4,656	5,764	4,791
Double Tangent	4,709	5,820	4,866
Brinch Hansen 80 %	5,623	6,742	5,962
Chin	6,629	7,804	7,061
Mazurkeiwicz	4,590	5,715	4,800
Mean	5,107	6,232	5,337
Displacement (mm)	11.2	11.1	10.9
End Bearing	521	782	580
Percentage of Total	10.2 %	12.6 %	10.8 %
Modified Mean	4,895	6,010	5,105
Mod. Displ. (mm)	8.6	8.9	8.4
Mod. End Bearing	488	752	558
Mod. %age of Total	10.0 %	12.5 %	10.9 %

constant decrease in end bearing as the driving depth increased. Arching within the tank inhibited the transfer of stresses from the higher layers of soil to the lower layers of soil. The arching effect manifested itself differently for fully tapered and partially tapered piles. The first of which was apparent in the 0.5° piles, where the load taken by the tip decreases with an increase in driving depth. This effect appeared in a more subtle manner with the 1° and 2° piles. These piles showed a peak in the bearing capacity for the 1.09 m long piles. This peak, or 'sweet spot', occurred due to a balance of the positive and negative variables which affected the bearing capacity of the piles. There was obviously a benefit

Table 4.10: Bearing Capacity of 2° Tapered Piles - Surcharge Pressure

Method	Bearing Capacity (N)		
	1.32 m	**1.09 m**	**0.73 m**
10 %	3,526	3,667	3,467
Single Tangent	3,740	3,948	3,651
Double Tangent	3,795	3,994	3,692
Brinch Hansen 80 %	4,764	4,739	4,358
Chin	5,762	5,596	5,025
Mazurkeiwicz	3,811	3,928	3,532
Mean	4,233	4,312	3,954
Displacement (mm)	10.9	11.3	10.0
End Bearing	583	572	570
Percentage of Total	13.8 %	13.3 %	14.4 %
Modified Mean	4,028	4,152	3,808
Mod. Displ. (mm)	8.7	9.5	8.1
Mod. End Bearing	556	557	548
Mod. %age of Total	13.8 %	13.4 %	14.4 %

to the extra driving depth versus the reduction in confining pressure. Up to a certain depth of driving, the depth of the 'sweet spot' appeared to decrease with the decrease in taper. This decrease in depth could have resulted from the decrease in angle of taper, decrease in volumetric displacement, or a combination of the two.

The settlement of the pile increased with an increase of the ultimate bearing capacity. This increase was similar to the no additional pressure condition where the greatest settlement

occurred at the point of greatest bearing capacity for all three types of tapered piles.

4.2.3 Surcharge and Confining Pressure

Figures 4.15 through 4.17 and Tables 4.11 to 4.13 summarize the data from the tests in which a surcharge pressure of 50 kPa and a confining pressure 25 kPa was applied to the soil. Similar to the unpressurized tank condition, the slow increase in percentage of load carried by the pile toe decreased with an increase in driving depth. Furthermore, the percentage of the load supported via end bearing was less in this pressurized state

Table 4.11: Bearing Capacity of 0.5° Piles - Surcharge and Confining Pressure

Method	Bearing Capacity (N)		
	1.32 m	**1.09 m**	**0.73 m**
10 %	11,554	5,729	4,183
Single Tangent	12,109	6,051	5,255
Double Tangent	12,271	6,240	5,340
Brinch Hansen 80 %	13,477	8,379	6,720
Chin	15,905	11,410	8,610
Mazurkeiwicz	11,941	6,233	8,289
Mean	12,876	7,340	6,400
Displacement (mm)	9.9	11.5	15.1
End Bearing	1,835	1,002	1,003
Percentage of Total	14.3 %	13.6 %	15.7 %
Modified Mean	12,450	6,726	6,401
Mod. Displ. (mm)	8.1	7.7	15.1
Mod. End Bearing	1,763	929	1,004
Mod. %age of Total	14.2	13.8	15.7

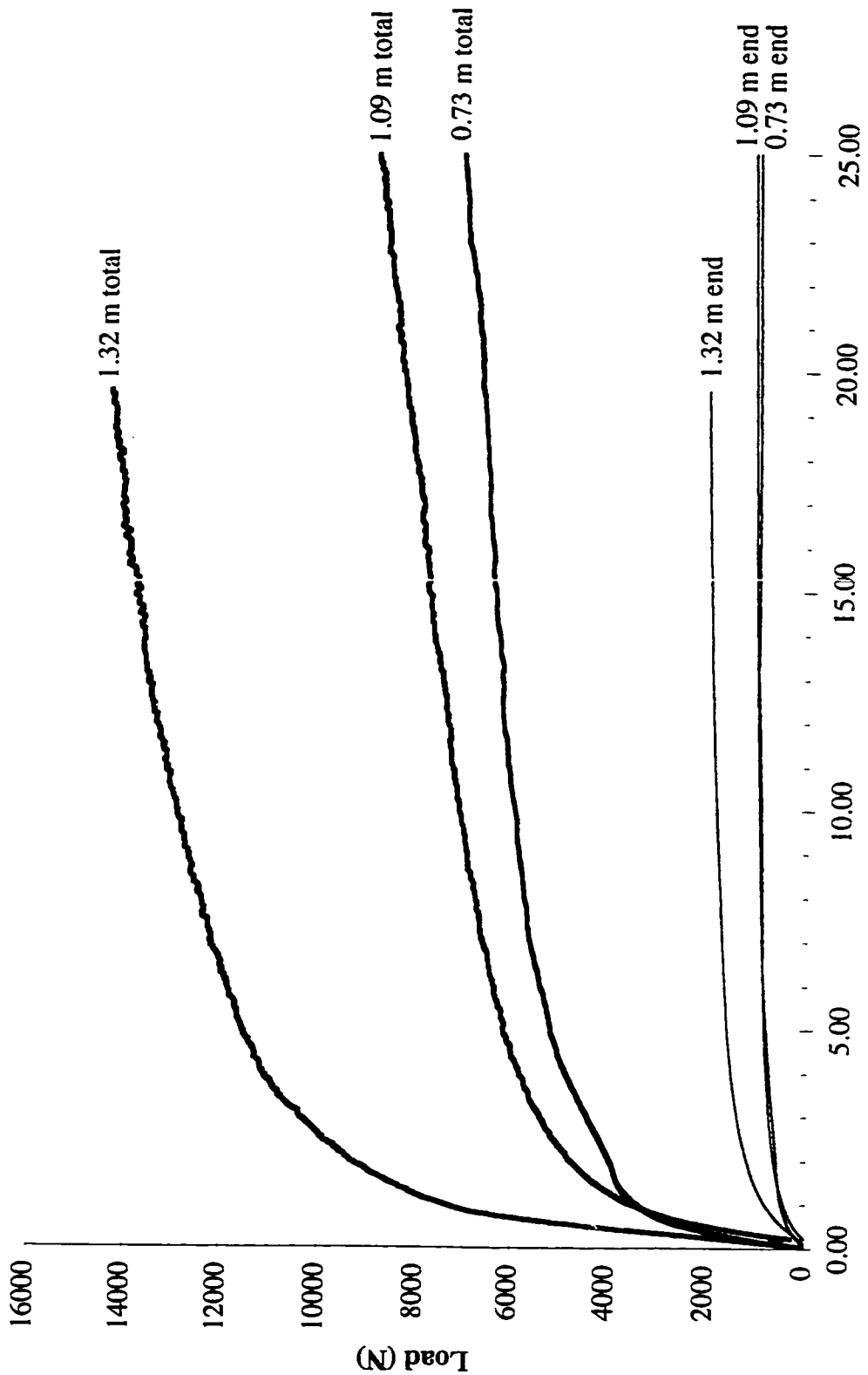

Figure 4.15 - 0.5° Tapered Piles with Surcharge and Confining Pressure

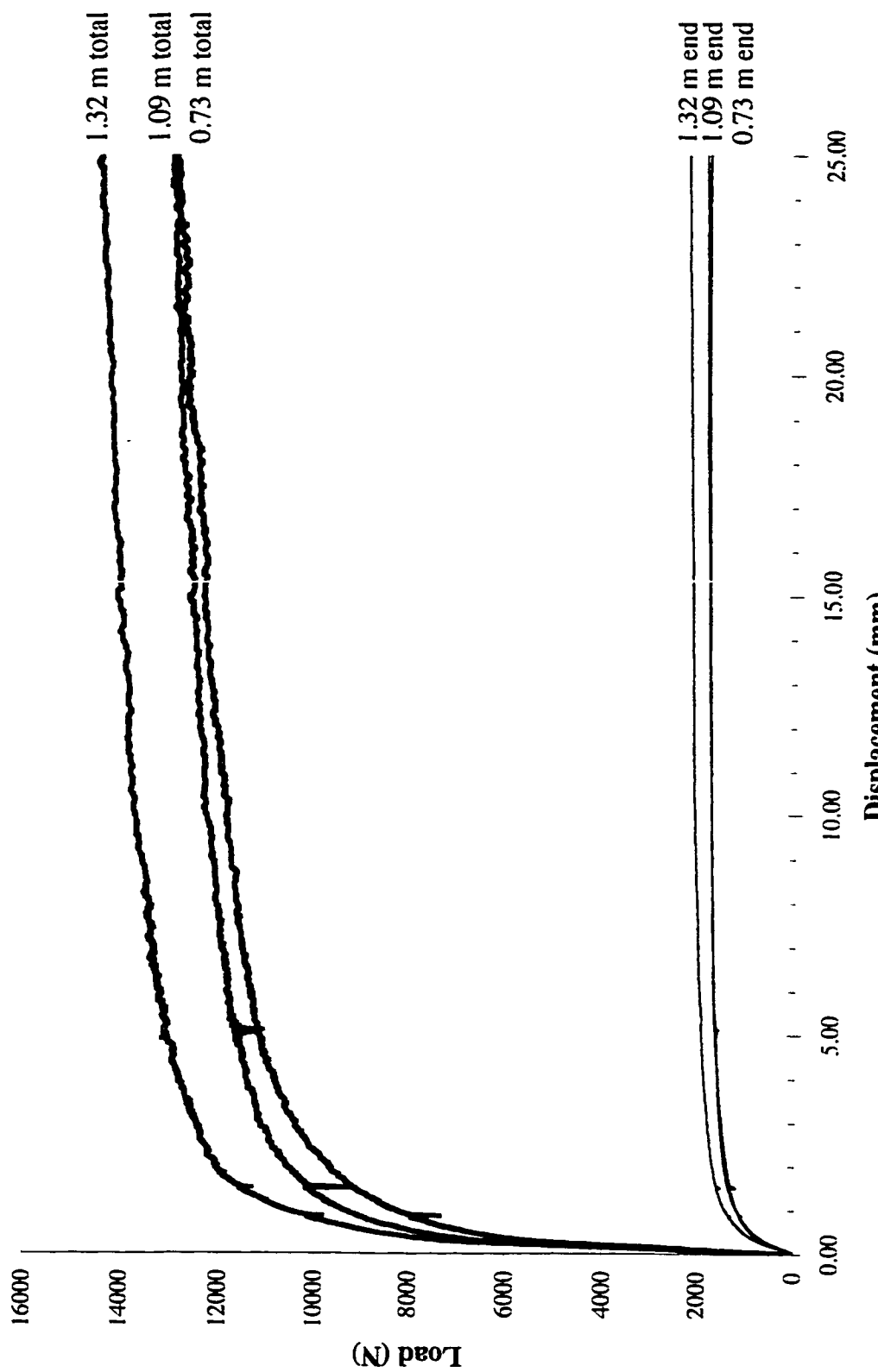

Figure 4.16 - 1° Tapered Piles with Surcharge and Confining Pressure

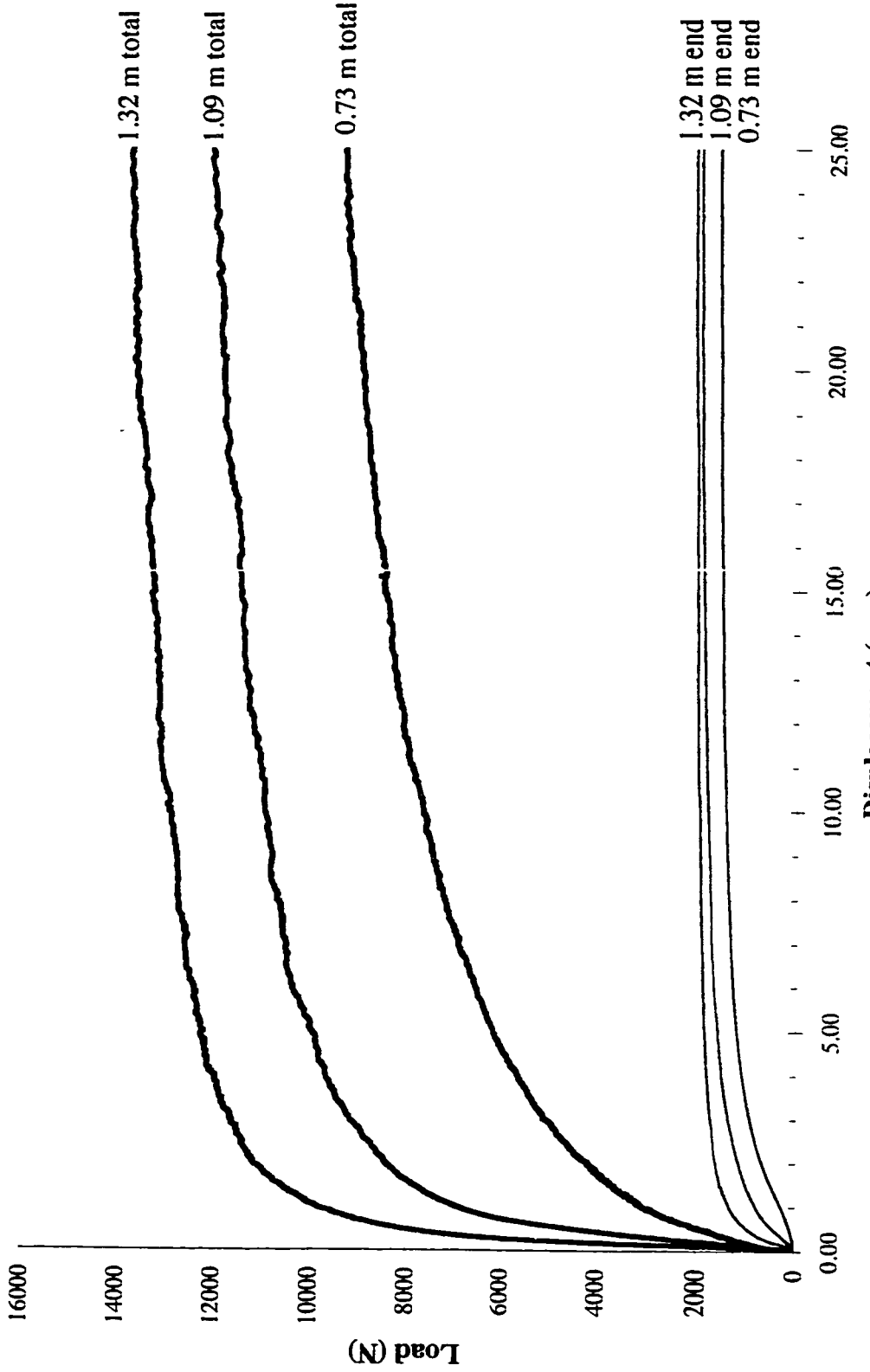

Figure 4.17 - 2° Tapered Piles with Surcharge and Confining Pressure

Table 4.12: Bearing Capacity of 1° Tapered Piles - Surcharge and Confining Pressure

Method	Bearing Capacity (N)		
	1.32 m	**1.09 m**	**0.73 m**
10 %	13,196	11,406	11,185
Single Tangent	13,348	11,923	11,300
Double Tangent	13,384	11,958	11,358
Brinch Hansen 80 %	14,515	13,002	12,269
Chin	14,984	13,525	13,624
Mazurkeiwicz	12,878	11,633	11,231
Mean	13,718	12,241	11,828
Displacement (mm)	10.1	9.9	9.4
End Bearing	2,083	1,733	1,721
Percentage of Total	15.2 %	14.2 %	14.6 %
Modified Mean	13,611	12,129	11,539
Mod. Displ. (mm)	9.2	9.0	7.1
Mod. End Bearing	2,066	1,709	1,691
Mod. %age of Total	15.2 %	14.1 %	14.7 %

compared to the unpressurized condition. This was particularly evident with the 0.73 m long pile with 0.5° taper for which the percentage of the load supported via end bearing, under pressurized conditions, was approximately one third that of the unpressurized condition. The percentage of the load supported by end bearing remained fairly consistent and therefore, it was concluded that under greater confining pressures the straight portions of the pile continued to provide only a small addition to the total bearing capacity of the partially tapered piles.

Table 4.13: Bearing Capacity of 2° Tapered Piles - Surcharge and Confining Pressure

Method	Bearing Capacity (N)		
	1.32 m	**1.09 m**	**0.73 m**
10 %	12,244	10,001	6,188
Single Tangent	12,488	10,463	7,100
Double Tangent	12,533	10,545	7,283
Brinch Hansen 80 %	13,772	11,803	9,481
Chin	14,474	13,009	11,031
Mazurkeiwicz	12,079	10,159	7,258
Mean	12,932	10,997	8,057
Displacement (mm)	10.1	10.7	11.7
End Bearing	1,995	1,847	1,506
Percentage of Total	15.4 %	16.8 %	18.7 %
Modified Mean	12,759	10,743	7,781
Mod. Displ. (mm)	8.7	8.3	10.6
Mod. End Bearing	1,968	1,774	1,472
Mod. %age of Total	15.4 %	16.5 %	18.9 %

Though the 1.09 m and the 0.73 m 1° pile tests showed the total bearing capacity to be very large compared to the 0.5° and 2° piles, the data appeared to indicate that the 1° piles provided the best equilibrium between the percentage of taper, volumetric displacement, and angle of taper. This was likely due to the fact that the increased confining pressure, in comparison to the unpressurized state, reduces the effects of volumetric displacement within the soil. The volumetric displacement of the pile became less important since the soil was already in a state of greater relative density. The 0.5° pile likely continued to

suffer from an insufficient volumetric displacement required to effectively densify the surrounding soil. While still within 10% of the bearing capacity of the 1° piles at the 1.32 m length, the lower capacity of the 2° piles demonstrated that the greater length of taper was more significant to load development than the greater angle of taper and volumetric displacement.

Even at elevated stress conditions, the end bearing failed to reach an ultimate stress condition. The rate of increase in end bearing appeared to be linear in most situations with the rate of increase being greatest for the 0.5° taper piles. This was likely a result of the lower taper angle.

Robinsky and Morrison (1964) concluded that, as the pile tip passed through the soil, vertical expansion within the soil resulted from the downward movement of the soil beneath the pile tip. The downward movement of the soil lowered the vertical stresses on the soil, thus creating a layer of loose sand immediately adjacent to the pile shaft surrounded by a dense ring of soil. As the tapered pile was driven further into the soil, the loose sand was recompacted into a densified state. Thus, it is likely that greater taper angles will reduce this vertical expansion of the soil. As illustrated in Figure 4.18 the soil would undergo less vertical expansion due to the greater downward movement of the soil adjacent to a pile with a greater anger of taper. Thus, the greater the angle the more quickly the soil beneath the tapered portion is recompressed. This will lead to a greater vertical stress in the expansion region and thus a reduction in the volumetric expansion

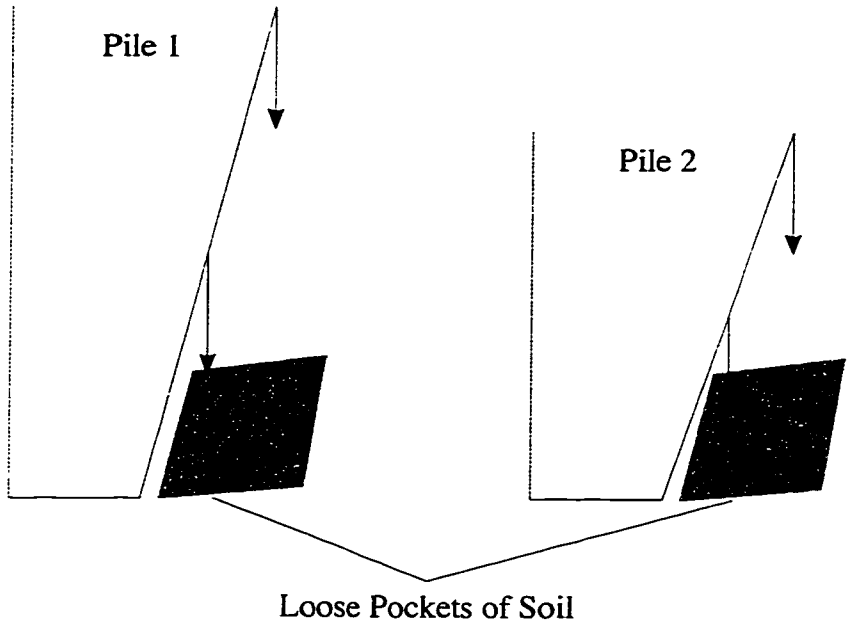

Figure 4.18 - Recompression of Loose Sands by Tapered Piles

within the soil. The reduction of volumetric expansion will lead to greater vertical stresses beneath the expansion zone. The increased stresses, in the region beneath the expansion zone, allows a smaller reduction of stress beneath the pile tip. Thus greater stresses would be possible along the pile toe resulting in a greater end bearing capacity.

The stress bubble observed by Robinsky and Morrison (1964) supports the recorded data. The size of the stress bubble was directly related to the ultimate bearing capacity of the pile. According to Robinsky and Morrison, the size of the stress bubble increased with sand density, pile taper, and volumetric displacement. This bubble theory agreed well with the test results, but did not include any recommendations on the effects of varying the percentage of the pile that is tapered. Results indicated that the greater the length of taper the greater the bearing capacity and therefore size of the bubble. A comparison of the

results, of the various tapered pile tests, illustrated that the soil stress was the most significant factor affecting the pile bearing capacity, and therefore the size of the stress bulb.

The acquired test data indicated that average settlements ranging from 7.9 to 9.2 mm were required to reach the ultimate bearing capacity. This was an increase in comparison to the average settlements under unpressurized conditions (7.8 to 8.2 mm). However, there was little or no difference between the settlements of the fully pressurized and the surcharge only conditions.

4.2.4 Pull Out Testing

A limited number of tension tests on 1.32 m long piles with 1° tapers were conducted to determine the effectiveness of tapered piles under tensile loading. The 1° piles were chosen for this series of tests due to their similarity to Monotube® piles, for which some test data was available. Figures 4.19 through 4.21 illustrate the differences in shear resistance developed between the regular and the pull out under the three different tank pressure conditions. All three tension tests reached a maximum frictional resistance, in less than 5 mm of displacement, subsequently followed by a constant reduction. Therefore, there is a reduction in the shear resistance along the surface of the pile.

The maximum compressive and tensile loads (see Tables 4.6, 4.9, and 4.12), are presented in Table 4.14. The ratio of tensile to compressive shear resistance under the surcharge

Figure 4.19 - Shear Friction for 1° Tapered Piles with No Additional Pressure

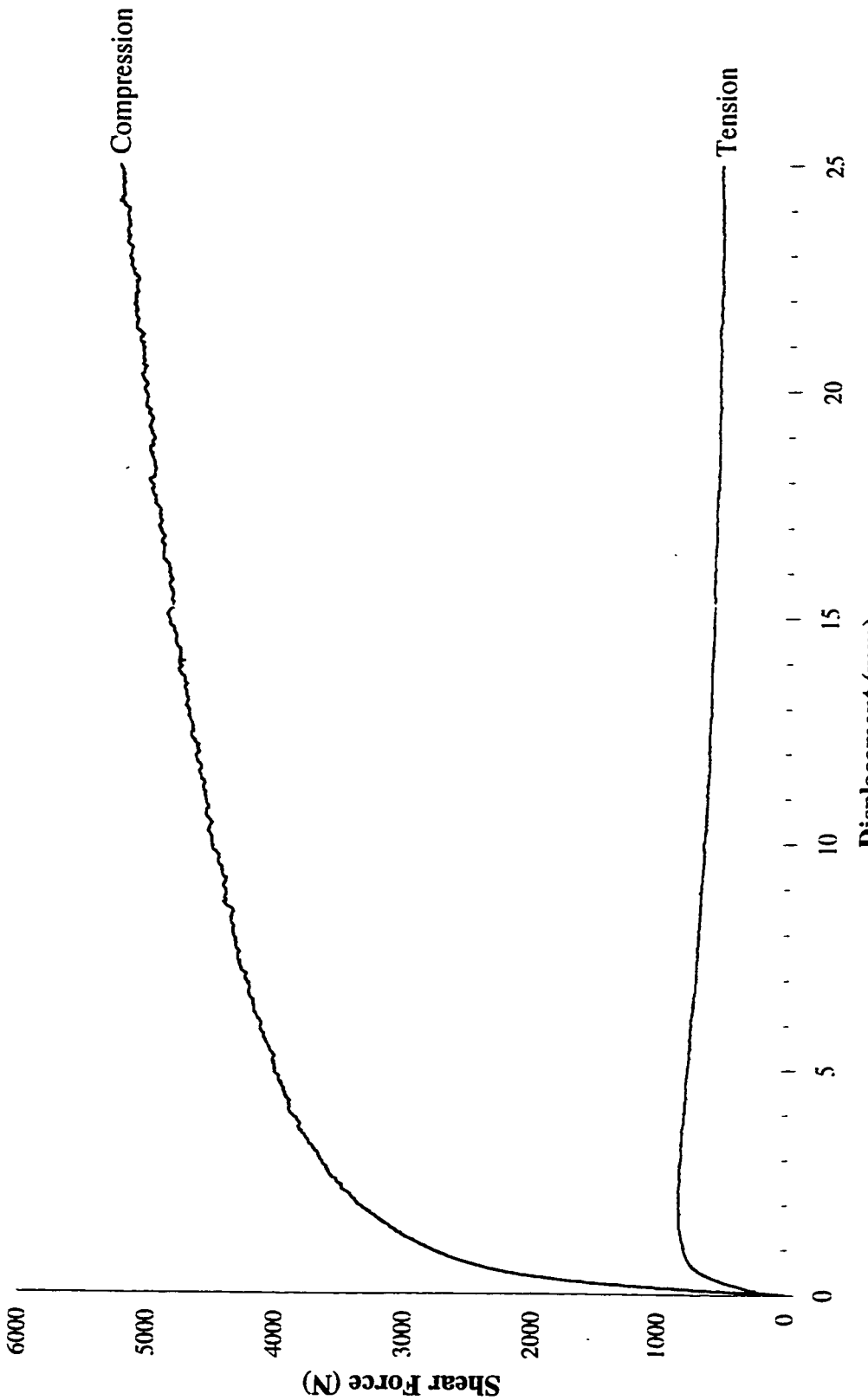

Figure 4.20 - Shear Friction for 1° Tapered Piles with Surcharge Pressure

Figure 4.21 - Shear Friction for 1° Tapered Piles with Surcharge and Confining Pressure

Table 4.14: Shear Friction of 1° Piles

Additional Tank Pressure	Shear Friction (N)		
	Compression	Tension	Tens:Comp
None	2,051	548	27 %
Top	4,407	845	19 %
Top & Side	11,545	3,290	29 %

tank condition was discontinuous with the other two tests. This agreed with earlier conclusions that the surcharge pressure alone altered the development of stresses within the soil. The completely unpressurized soil condition may have had an overestimated value of shear in compression due to the previously discussed problem with the load cell. Increasing the compression test end bearing of the 1° tapered pile by 150 N brought the ratio of end bearing to total load into line with the 0.5° and the 2° tapered piles. This increase in end bearing reduced the ultimate shear resistance to approximately 1900 N. This reduction resulted in an increase of the tensile to compressive shear ratio to 29 %.

It may be noted that the ratio of tensile to compressive capacity was relatively small. One particularly significant difference was the loss of the end bearing component along the tapered surface. The loss of this portion of the load was a very significant portion of the difference between the two load cases. The other aspect was the decreased ability of the sand to provide similar resistance in compression as in tension. When a pile is pulled out of the sand there is a tensile force induced into the soil. The absence of any cohesion within the soil allows the grains to be pulled apart thus loosening the soil and reducing the

pressure applied to the pile walls.

4.3 Comparison of Straight and Tapered Piles

4.3.1 No Additional Pressure

Figures 4.22 through 4.24 compared all of the piles tested under unpressurized test tank conditions. Tables 4.15 through 4.17 compare the modified average pile capacities to each other at the various driving lengths.

Table 4.15: 0.73 m Long Piles - No Additional Pressure

	Straight	0.5°	1°	2°
Total (N)	1,009	968	757	1,116
Tip (N)	938	403	111	233
Tip (kPa)	463	855	235	494
Settlement (mm)	7.9	7.7	8.2	7.5
Volume (cm^3)	1,480	583	863	1,171
%age of Str. Vol.	100 %	39.4 %	58.3 %	79.1 %

Tables 4.15 to 4.17 illustrate that the tapered piles sometimes provided greater bearing capacity than straight piles, for an equivalent driving length and top diameter, under low soil pressure conditions. At the shorter lengths of 0.73 m and 1.09 m only the 2° piles provided greater bearing capacity than the straight piles. This was likely due to insufficient volumetric displacement on the part of the 0.5° and 1° piles at these depths. At a driving depth of 1.32 m, all of the tapered piles developed total bearing capacities that were equivalent to or greater than that of the straight pile. This was likely due to the increased

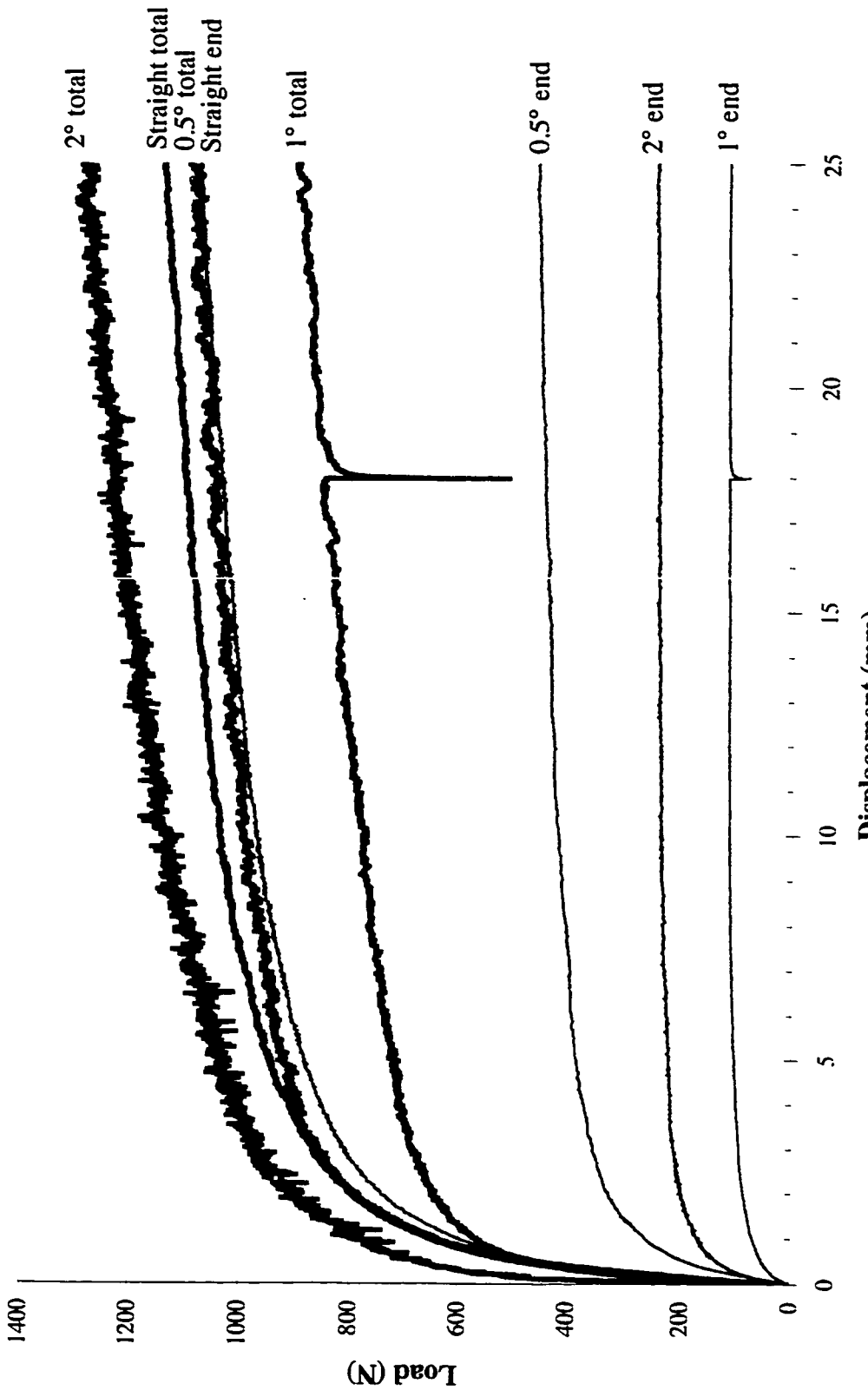

Figure 4.22 - 0.73 m Long Piles with No Additional Pressure

Figure 4.23 - 1.09 m Long Piles with No Additional Pressure

Figure 4.24 - 1.32 m Long Piles with No Additional Pressure

Table 4.16: 1.09 m Long Piles - No Additional Pressure

	Straight	0.5°	1°	2°
Total (N)	1,781	1,342	1,554	2,365
Tip (N)	1,620	339	156	476
Tip (kPa)	799	719	331	1,010
Settlement (mm)	8.6	7.8	8.2	8.6
Volume (cm^3)	2,209	1,070	1,593	1,901
%age of Str. Vol.	100 %	48.4 %	72.1 %	86.1 %

Table 4.17: 1.32 m Long Piles - No Additional Pressure

	Straight	0.5°	1°	2°
Total (N)	1,978	2,088	2,357	2,220
Tip (N)	1,564	509	306	407
Tip (kPa)	772	1,080	649	863
Settlement (mm)	8.2	7.9	8.9	7.9
Volume (cm^3)	2,675	1,459	2,059	2,367
%age of Str. Vol.	100 %	54.5 %	77.0 %	88.5 %

volumetric displacement of the tapered piles as a percentage of the straight piles and the increased pressure along the tapered surfaces due to the increased driving depth.

Figure 4.25 depicts the ultimate capacities of all the piles tested as well as a nearly linear interpolation between the data points. The plotted data indicated a trend of increasing bearing capacity with length and angle of taper. All of the tapered piles showed a rate of

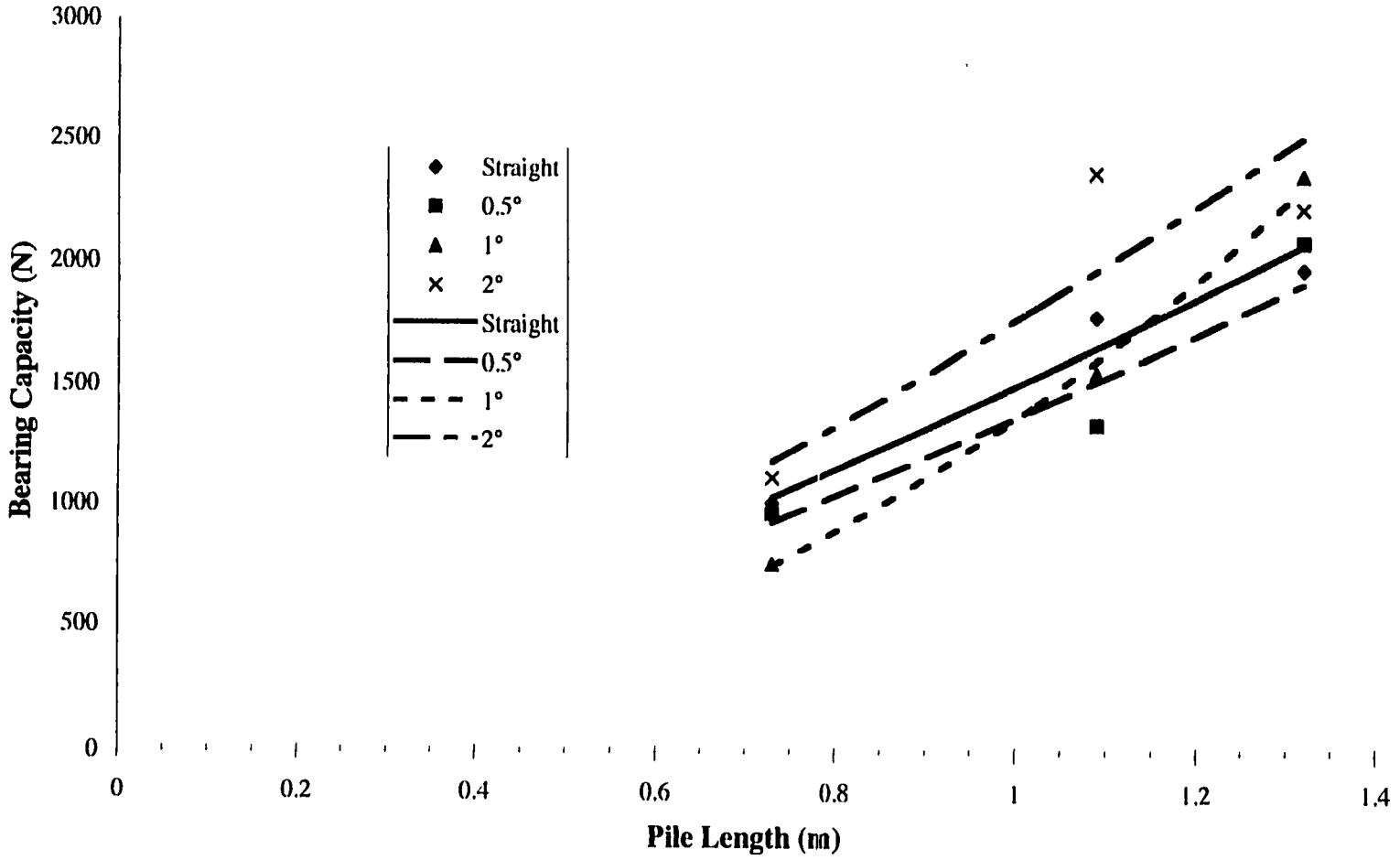

Figure 4.25 - Bearing Capacity of All Piles with No Additional Pressure

increase in bearing capacity which was greater than that of the straight piles. The relatively large increase in the bearing capacity of the 1° taper piles was possibly the result of a very low bearing capacity at the 0.73 m length.

As shown in Tables 4.15 through 4.17, the settlements required to reach the ultimate bearing capacity were relatively constant for piles of the same length. In terms of settlement there appeared to be little difference between the straight and the tapered piles. There also appeared to be a trend of increased settlement with increased depth of driving. While this increase was small, only 0.5 mm, it was noticeable.

While the load on the pile toe was significantly greater for straight piles than for tapered piles, it resulted from the former having a larger bearing area. In general, the tapered piles actually had a greater end bearing stress than the straight piles. Excluding the 1° piles from the data, due to the previously discussed problem with the load cell, the straight piles constantly had the lowest stress on the pile toe except for in one test.

4.3.2 Surcharge Pressure

Figures 4.26 through 4.28 illustrate the load-settlement curves for piles, of the same driving depth, when the sand in the test tank is under a 50 kPa surcharge pressure. The modified average of the bearing capacities, calculated in sections 4.1 and 4.2 are presented in Tables 4.18 through 4.20.

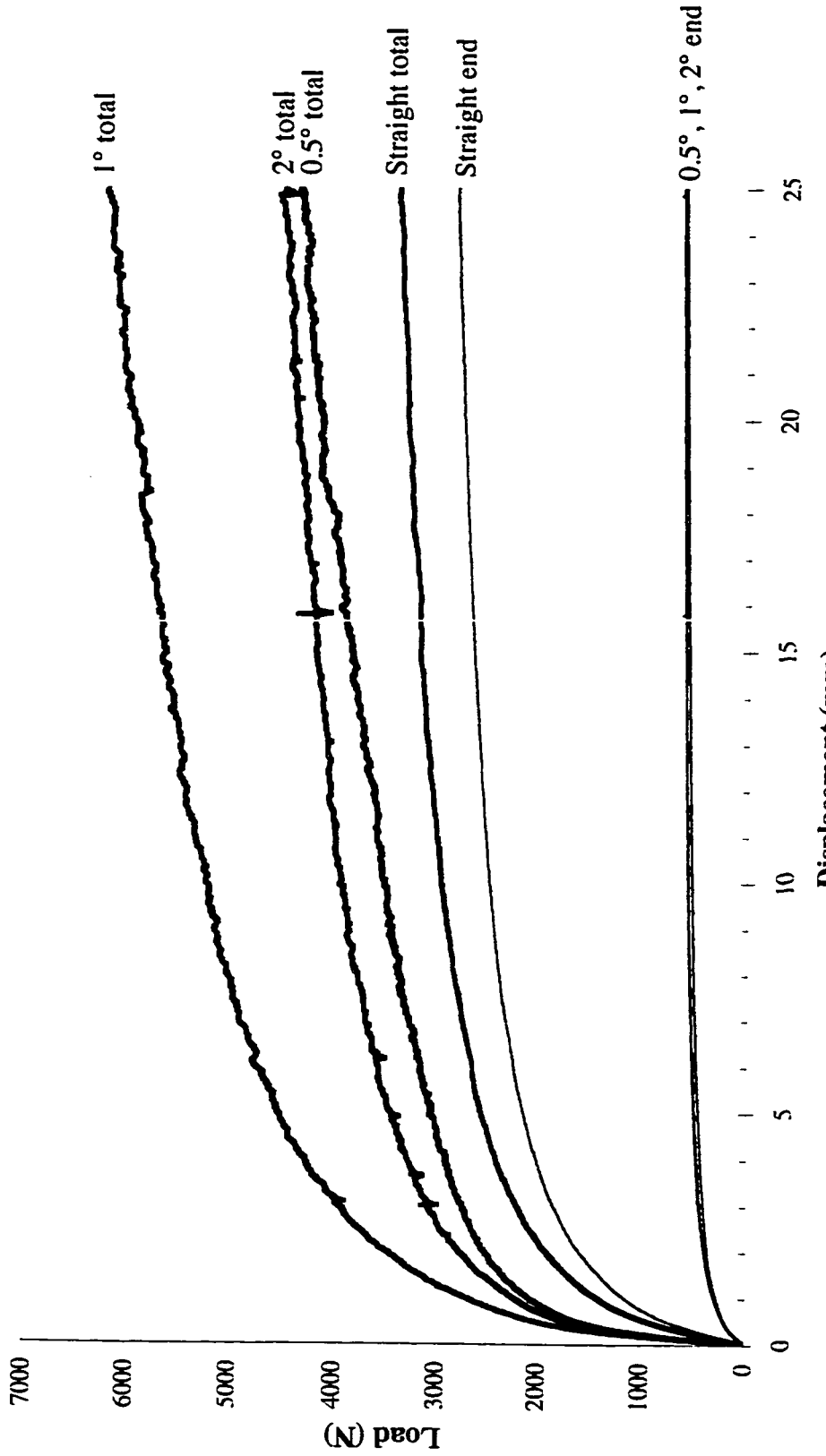

Figure 4.26 - 0.73 m Long Piles with Surcharge Pressure

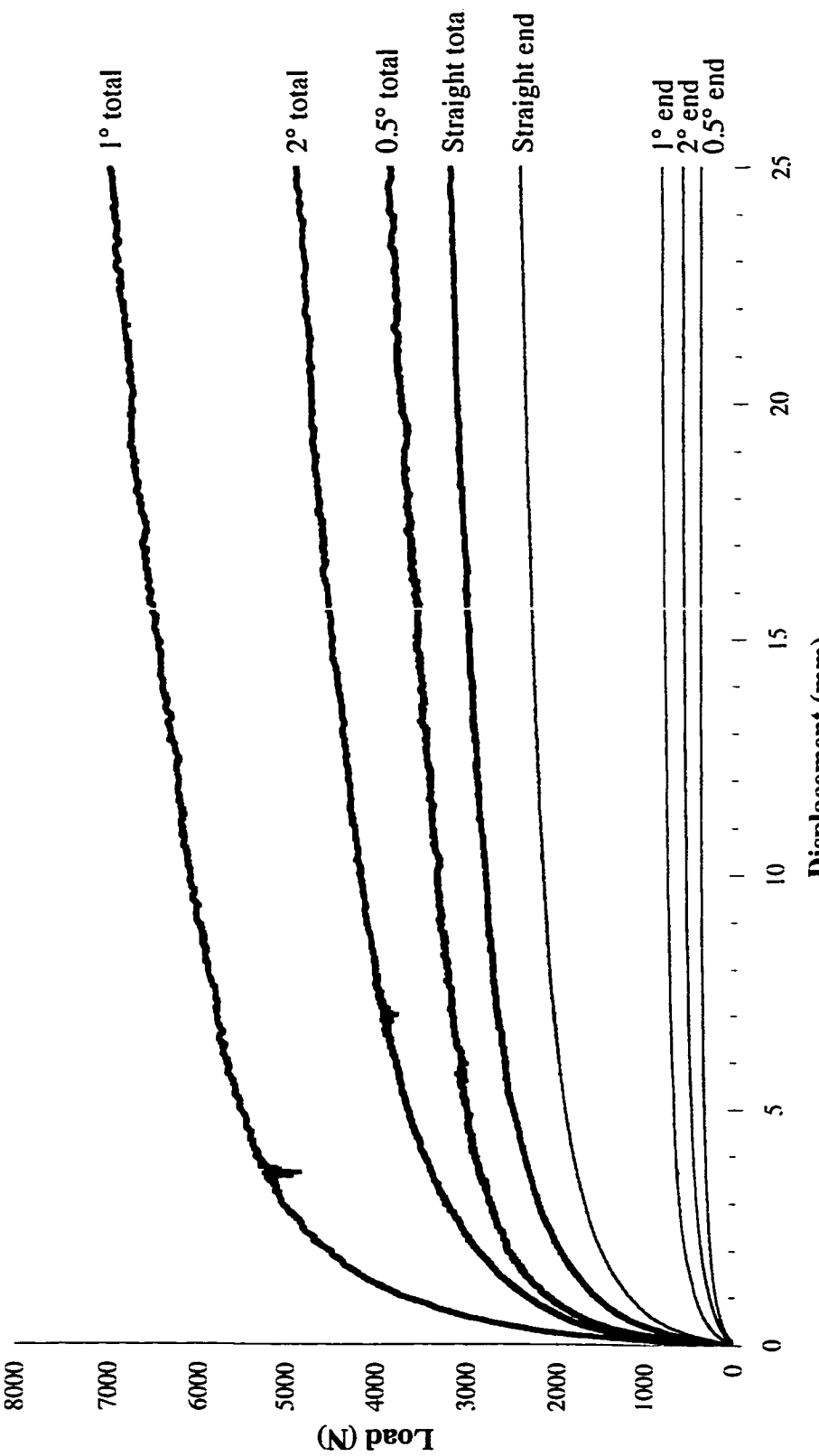

Figure 4.27 - 1.09 m Long Piles with Surcharge Pressure

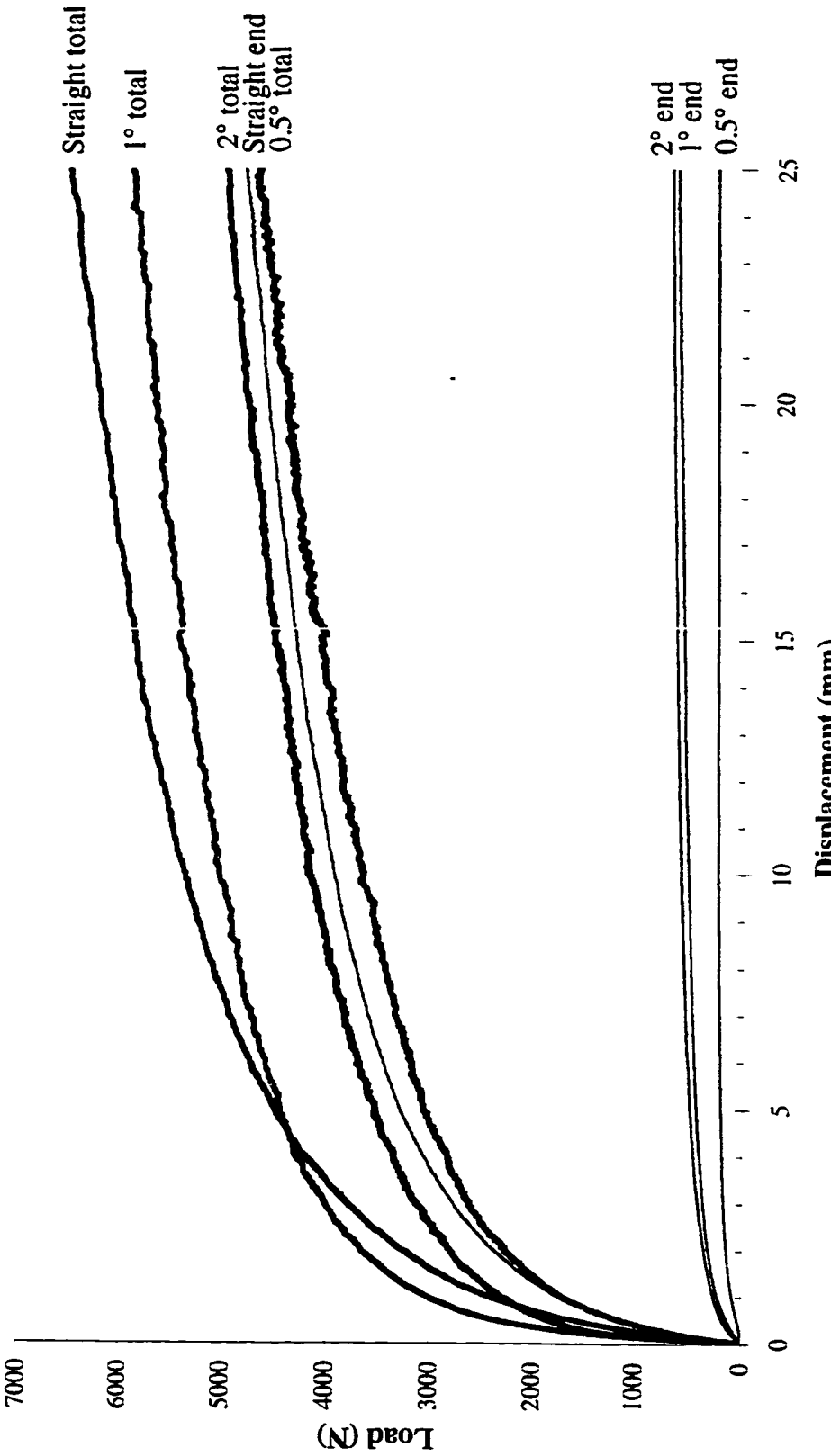

Figure 4.28 - 1.32 m Long Piles with Surcharge Pressure

Table 4.18: 0.73 m Long Piles - Surcharge Pressure

	Straight	0.5°	1°	2°
Total (N)	2,924	3,331	5,105	3,808
Toe (N)	2,452	501	558	584
Toe (kPa)	1,210	1,063	1,184	1,239
Settlement (mm)	9.1	7.4	8.4	8.1
Volume (cm^3)	1,480	583	863	1,171
%age of Str. Vol.	100 %	39.4 %	58.3 %	79.1 %

Table 4.19: 1.09 m Long Piles - Surcharge Pressure

	Straight	0.5°	1°	2°
Total (N)	2,769	3,237	6,010	4,152
Toe (N)	2,122	369	752	557
Toe (kPa)	1,047	783	1,595	1,183
Settlement (mm)	8.4	7.8	8.9	9.5
Volume (cm^3)	2,209	1,070	1,593	1,901
%age of Str. Vol.	100 %	48.4 %	72.1 %	86.1 %

The erratic nature of the results illustrated the low reliability of the data acquired when only a surcharge pressure was applied in a tank of such small dimensions. The bearing capacity of the straight piles appeared to be the least affected. The data obtained for the tapered piles was inconsistent, especially for the values of end bearing under the surcharge load condition.

Table 4.20: 1.32 m Long Piles - Surcharge Pressure

	Straight	0.5°	1°	2°
Total (N)	5,294	3,553	4,895	4,028
Toe (N)	3,886	227	488	556
Toe (kPa)	1,917	482	1,035	1,179
Settlement (mm)	9.5	9.0	8.6	8.7
Volume (cm^3)	2,675	1,459	2,059	2,367
%age of Str. Vol.	100 %	54.5 %	77.0 %	88.5 %

Figure 4.29 plots all of the ultimate capacities as previously determined in Sections 4.1 and 4.2. The straight piles showed an increase in total bearing capacity with driving depth, but the tapered piles showed nearly flat curves indicating the same total bearing capacity for all the piles in this series of tests. These flat curves along with the erratic nature of the tests was a further indication of the soil arching present in the soil that prevented stresses from being transferred to the deeper layers of sand. Furthermore, the development of arching was not consistent under these conditions, but varied to a large degree between the various tests.

Another noticeable effect of arching was the difference in end bearing stress between the straight and the tapered piles. Under unpressurized conditions, the stress under the toe of the tapered piles was generally equivalent to or greater than that of the straight piles. However, under surcharge conditions the straight piles regularly had an equivalent or greater bearing capacity than that of the tapered piles. With the increase in pile length the

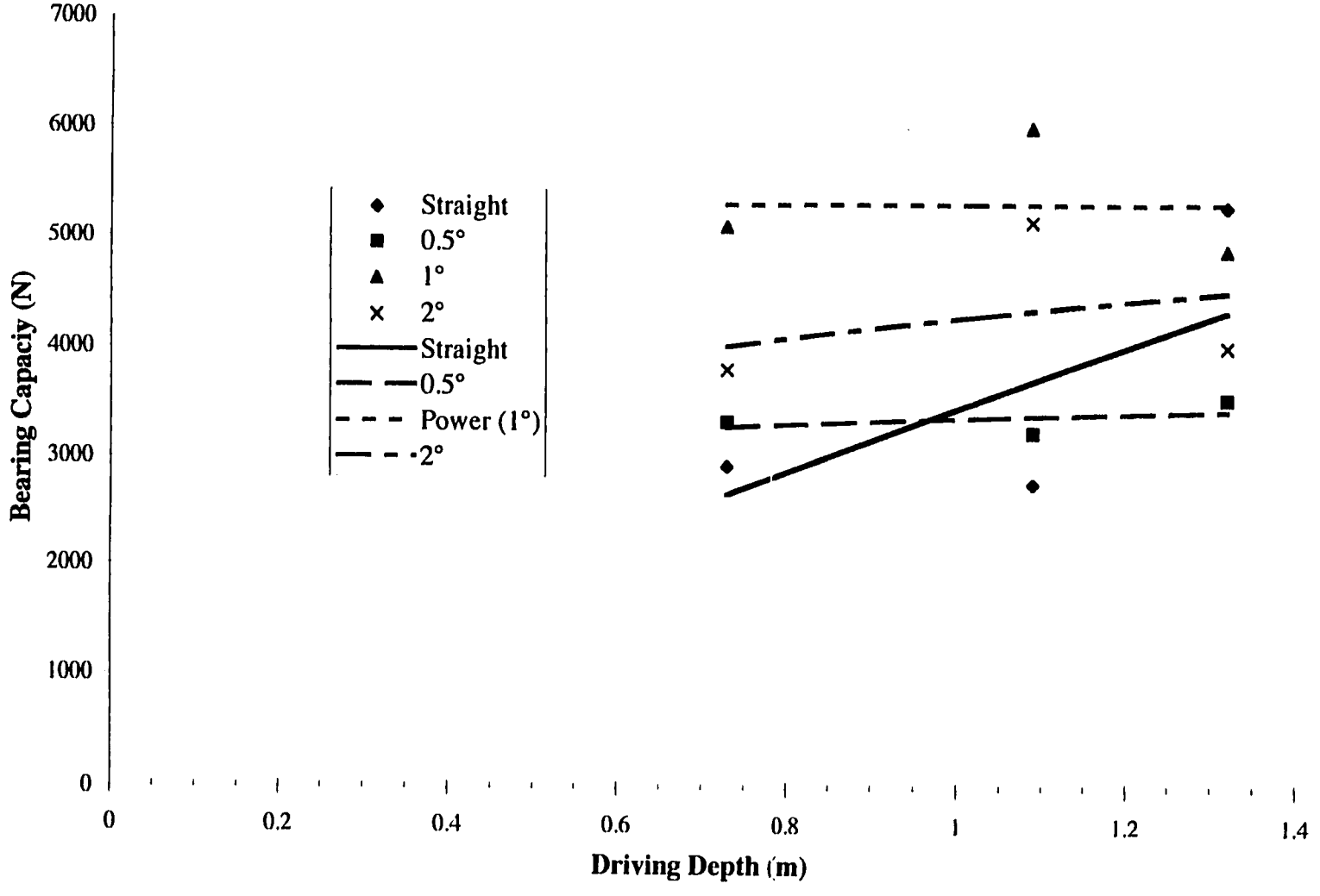

Figure 4.29 - Bearing Capacity of All Piles with Surcharge Pressure

straight piles showed an increase in end bearing. Whereas the tapered piles either showed a peak end bearing stress at a length of 1.09 m or constantly decreased. This further exemplified the difficulties encountered by tapered piles due to the arching present in the test tank.

Likewise, the range of settlements required to reach the ultimate bearing capacity was very erratic. While the general trend of the settlement was to increase with driving depth, the actual values themselves were inconsistent. The straight piles tended to have larger settlements, but this may have been due to the smaller effect of arching upon the straight piles.

4.3.3 Surcharge and Confining Pressure

A summary of the bearing capacities, illustrated in Figures 4.30 through 4.32, compared all piles under a surcharge stress of 50 kPa and a confining stress of 25 kPa and is presented in Tables 4.21 through 4.23.

Comparisons of the individual test data indicated that under the higher stress conditions, represented by the application of both a surcharge and a confining stress, tapered piles provided significantly greater bearing capacity than similar straight piles. Both the 1° and the 2° tapered piles provided significantly greater bearing capacity than the straight piles at all depths of driving. The 0.5° tapered pile showed a significant total bearing capacity advantage over straight piles only at a driving depth of 1.32 m. The bearing capacity of

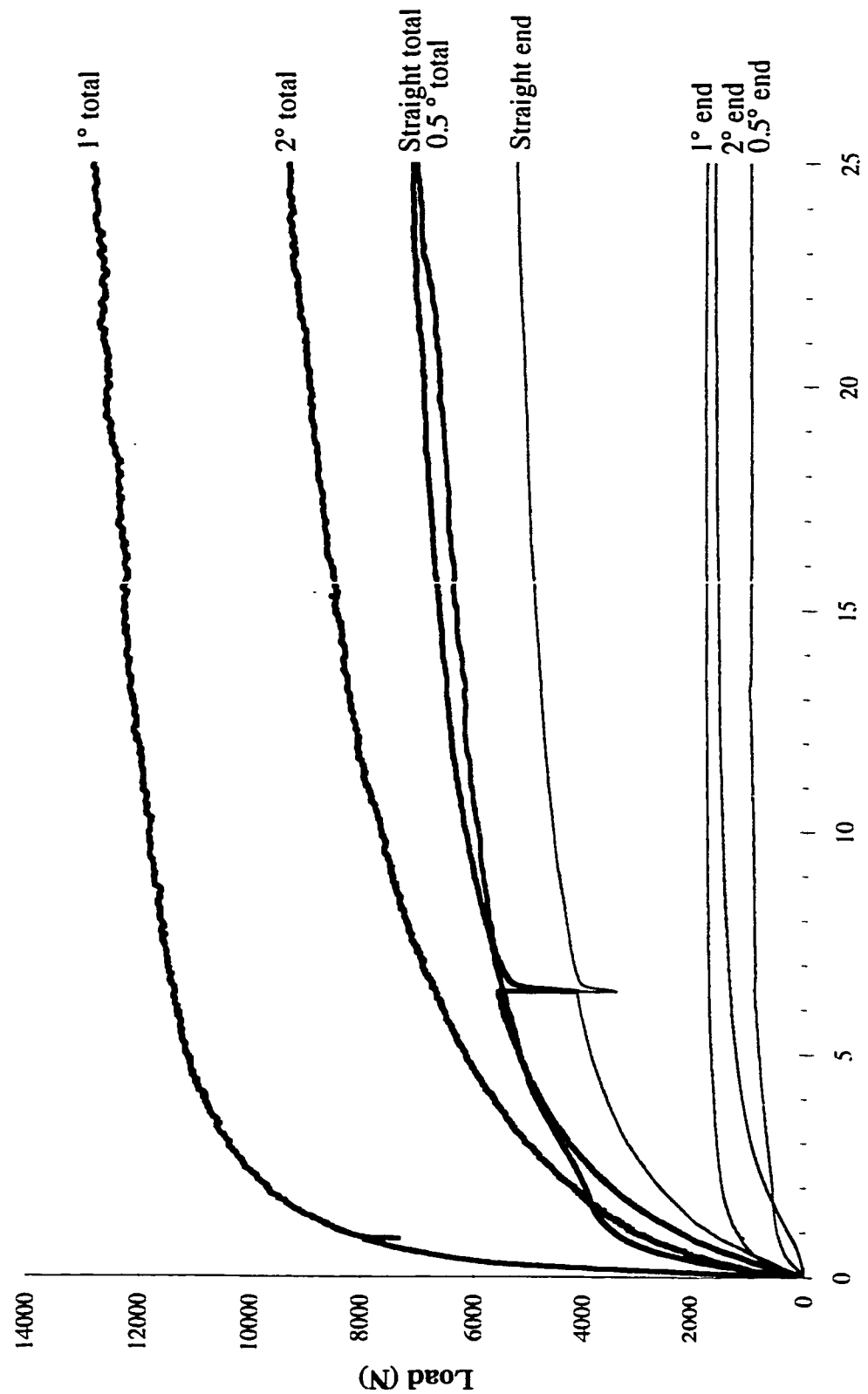

Figure 4.30 - 0.73 m Long Piles with Surcharge and Confining Pressure

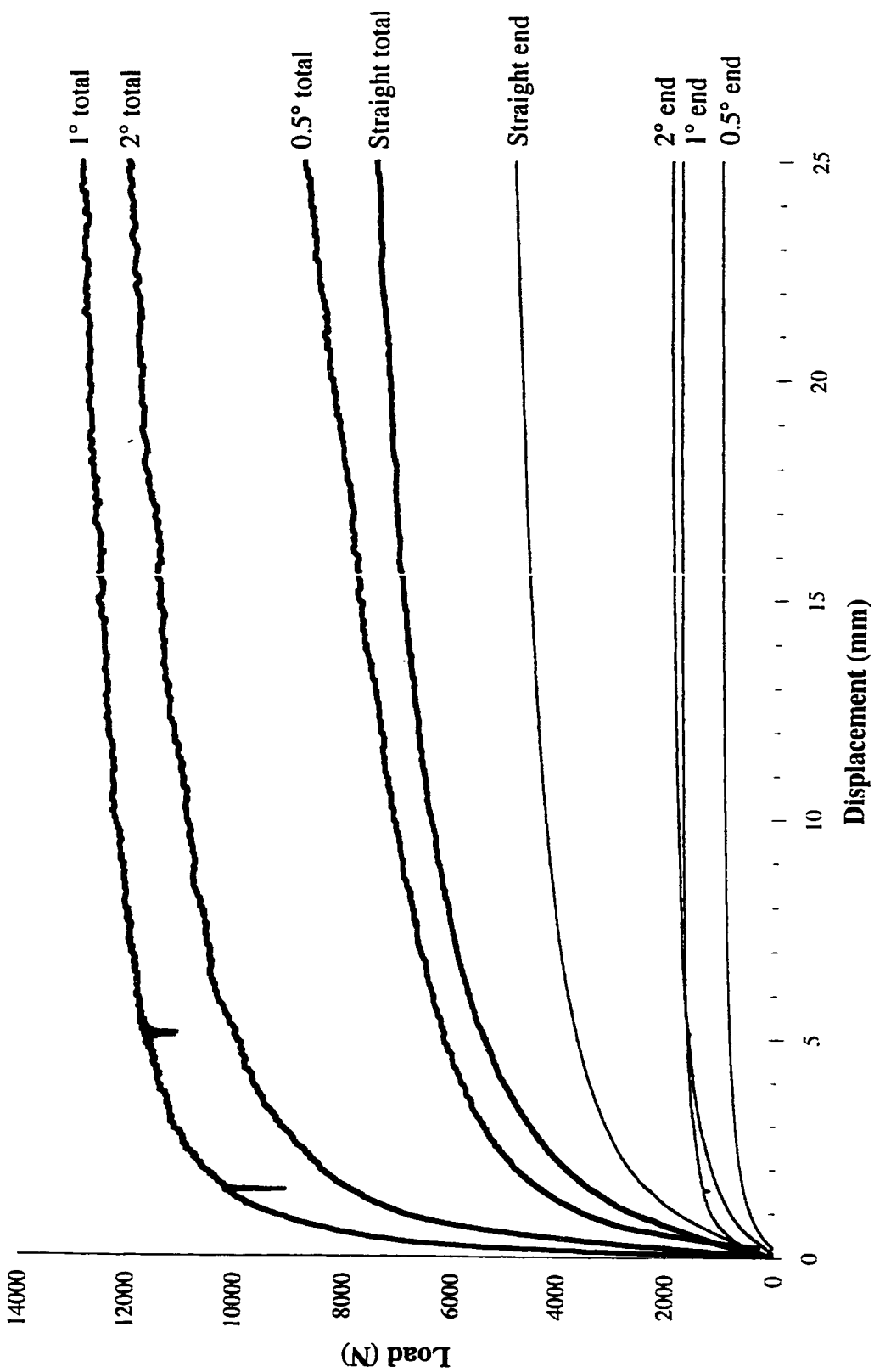

Figure 4.31 - 1.09 m Long Piles with Surcharge and Confining Pressure

Figure 4.32 - 1.32 m Long Piles with Surcharge and Confining Pressure

Table 4.21: 0.73 m Long Piles - Surcharge and Confining Pressure

	Straight	0.5°	1°	2°
Total (N)	6,230	6,401	11,539	7,781
Toe (N)	4,626	1,004	1,691	1,472
Toe (kPa)	2,282	2,130	3,587	3,122
Settlement (mm)	10.2	15.1	7.1	10.6
Volume (cm^3)	1,480	583	863	1,171
%age of Str. Vol.	100 %	39.4 %	58.3 %	79.1 %

Table 4.22: 1.09 m Long Piles - Surcharge and Confining Pressure

	Straight	0.5°	1°	2°
Total (N)	6,381	6,726	12,129	10,743
Toe (N)	4,248	929	1,709	1,774
Toe (kPa)	2,096	1,971	3,625	3,763
Settlement (mm)	9.7	7.7	9.0	8.3
Volume (cm^3)	2,209	1,070	1,593	1,901
%age of Str. Vol.	100 %	48.4 %	72.1 %	86.1 %

the 0.5° tapered pile was only slightly greater than that of the straight pile at the 1.09 m and 0.73 m depths.

Figure 4.33 depicts the trend of the bearing capacity with the change in the driven depth. The straight piles showed only a marginal increase in bearing capacity, this was likely the result of only having 3 tests on which to base the trend. While this increase was smaller than general theory would indicate, it was indicative of the slow increase in bearing

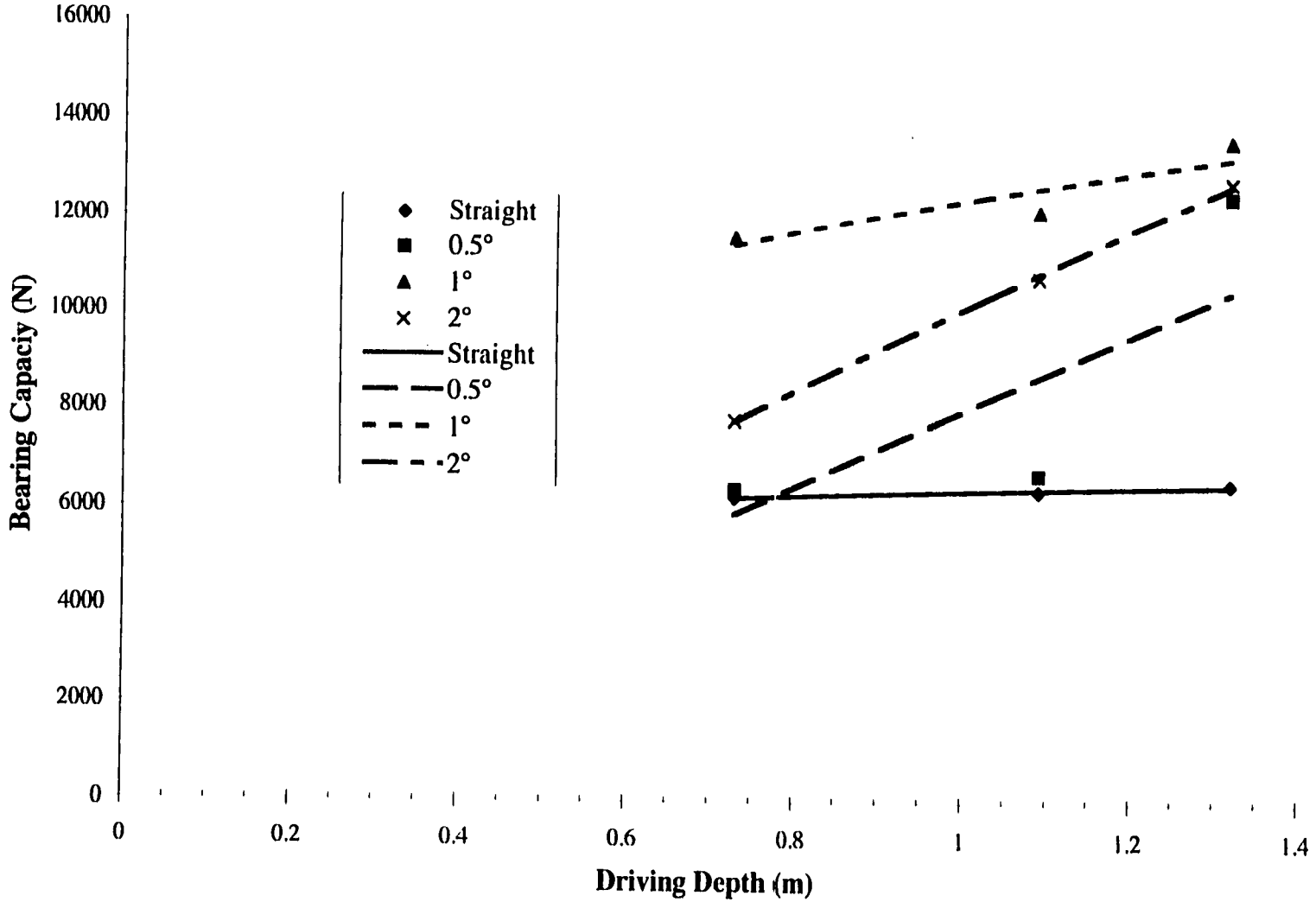

Figure 4.33 - Bearing Capacity of All Piles with Surchage and Confining Pressure

Table 4.23: 1.32 m Long Piles - Surcharge and Confining Pressure

	Straight	0.5°	1°	2°
Total (N)	6,552	12,450	13,611	12,759
Toe (N)	4,538	1,763	2,066	1,968
Toe (kPa)	2,239	3,740	4,382	4,174
Settlement (mm)	8.9	8.1	9.2	8.7
Volume (cm^3)	2,675	1,459	2,059	2,367
%age of Str. Vol.	100 %	54.5 %	77.0 %	88.5 %

capacity in comparison to that of the tapered piles. The slow increase in the total bearing capacity is likely the result of a low end bearing of the 1.09 m long pile and a low shear value of the 1.32 m long pile.

Using the 2° tapered pile as the benchmark, due to a consistent trend of the data with the trend line, the rate of increase in the total bearing capacity of the 0.5° and 1° taper piles should have been greater. The 0.5° pile should have had a greater rate of increase, due mainly to the increasing diameter at the top of the pile. The longer length of taper was another potential reason for a greater rate of increase. The data tended to indicate that the 1.09 m long pile was likely on the low end of the average of that which would be expected of a pile of this length and shape. The 1° tapered piles should have a rate from increase equal to or greater than the 2° tapered piles. Since both piles had their tapered portion completely driven into the sand at the 0.73 m length, the only change to the pile at greater driving depths was the addition of straight portions. If the tapered portions increased at

the same rate with increased driving, then the bearing capacity should have increased at the same rate. Since the tapered portion of the 0.73 m long 1° pile was just below the surface, it was probable that it would increase at a greater rate. The curve would have fit this assumption reasonably well if the 0.73 m pile had a significantly lower bearing capacity.

The addition of both surcharge and confining pressures on the soil resulted in a sizable increase in the bearing capacity of all the piles. This increase in bearing capacity was significantly greater for tapered piles than for untapered piles. Since straight piles were primarily end bearing, the best way to compare this increase was to compare the end bearing of the piles. The end bearing stress of the straight piles was smaller than that of the tapered piles under both the no additional pressure condition, and the condition in which both surcharge and confining stresses were applied. However, the magnitude of the difference was significantly greater under the surcharge with confining stress condition. As previously stated, while the end bearing of tapered piles was not directly responsible for the majority of the bearing capacity, it was a good indicator of the ultimate bearing capacity. Though the percentage of the load supported through end bearing decreased in the fully pressurized tests, the end bearing remained a good indicator of the ultimate bearing capacity of the pile.

Smith (1995) determined that the sand bed created via the pluviation method had a density of 16.5 kN/m^3. Thus the surcharge pressure was approximately equivalent to an additional

3 m of soil. While this did not exactly replicate the field conditions, all of the end bearing data from the tests in which no additional pressure was applied to the test tank as well as that from the surcharge with confining pressure tests, adjusted for simulated depth of driving, are presented in Figure 4.34. The plotted data is erratic and difficult to interpret.

Figure 4.35 is the same plot with the data that was previously determined to be unreliable or excessively out of line with the trend of the remaining data, e.g. the end bearing of the 1° taper piles with no additional pressure due to load cell failure. The trend seemed to suggest that the end bearing increased in a linear manner with increased depth of driving and therefore overburden pressure. This indicated that the end bearing of piles increased in a near linear manner past a D/B ratio of 100. This was contrary to the findings of Vesic (1967), Coyle and Castello (1981), and Meyerhoff (1983) who concluded that the end bearing reached a maximum value at a D/B ratio of no greater than 30. It was also contrary to the findings of Hanna and Tan (1973), Kulhawy (1984), and Randolph *et al.* (1994) who concluded that the end bearing did not reach a maximum value at these depths, but that it continued to increase at a decreased rate. There were several possible explanations for these discrepancies, the first of which being that the shorter physical pile length may not have accurately replicated the natural soil arching effects. Furthermore, the tank dimensions may not have been sufficiently large to allow the soil to behave as it otherwise would under in situ conditions. A distance of 0.6 m from the bottom of the tank may have been insufficient, and therefore may have artificially enhanced the end bearing capacity of the pile.

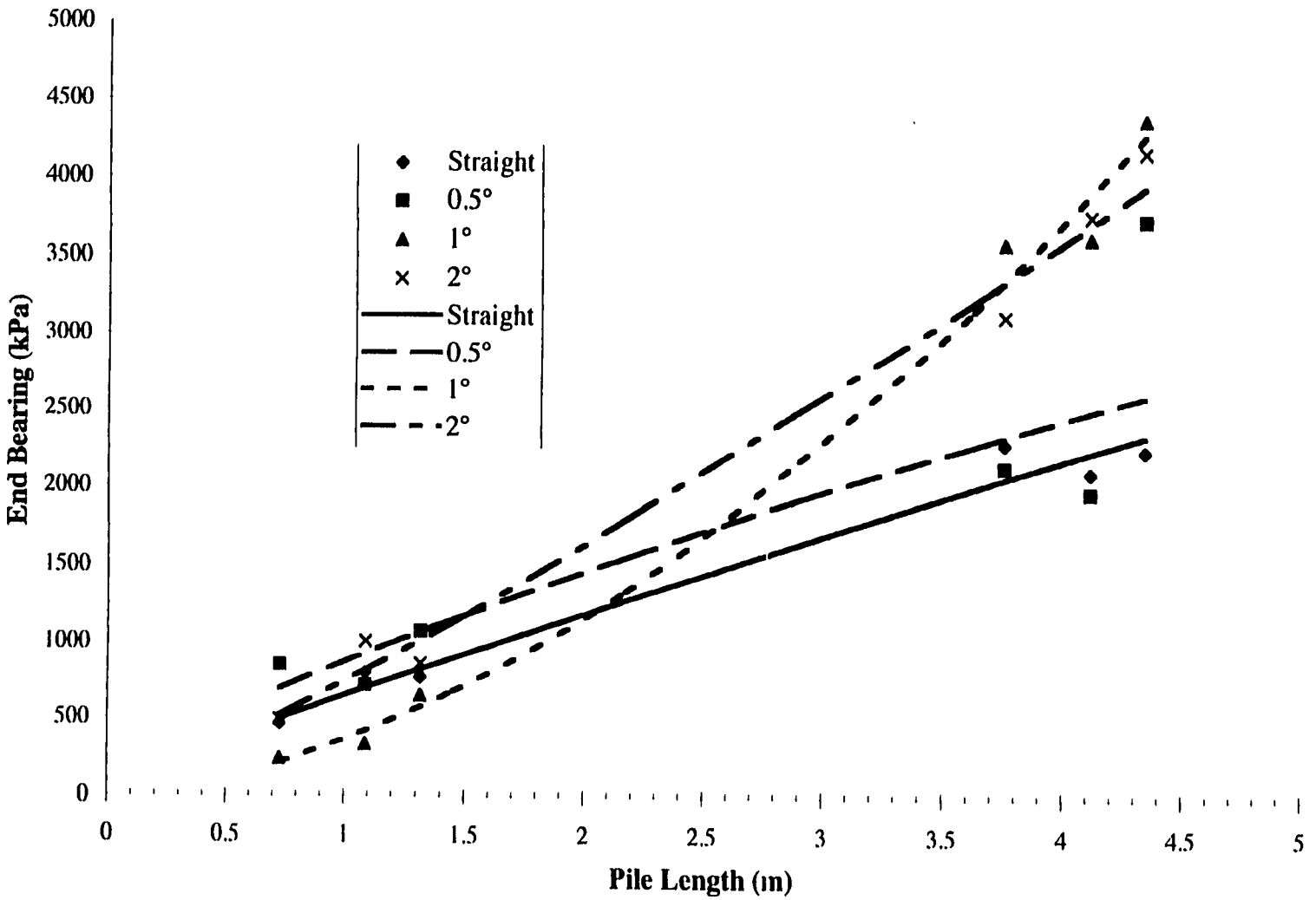

Figure 4.34 - Pile End Bearing

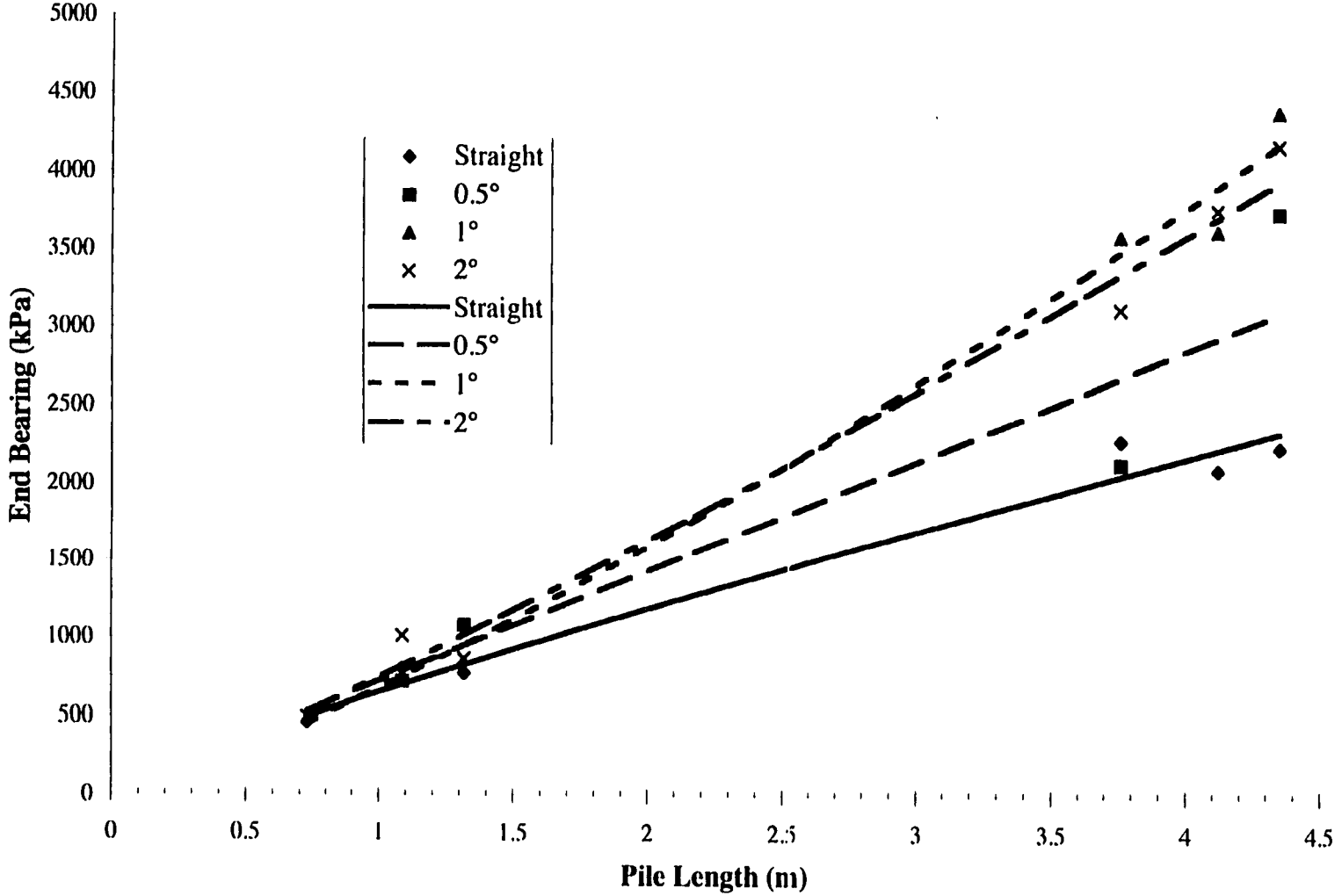

Figure 4.35 - Modified Pile End Bearing

There may have been some scaling effects between the test conditions and field conditions not regularly accounted for. While not completely recreating the effects of the field data, several comparative observations were made. The chart showed that tapered piles developed greater end bearing stresses than did straight piles. This effect became more predominant with increased confining pressure around the soil. As previously stated, Kraft (1991) described the process of the 'fluffing' of the soil along the pile wall as the pile toe passes through the soil. Furthermore, the amount of fluffing increased as the soil density increased. This fluffing affected the shear friction along the pile wall, but did not seem to affect the end bearing of the pile as well. Due to a reduction in vertical pressure, the fluffing process resulted in a reduction in soil stress above the pile toe. With tapered piles the reduction in pressure was still present but of a smaller magnitude. The amount of fluffing in this region is reduced due to the application of vertical pressure on the soil from the tapered portion of the pile. This kept the soil around the pile in a state of greater pressure. When the soil near the pile toe was under greater stress the soil under the pile toe was able to attain a state of higher compression as well. This resulted in the slopes of the tapered pile curves in Figure 4.35 being steeper than that of the straight pile.

The ultimate bearing capacity data agreed well with the stress bulb of Robinsky and Morrison (1964). While it was stated that there was an increase in bearing capacity with an increase in density, it was not determined what effect stress had upon the size of the bulb. The soil stress, and therefore depth of driving, had a significant impact upon the size

of the resulting stress bulb. The size of the bulb under those conditions was enhanced more for tapered piles than for straight piles. Robinsky and Morrison (1964) attributed this to the same concept of fluffing as later proposed by Kraft (1991).

The trend for the pile settlement, at the ultimate bearing capacity, seemed to increase with an increase in driving depth. This trend continued with the pressurized conditions where the settlement under pressurized conditions was greater than that under unpressurized conditions. It thus appeared that an increase in confining pressure increased the settlement required to reach the ultimate bearing capacity. While the straight piles were consistently at the high end of the settlement of the individual driving depths, they were well within the range of the other piles. Therefore, straight piles likely have similar or marginally greater settlements than tapered piles.

4.3.4 Tension Testing

Figures 4.36 to 4.38 illustrate the differences between the shear friction developed along the pile face in both compression and tension for the 1.32 m straight and 1° tapered piles. Table 4.24 summarizes the maximum frictional resistance developed during the tension testing.

As previously stated, a significant portion of the recorded shear friction of tapered piles under compressive loading was actually end bearing along the tapered surface. While the

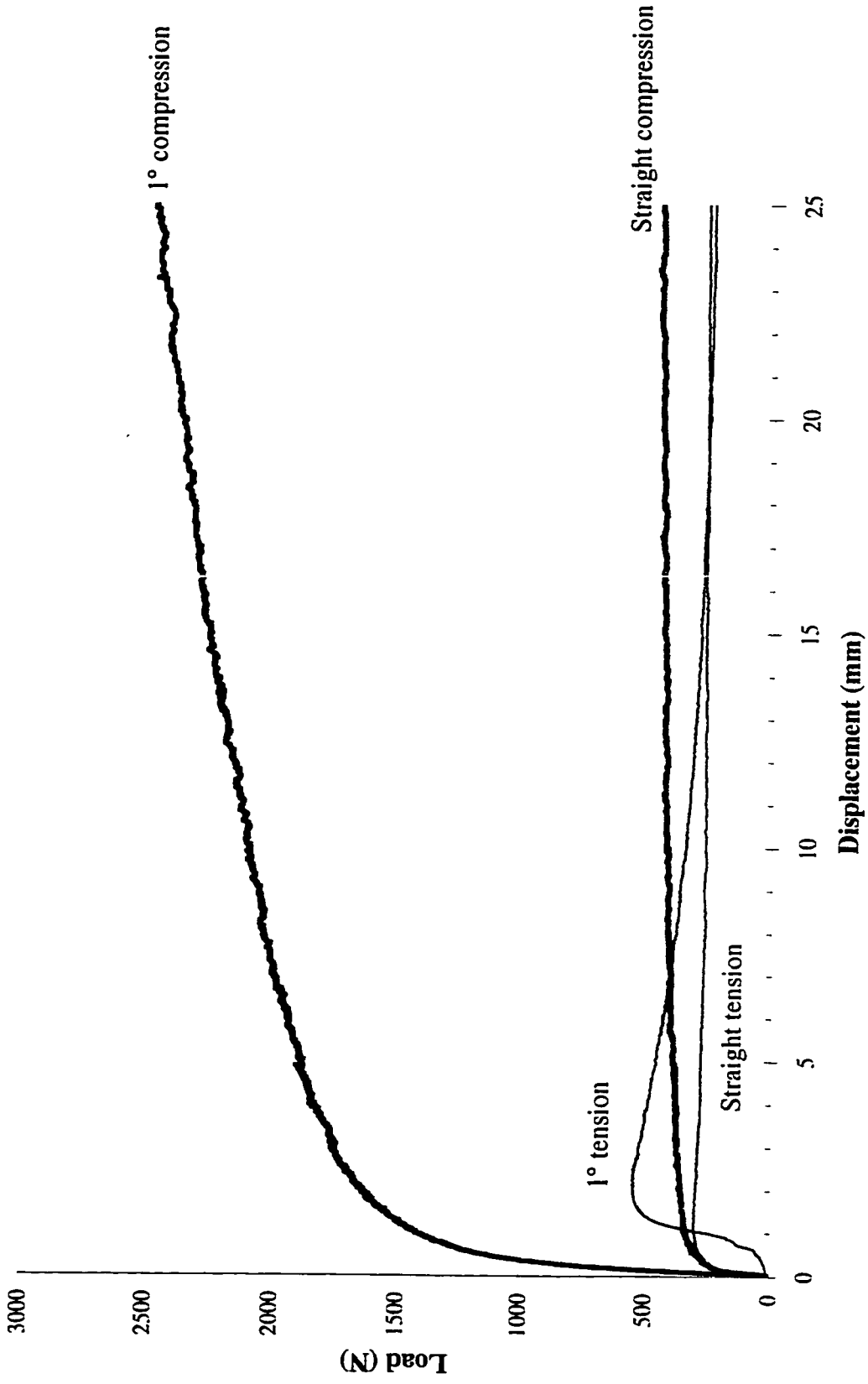

Figure 4.36 - Shear Friction for All Piles with No Additional Preesure

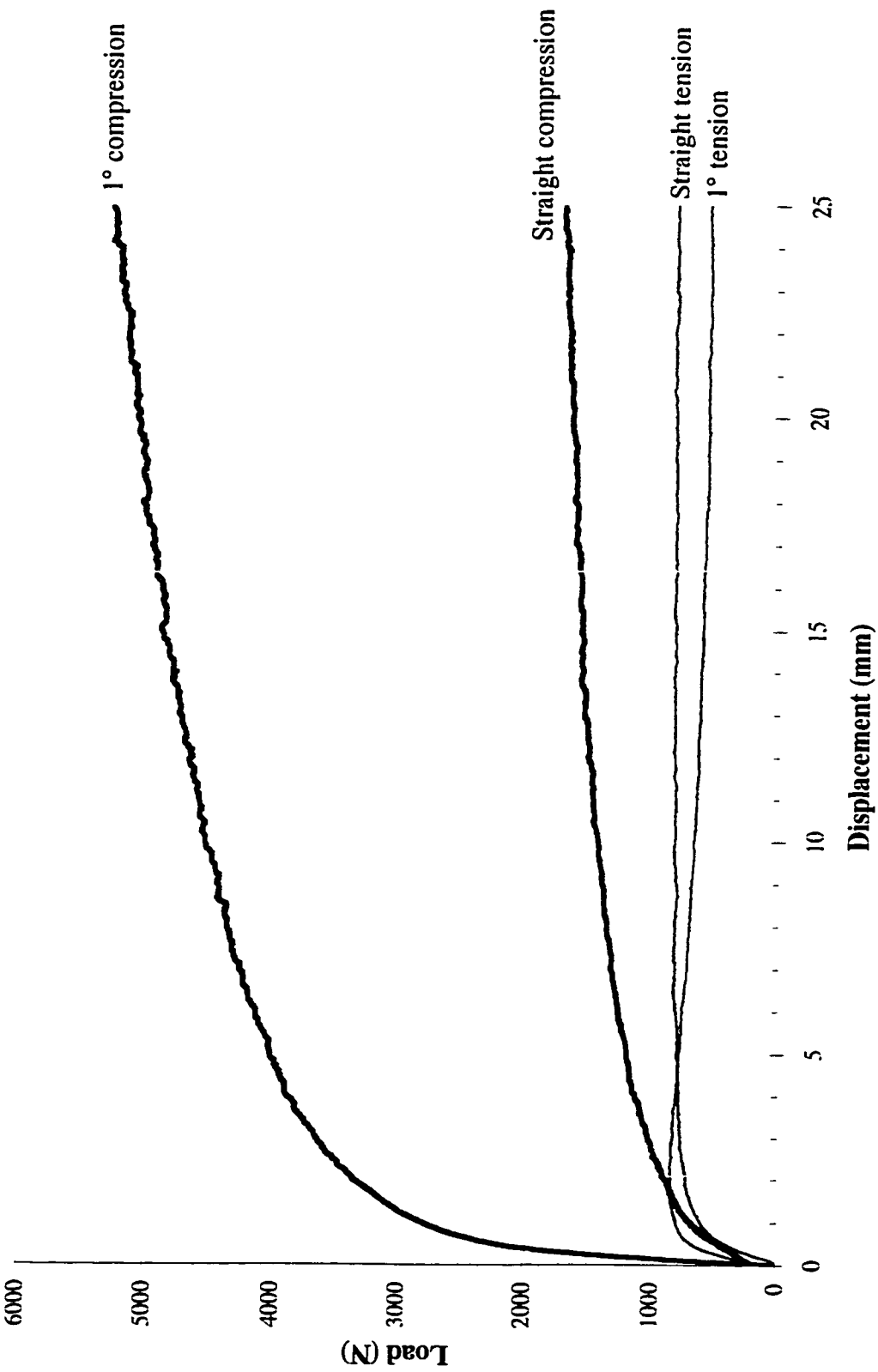

Figure 4.37 - Shear Friciton for All Piles with Surcharge Pressure

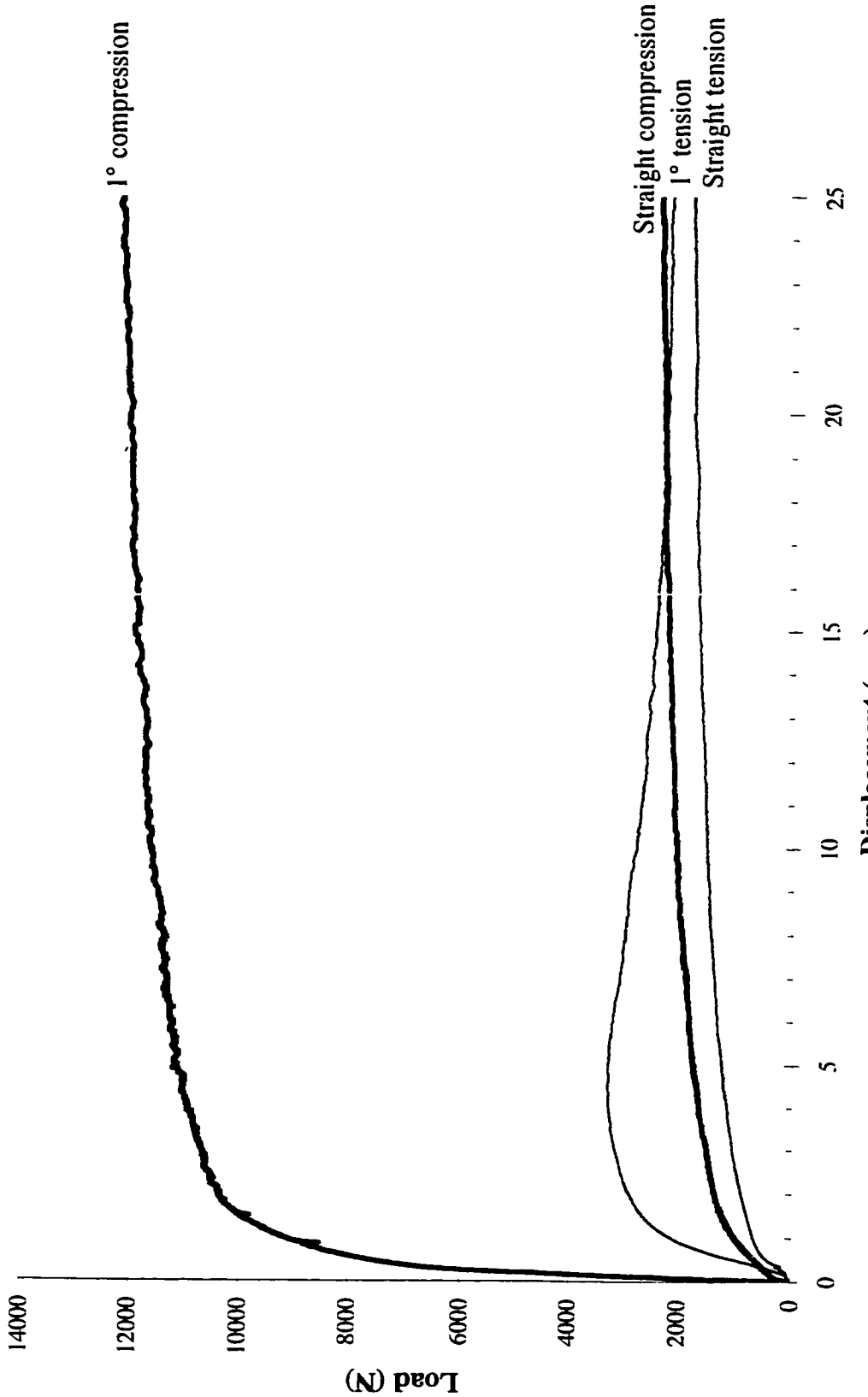

Figure 4.38 - Shear Friction for All Piles with Surcharge and Confining Pressure

Table 4.24: Shear Friction of Straight and 1° Piles

Pressure Location	Straight	1° Taper	Straight:Tapered
None (N)	301	548	55 %
Surcharge (N)	830	845	98 %
Surcharge and Confining (N)	1,465	3,290	45 %

shear friction of tapered piles was likely greater than that of straight piles, a large portion of the difference in the compression curves of Figures 4.36 to 4.38 is the end bearing along the tapered surface.

The pull out resistance of the shear friction, of the straight and tapered piles, were much closer to each other than the compressive values. The pull out resistance that resulted from the application of surcharge pressures further illustrated the negative impacts of pressurization upon tapered piles as compared to straight piles. A similar trend was observed with the compressive shear friction, as depicted in Figure 4.37, as compared to those in Figures 4.36 and 4.38. The shear resistance of the straight pile in tension was significantly larger as a percentage of that developed by the tapered pile under surcharge conditions, as compared to either of the other conditions.

Except for the surcharge load condition, the tapered piles provided significantly greater tensile capacity than the straight piles. The difference in tensile shear friction between the straight and tapered piles resulted primarily from the reduction of 'fluffing' in the soil

along the pile walls. This reduction in fluffing increased the pressure applied to the pile walls allowing for a greater shear resistance. However, the tapered piles showed a significant drop off in uplift capacity upon reaching an ultimate capacity. This reduction in capacity was due to the shape of the tapered piles. Upward movement caused the tapered portion of the pile to be pulled out of contact with the soil, in turn the soil expands in the vicinity of the pile wall under the reduced pressure. The result was the continuous degradation of uplift capacity of the tapered piles.

These finding are contrary to those of El Naggar and Wei (1998) who concluded that tapered piles provided less uplift capacity than straight piles. However, two major differences existed between the two series of tests. The piles for this series of tests were only partially tapered, not completely tapered as those of El Naggar and Wei, and the piles for this series of tests were driven not placed into the sand bed. It was unknown what effect partially tapered piles versus fully tapered piles would make, but it can be concluded that the driving process accounted for a significant difference. This difference was primarily in the build up of stresses around the pile. The results of this testing agreed with the findings of pull out capacities of *Monotube*® piles in field testing which showed greater uplift capacity than untapered piles.

The tapered piles also showed increasing effectiveness with increasing soil pressure, and therefore driving depth. Kraft (1991) concluded that both a decrease in δ and an increase in contractive behaviour of the soil occurred with increased depth of driving. These two

effects were related to the development of arching within the soil and limited the frictional resistance of the pile. It was possible that the shape of the tapered piles reduces the magnitude of these effects. This was evidenced by the development of higher end bearing stresses in the presence of greater confining stresses with tapered piles as compared to straight piles. The greater stresses evident under the pile toe were likely accompanied by greater stresses surrounding the pile. As such, the tapered piles became increasingly effective, relative to straight piles, with an increase in soil stresses.

It may be noticed that in Figure 4.36 that the curve of the tension test of the 1° tapered pile initially increased at a slow rate and then increased in rate of pullout resistance. This was due to the method in which the tension testing occurred. If the equipment was not exactly aligned at the beginning of the test it would align itself during the test. This slow rate of initial increase seen in Figure 4.36 is likely the result of the equipment aligning itself, therefore the ultimate tensile capacity will be correct, but the accompanying displacement will be slightly greater than it should be.

4.4 Numerical Analysis of the Data

Several methods of determining the bearing capacity of tapered piles were described earlier in Section 2.4.4 but most of them provided unacceptable results. Kodikara and Moore's (1993) method could not be used due to the fact that the method was developed for the bored cast-in-place piles of Rybnikov (1990). Also, the correction factors to the shear friction and end bearing of Dennis and Olson (1985) are ineffective due to the short

length of the piles, and the empirical nature of the formula.

4.4.1 Straight Piles

The theoretical bearing capacities of the straight piles were calculated in accordance with API RP-2A (1989). The Potyondy (1961) ratio of the soil-pile friction angle to the soil internal angle of friction of $\delta = 0.54 \cdot \phi'$, for smooth steel in a dry sand provided the best fit to the data.

The results best fit the test data when the end bearing was allowed to increase linearly with depth without limit and the shear friction increased linearly with depth up to 10 pile diameters after which time it was kept constant. As seen in Figure 4.39 the shear friction was overestimated and the end bearing was underestimated. This resulted in the total estimated bearing capacity averaging out to a reasonably good approximation of the results obtained during testing. No attempts were made to calculate the pile resistance under the fully pressurized tank conditions, due to an inability to properly calculate the effects that these conditions have upon regular formulae.

4.4.2 Tapered Piles

The computations of shear resistance for the tapered piles was restricted to the 0.5° taper piles due to the unknown factors when dealing with partially tapered and straight section piles. The method of calculation followed the API RP 2A (1989) as with the straight piles, but was modified as per Equations (16) and (17) (Olson and Long, 1989). As can be seen

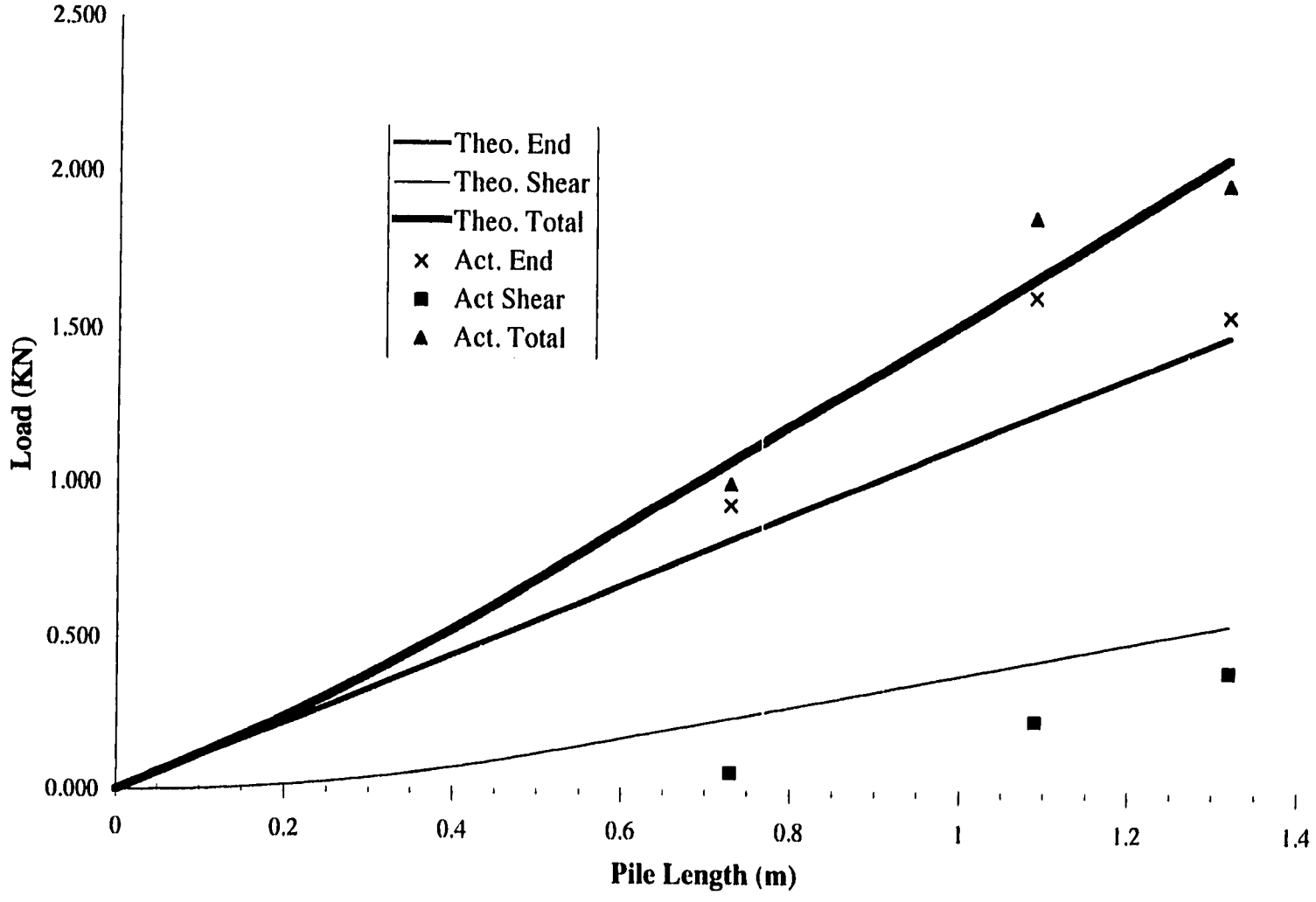

Figure 4.39 - Actual Capacity versus Theoretical API Capacity for Straight Piles

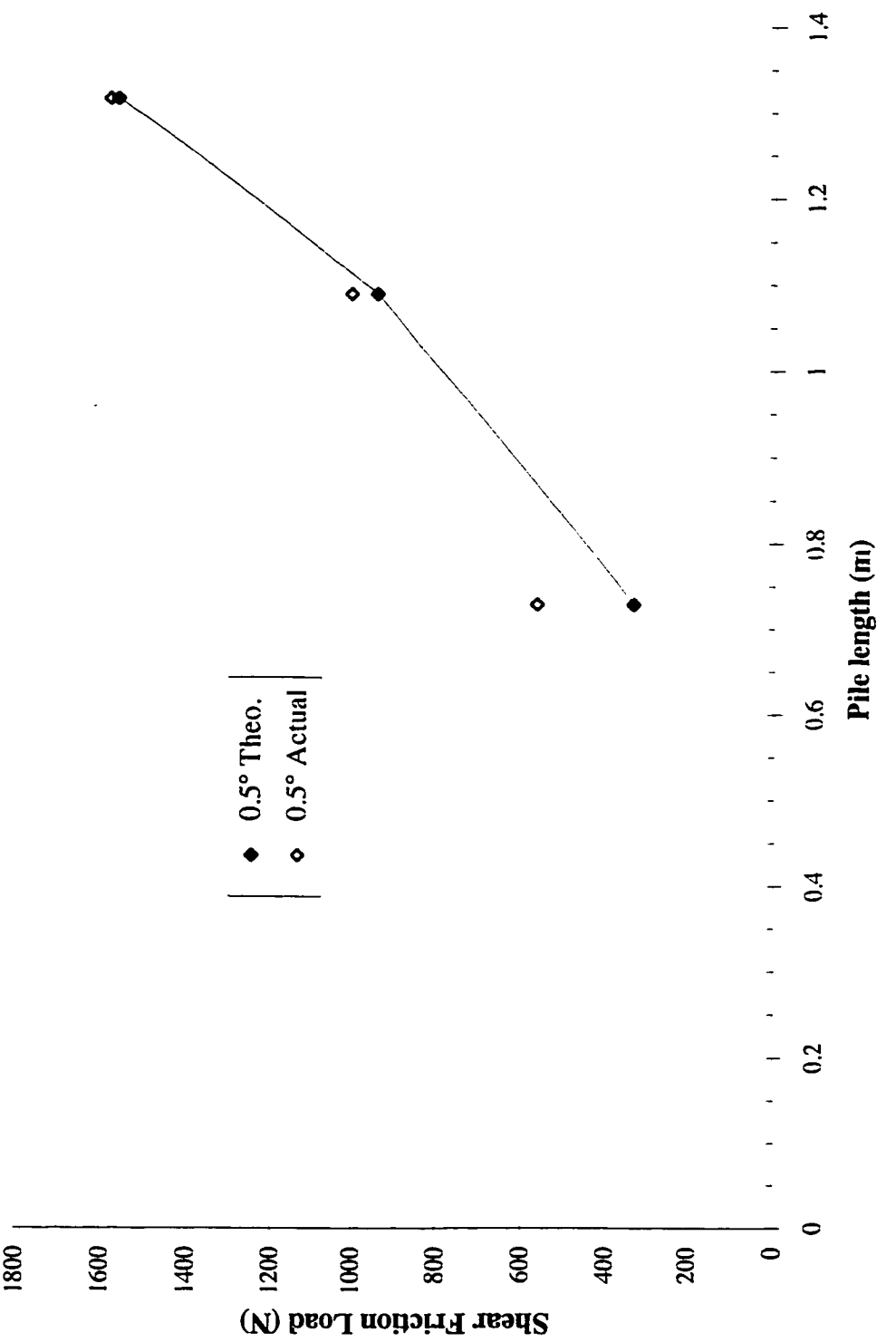

Figure 4.40 - Actiual versus Theoretical Shear Stress for 0.5° Tapered Piles

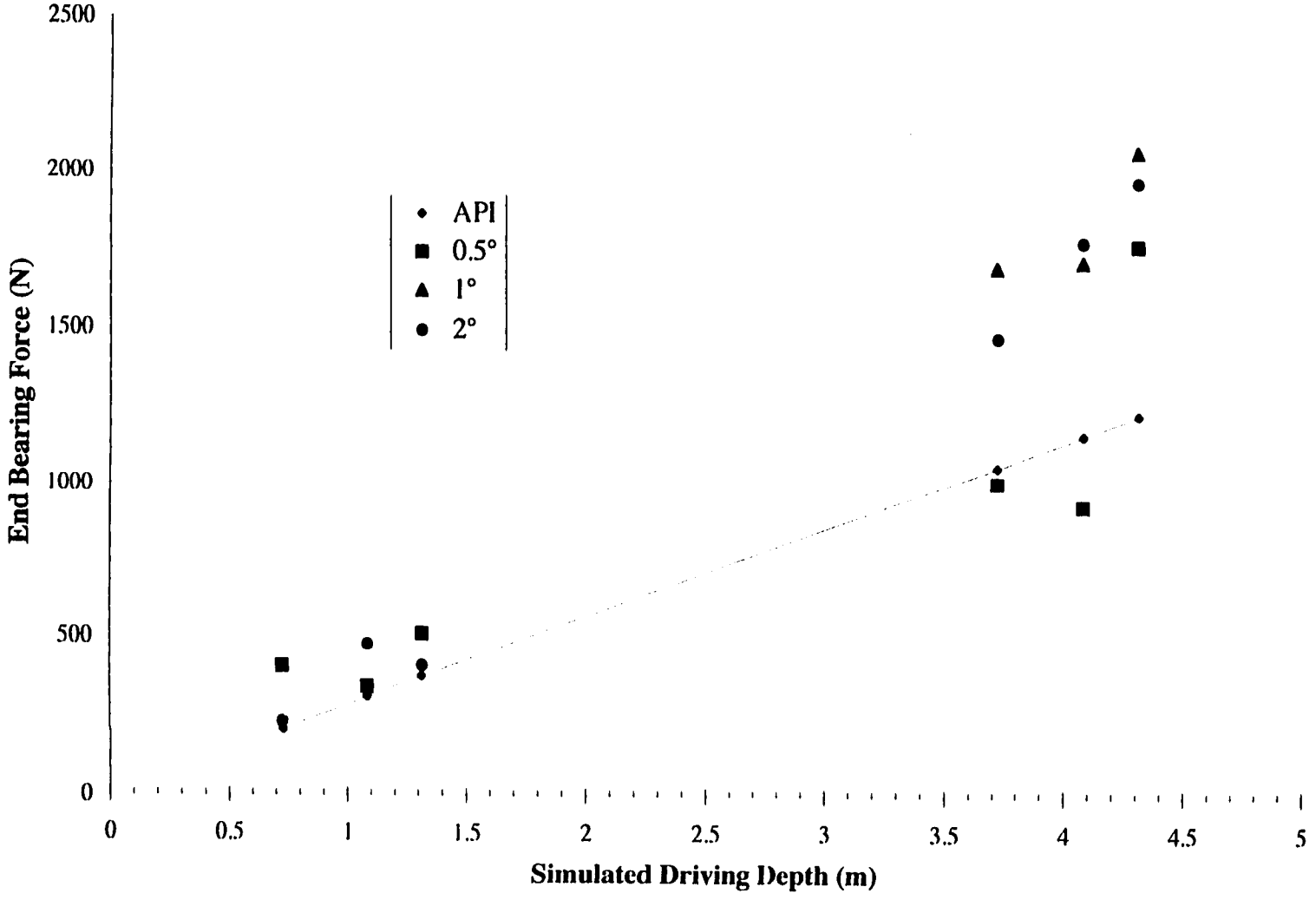

Figure 4.41 - Actual versus Theoretical End Bearing Stress for Tapered Piles

in Figure 4.40 the correlation between the theoretical and the actual test results were reasonably close, with the theoretical underestimating the actual shear resistance.

Figure 4.41 illustrated that the API RP-2A under estimated the end bearing capacity of the piles in both the no additional pressure tests and the surcharge with confining pressure tests, which simulated driving the piles 3 m further into the soil. Therefore a different method of determining the end bearing of tapered piles was considered necessary.

Using basic principles of geotechnical engineering such a method was developed which provided good results when compared to the laboratory testing. This method was based on one of the oldest engineering principals, Mohr's Circle. Figure 4.42 illustrates the concept of Mohr's circle as it relates to passive soil pressure. For a confining soil stress of σ_3 the primary stress σ_1 may be increased until the Mohr's Circle comes in contact with the failure plane defined by ϕ. Any further increase in σ_1 will cause the soil to flow, since the passive pressure condition has been reached.

Figure 4.43 illustrates the basic concepts of the presented end bearing theory. The stress at the pile toe from the surcharge pressure is represented by σ_{3-1}. The corresponding passive pressure to σ_{3-1} is thus defined as σ_{1-1}. σ_{3-2} represents a new confining pressure beneath the pile toe which is equal in magnitude to σ_{1-1}. σ_{1-2} is thus defined as the passive pressure of the new confining pressure σ_{3-2}. Therefore the maximum end

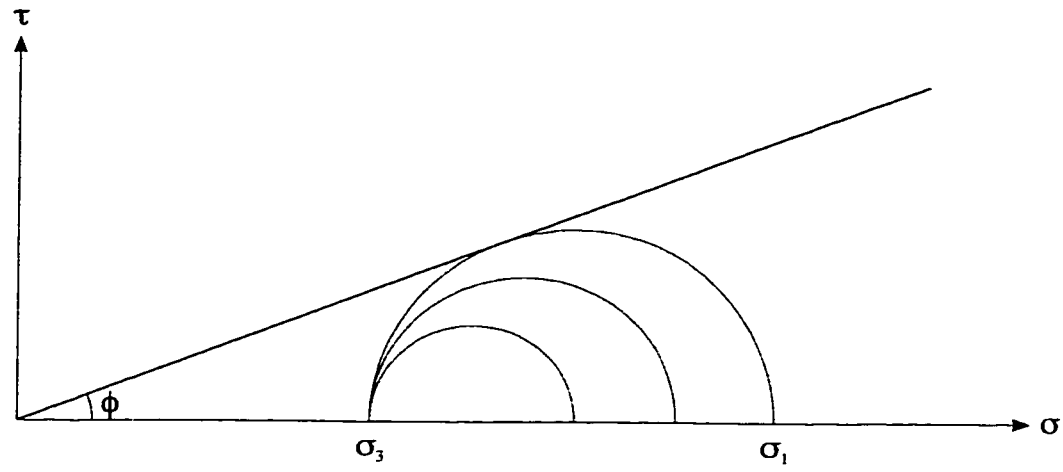

Figure 4.42 - Passive Pressure Defined by Mohr's Circle

bearing stress, that a pile can sustain, is the passive pressure of the passive pressure of the soil.

Figure 4.44 shows a modification to this theory which reduces the end bearing capacity. According to Vesic (1977) there is a wedge of very dense soil directly beneath the pile toe. This wedge is likely the result of a rotation in the principal stress planes in the region of the pile tip. Therefore σ_{1-2} is parallel to the adjoining side of the wedge. The net result is that the σ_{X-2} plane is rotated from its regular orientation by $(45 - \phi/2)$. The maximum load is reduced by $\cos(45 - \phi/2)^2$ because after rotating the σ_{X-2} plane there is an angle of $(45 - \phi/2)$ between the pile toe and σ_{1-2}, and between σ_{1-1} and σ_{3-2}. Therefore the end bearing may be determined from the following equation:

$$Q_p = \gamma \cdot H \cdot K_{p2} \cdot K_{p2} \cdot \cos^2(45 + \phi_2/2) \cdot A_p \qquad (23)$$

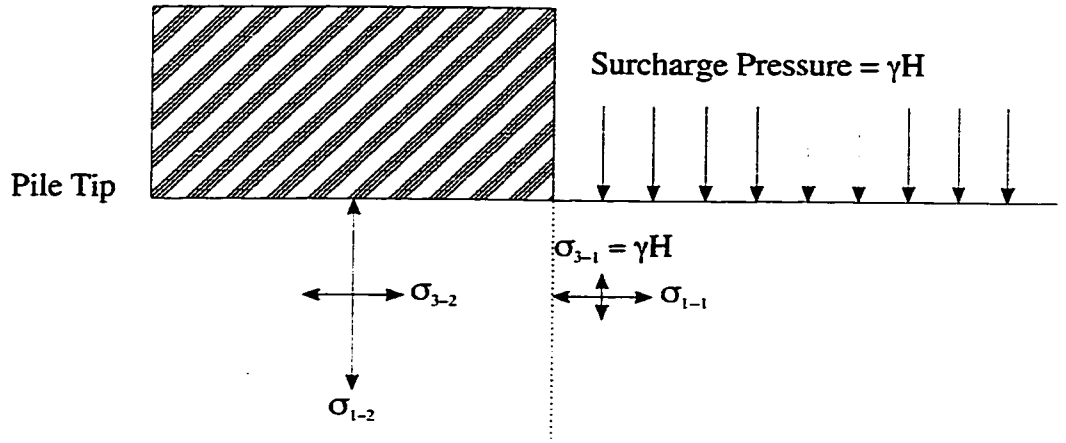

Figure 4.43 End Bearing Theory

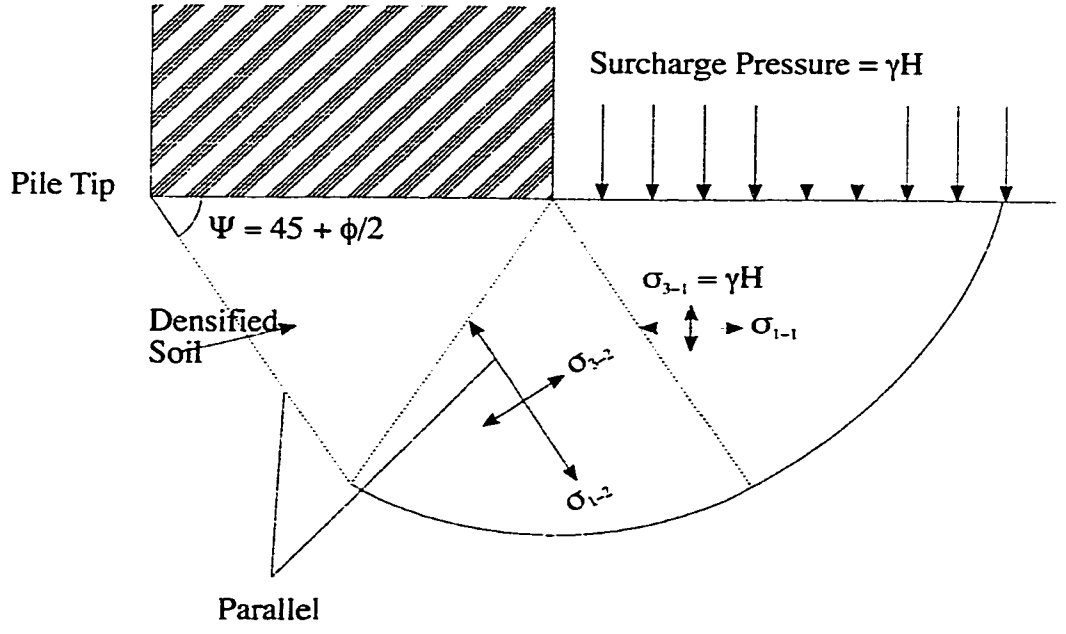

Figure 4.44 Modified End Bearing Theory

Combining Equation (23) with the definition of passive pressure from Equation (12) yields the final Equation (24):

$$Q_p = \gamma \cdot H \cdot \tan^2(45 + \phi_1/2) \cdot \tan^2(45 + \phi_2/2) \cdot \cos(45 + \phi_2/2) \cdot A_p \qquad (24)$$

where γ = unit weight of the soil

H = depth of driving

ϕ_1 = internal angle of friction in the soil adjacent to the pile toe

ϕ_2 = internal angle of friction in the soil directly under the pile toe

A_p = area of pile tip

$\tan(45 + \phi/2)$ = passive soil pressure, Equation (12)

The driving process densifies the soil directly under the pile toe, and therefore the internal angle of friction directly under the pile, ϕ_2, should be taken at a relative density of 100% and not the in situ soil density. Additional soil densification and vertical stress on the soil adjacent to the pile toe warrants an increase in the value of ϕ_1 to the value at a relative density of 100% for tapered piles. For untapered piles the value of ϕ_1 would be a value equal to the in situ value due to the smaller soil stresses and densification resulting from untapered piles as compared to tapered piles.

Figure 4.45 depicts the two conditions previously mentioned and all of the pile end bearing data for both the no additional pressure and the surcharge with confining pressure

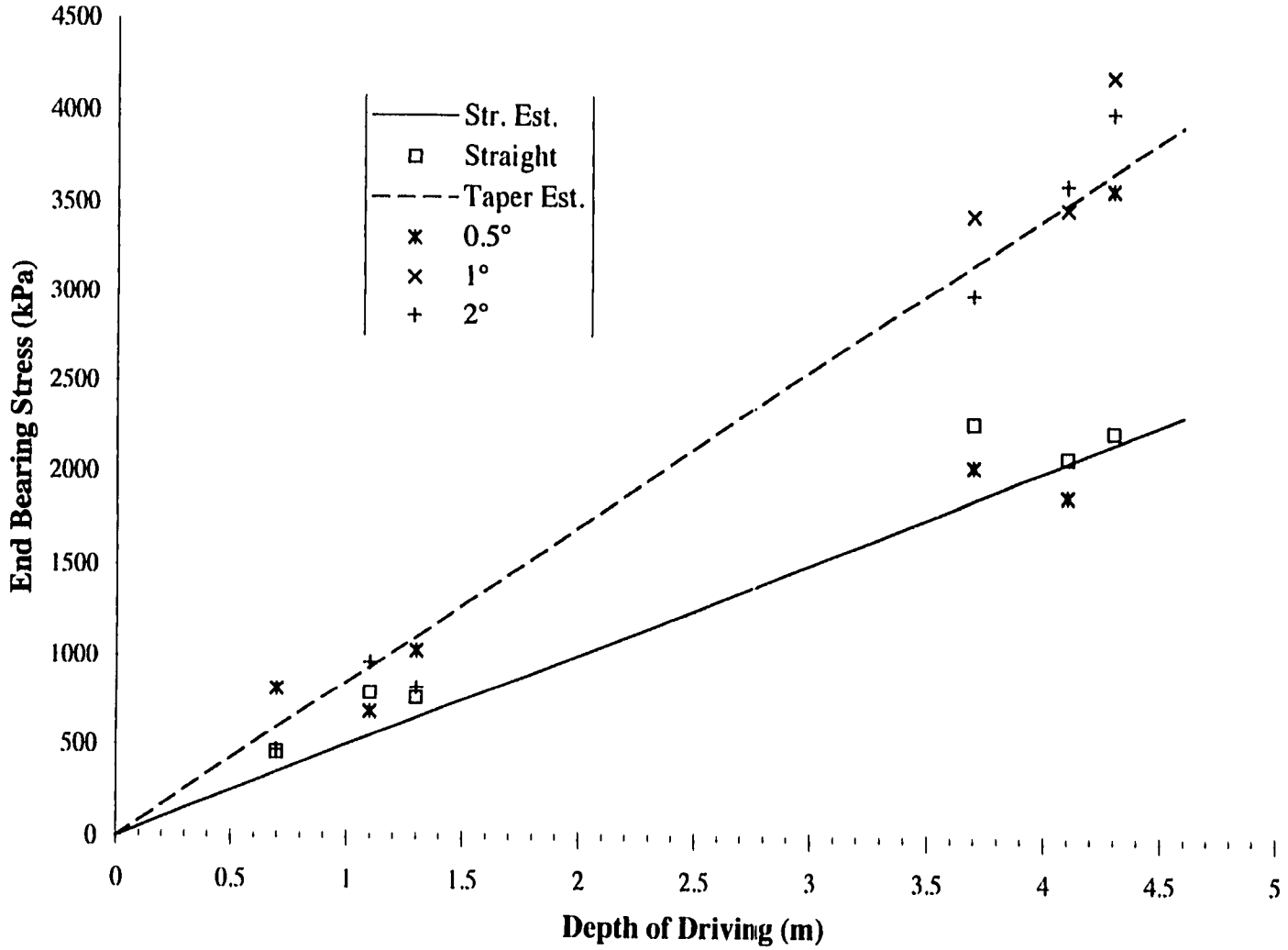

Figure 4.45 - Double Passive Pressure End Bearing Method

conditions. This provided end bearing data for piles 0.73 m to 4.32 m long, with $\phi_1 = 40°$ for straight piles, 50° for tapered piles, and $\phi_2 = 50°$ for both straight and tapered piles. The theory presented provided an excellent estimate of the end bearing of the tapered piles which appeared to increase linearly with depth of pile. However, the end bearing of straight piles was underestimated illustrating the need to modify the theory.

Figure 4.46 illustrates the trend when $q_{calculated}$:q_{actual} was averaged to a value of 1. To achieve this ϕ_1 was reduced from 50° to 49° for the tapered piles and increased from 40° to 44° for the straight piles. The the change in the estimate for the tapered piles was mainly driven by the two very low values of the 0.5° tapered piles under surcharge with confining pressure conditions. This had the net effect of increasing the safety factor of the calculated end bearing of the tapered piles. The data for straight piles indicated a decreasing rate of increase in the end bearing stress with increased depth of driving. Therefore the increase in the value of ϕ_1 underestimated the unpressurized tests and overestimated the tests which were fully pressurized. All the predicted values were within a safety factor of 2, i.e. no test was 50% less or 100% greater than the estimated value, for both the modified and unmodified proposals.

4.4.3 Pile Driving Formula

Regular pile driving formulae did not provide acceptable results. The driving formula presented here in Equation (21) provided results that underestimated the results by a factor

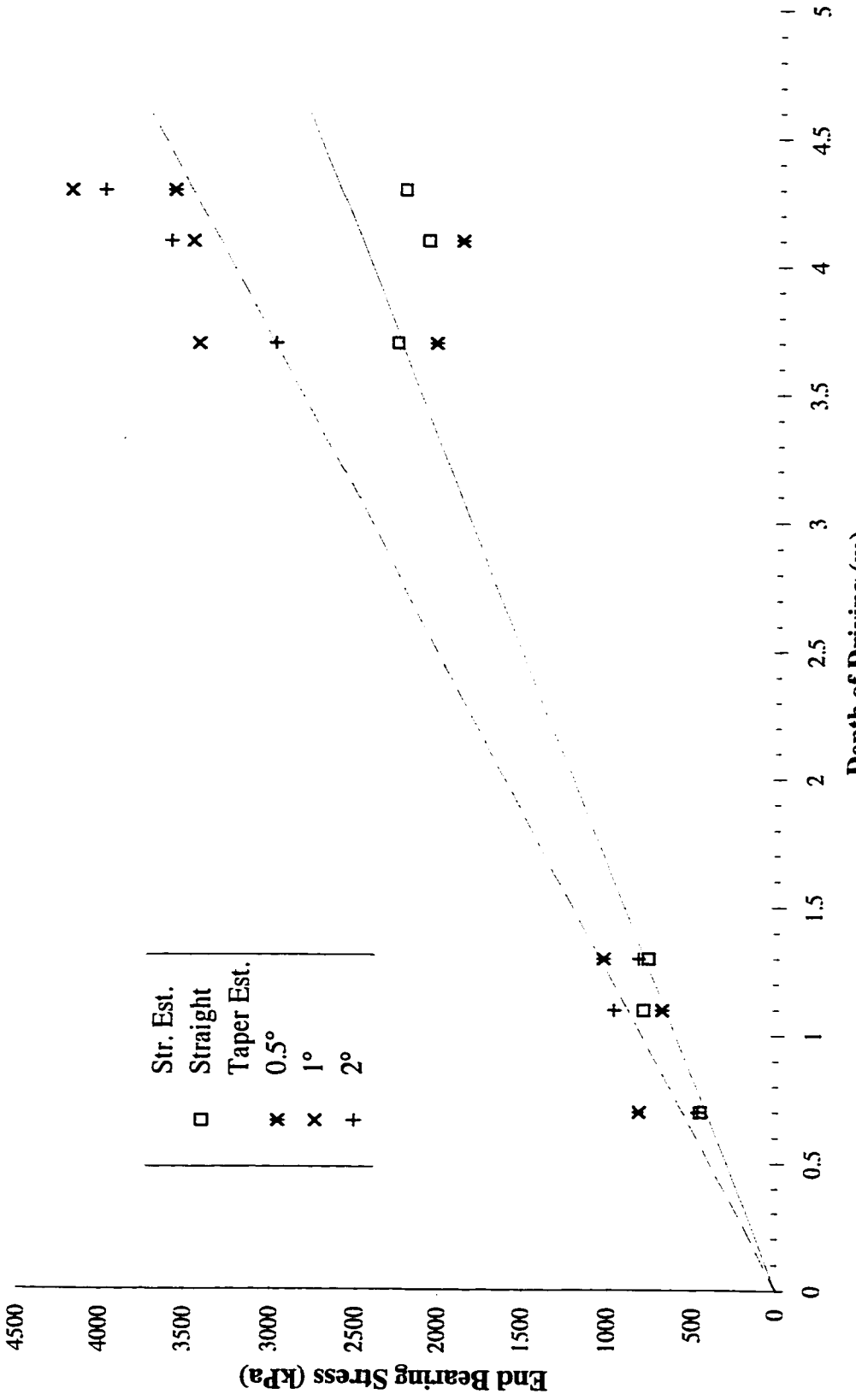

Figure 4.46 - Modified Double Passive Pressure End Bearing Method

of 7 or more. This error likely resulted from a scaling problem between the test piles and the field data on which the formula is based.

Figures 4.47 and 4.48 showed the average number of blows per 25 mm (1 inch) for the last 362 mm section of the pile driven. The data in Figures 4.47 and 4.48 indicated the lower blow count of straight piles at greater depths and pressures.

Figure 4.49 plots the bearing capacity versus the blows per inch. Equation (24) provided the best fit to the data:

$$y = 2656.1\ x^{0.9834} \tag{25}$$

The data from the tests with no additional pressure were more consistent and fit the curve better than the tests with both surcharge and confining pressures.

It must be noted that with only one test at each of the different test conditions, previously discussed in this chapter, that there is an inherent level of uncertainty in the recorded loads. This is the result of the variations naturally present when testing in a non-homogeneous material such as sand. While use of the pluviation method to create the sand bed reduced the magnitude of these variations, it cannot completely eliminate them.

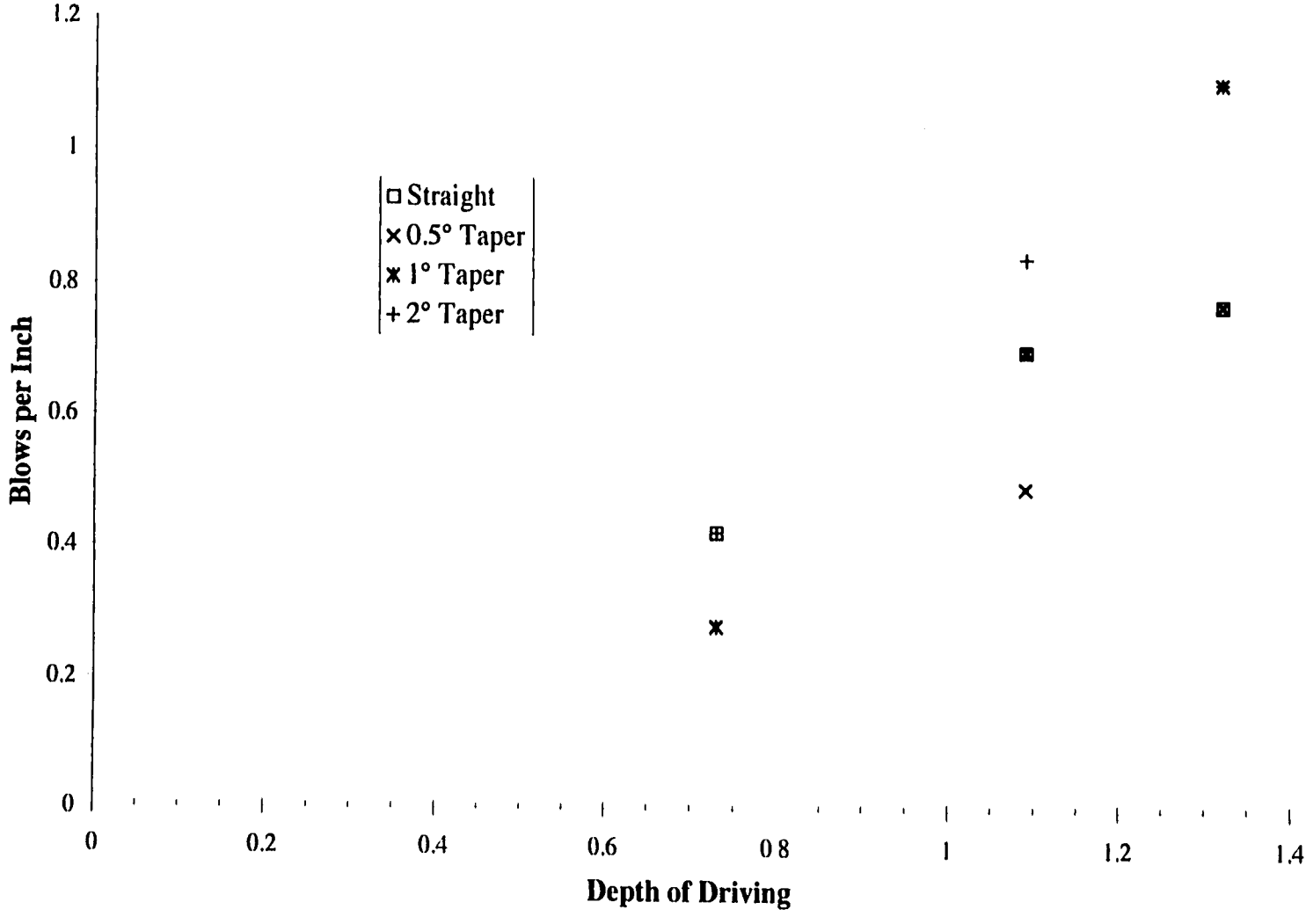

Figure 4.47 - Blows per 25 mm with No Additional Pressure

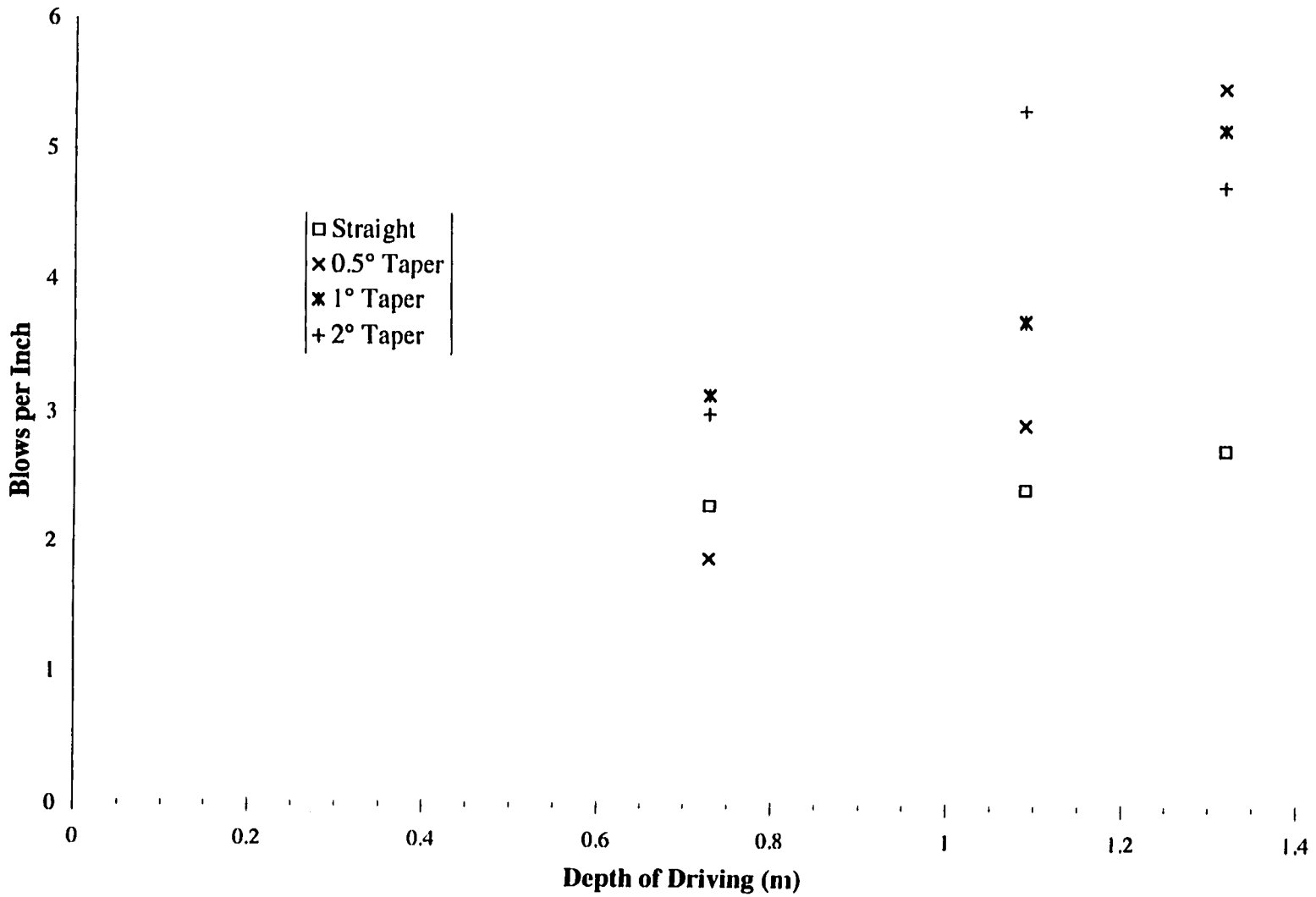

Figure 4.48 - Blows per 25 mm with Surcharge and Confining Pressure

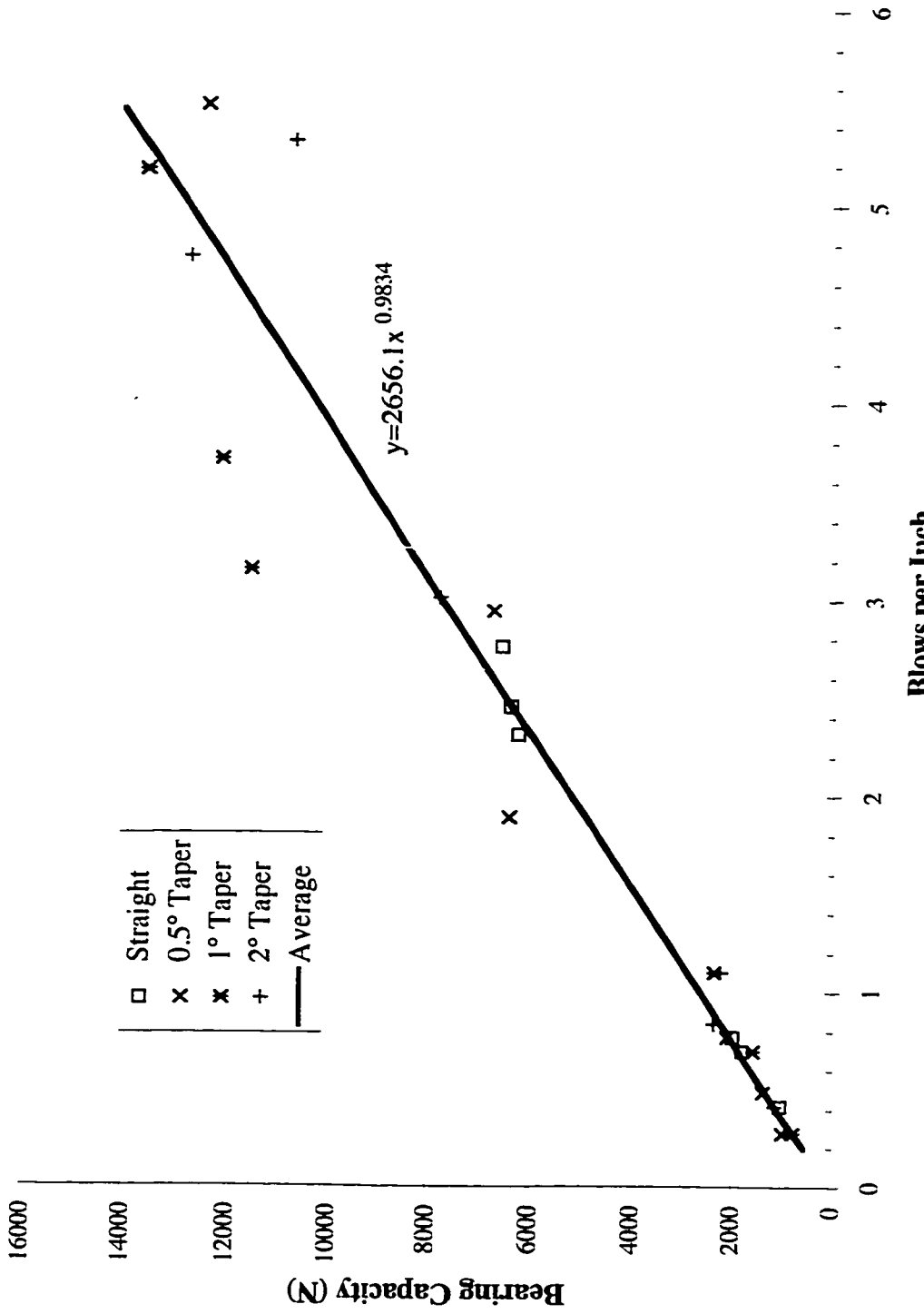

Figure 4.49 - Bearing Capacity versus Blows per 25 mm

Chapter 5

Conclusions and Recommendations

5.1 Conclusions

Based on the observations of the test data presented in Chapter 4 the following conclusions may be drawn.

5.1.1 Straight versus Tapered Piles

- The settlement required to achieve ultimate bearing capacity is approximately the same for both straight and tapered piles.
- The settlement required to reach the ultimate bearing capacity shows a small increase with an increase in ultimate bearing capacity.
- Tapered piles develop greater shear friction than straight piles.
- Tapered piles develop greater end bearing stress.
- Under low soil pressure conditions, the end bearing stress was similar for both straight and tapered piles.
- Under higher soil pressure conditions the tapered piles had a greater end bearing stress.
- The driving force required to drive straight piles increases at a slower rate, with increasing depth and pressure, than for tapered piles.
- The bearing capacity of the piles increases with increasing depth of driving.
- Straight piles support the load primarily on the pile toe, whereas tapered piles carry the load primarily along the pile walls.
- An increase in the depth of driving decreases the percentage of the load taken in end

bearing.

- Partially tapered piles provide greater uplift capacity than straight piles.

5.1.2 Tapering

- There is an increase in bearing capacity between the various tapered piles with an increase in:
  - Volumetric displacement
  - Angle of taper
  - Percentage of pile that is tapered
  - Initial stress level in the soil

5.1.3 Calibration Chamber Conditions

- Under no additional pressure, and confining with surcharge pressures conditions the results appear to be reliable.
- The application of a surcharge pressure without a confining pressure leads to arching within the tank, and therefore unreliable results.
- Unpressurized tests were more consistent than pressurized tests.

5.1.4 Analysis Methods

- The method proposed by the American Petroleum Institute (API RP-2A) over estimated the shear friction and underestimated the end bearing of the model straight piles.
- The equations proposed by Olson and Long (1989) provided a reasonably good

estimation of the shear friction of tapered piles.

- For the available data, the end bearing method presented in this paper provided a better estimation of the end bearing of tapered piles than did the API RP-2A.
- It is also possible to estimate the end bearing capacity from the blows per inch during the driving process. This cannot be done via regular driving formulae, but through a specific formula for the sand, hammer, and drop height used.
- Vesic's 10% method proved to be the most conservative estimation of the bearing capacity for a given load versus displacement curve, Chin's method was the least conservative.

5.2 Recommendations

Future study on model tapered piles should consider the following:

- Tapered piles with toe diameters both smaller and larger than 25.4 mm (1 inch).
- Larger maximum diameters and longer piles.
- Testing in sand beds of different initial relative density.
- Testing in a different sand with different internal properties.
- Effects of other loading methods such as long term sustained loading and cyclic loading, particularly in pull out conditions.
- Field testing of straight, tapered, and partially tapered piles.
- Larger diameter test tank to reduce the effects of the pile to tank aspect ratio.

Chapter 6

References

Abendroth, Robert E. and Greimann, Lowell F., (1990). "Pile Behavior Established from Model Tests", Journal of Geotechnical Engineering,Vol. 116, No. 4, pp. 571-588.

Achari, G.; (1991). "Load - Displacement Behavior of Piles." MSc. Thesis, University of Calgary, Calgary, Alberta.

Anderson, W.F. and Pyrah, I.C., (1991). "Pressuremeter Testing in a Clay Calibration Chamber", Proceedings, 1st International Symposium of Calibration Chamber Testing, New York, pp. 55-66.

Backholdin, B.V., (1971). "Bearing Capacity of Pyramidal Piles", Proceedings, 4th Conference on Soil Mechanics, pp.507-510.

Bartolomei, A.A., (1995). "Bases for Predition of the Settlements of Pile Foundations", Soil Mechanics and Foundation Engineering, Vol. 32, No. 3, pp. 76-79.

Berezantzev, V.G., Khristoforov, V.S., and Golubkov, V.N., (1961). "Load Bearing Capacity and Deformation of Piled Foundations", Proceedings, Fifth International Conference on Soil Mechanics and Foundation Engineering, Paris, pp. 11-15.

Bhushan, Kul, (1982). "Discussion: New Desing Correlations for Piles in Sands", Journal of Geotechnical Engineering,Vol. 108, No. 11, pp. 1508-1528.

Bishop, A.W., (1972). "Shear Strength Parameters for Undisturbed and Remoulded Soils Specimens", In Stress-Strain Behaviour of Soils, Foulis, London, pp. 69-80.

Bolton, M.D., (1986). "The strength and dilatancy of sands", Geotechnique, Vol. 36, No. 1, pp. 65-78.

Bolton, M.D., (1987). "The strength and dilatancy of sands", Geotechnique, Vol. 37, No. 2, pp. 219-226.

Boulon, M. and Foray, P., (1986). "Physical and Numerical Simulation of Lateral Shaft Friction Along Offshore Piles in Sand", Proceedings, 3rd Internation Conference on Numerical Methods in Offshore Piling, pp. 127-147.

Briaud, Jean-Louis and Tucker, Larry, (1984). "Piles in Sand: A Method Including Residual Stresses", Journal of Geotechnical Engineering, Vol. 110, No. 11, pp. 1666-1680.

Brinch-Hansen, J., (1963). Discussion:"Hyperbolic Stress-Strain Response in Cohesive Soil", Journal of Soil Mechanics and Foundation Engineering, ASCE, Vol. 89, SM4, pp. 241-242.

Buisman, A.S.K., (1935). "De Weerstand van Paalpunten in Zand", De Ingenieur 50, pp. 25-35.

Caquot, A., (1934). "Equilibre des Massifs a Frottement Interne". Paris (Gauthier-Villars).

Chin, F.K., (1970). "Estimation of the Ultimate Load of Piles not Carried to Failure", Proceedings, 2nd South East Asian Conference on Soil Engineering, Singapore, pp

Cooper, S.S., (1976). "Laboratory Investigation of Undisturbed Sampling of Cohesionless Material Below the Water Table", U.S. Army Engineerin Waterways Experiment Station, Vicksburg, MS.

Chan, W.T., Chow, Y.K. and Liu, L.F., (1995). "Neural Network: An Alternative to Pile Driving Formulas", Computers and Geotechnics, Vol. 17, No. 2, pp. 135-156.

Chow, F.C., Jardine, R.J., Nauroy, J.F. and Brucy, F., (1997). "Time-related increases in the shaft capacities of driven piles in sand", Geotechnique, Vol. 47, No. 2, pp. 353-361.

Coyle, Harry M. and Castello, Reno R., (1981). "New Design Correlations for Piles in Sand", Journal of the Geotechnical Engineering Division, Vol. 1981, No. GT7, pp. 965-986.

D'Appolonia, E. and Hribar, J.A., (1963). "Load Transfer in a Step-Taper Pile", Journal of the Soil Mechanics and Foundation Division, ASCE, Vol. 89, No. SM6, pp. 57-77.

Das, B.M., (1984). "Principles of Foundation Engineering", PWS - Kent Publishing Company, Boston, Massachusetts, pp. 330-415.

Das, B.M., (1990). "Principles of Foundation Engineering", 2nd Ed., PWS - Kent Publishing Company, Boston, Massachusetts, pp. 330-415.

Das, B.M., (1992). " Soil Mechanics Laboratory Manual", Engineering Press Inc., San Jose.

De Beer, E.E., (1945). "Etude des Fondations sur Pilotis et des Fondations Directes", Annales des Travaux Publics de Belgique, pp. 1-78.

De Nicola, Anthony and Randolph, Mark F., (1993). "Tensile and Compressive Shaft

Capacity of Pile in Sand", Journal of Geotechnical Engineering, Vol. 119, No. 12, pp. 1952-1973.

Dennis, Norman D. and Olson, Roy E., (1985). "Axial Capacity of Steel Pipe Piles in Sand", ASCE Geotechnical Engineering Division Specialty Conference, pp. 389-402.

Dickin, E.A. and Leung, C.F., (1990). " Performance of piles with enlarged bases subject to uplift forces", Canadian Geotechnical Journal, Vol. 27, pp. 546-1990.

Dutta, S., (1986). "Influence of Surface Taper and Shape of Pile on Ultimate Bearing and Uplift Capacity", Indian Geotechnical Journal, Vol. 16, pp. 167-180.

Dunn, I.S., Anderson, L.R. and Kiefer, F.W., (1980). "Fundamentals of Geotechnical Analysis", John Wiley and Sons, Toronto.

El Naggar, M.H. and Wei, J.Q., (1998). "Axial Loading Behaviour of Tapered Piles", Proceedings, 51st Canadian Geotechnical Conference, Edmonton, Vol. 1, pp. 367-374.

Fioravante. V., Jamiolkowski, M., Tanizawa, F., and Tatsuoka, F., (1991). "Results of CPT's in Toyoura Quartz Sand", Proceedings, 1st international Symposium of Calibration Chamber Testing, New York, pp.

Foray, P., (1991). "Scale and Boundary Effects on Calibration Chamber Pile Tests", Proceedings, 1st international Symposium of Calibration Chamber Testing, New York, pp. 147-160.

Gendron, G.J., (1970). "Pile Driving: Hammers and Driving Methods", Higway Research Board, No. 333, pp 16-22.

Ghionna, V.N. and Jamiolkowski, M., (1991). "A Critical Appraisal of Calibration Chamber Testing of Sands", Proceedings, 1st international Symposium of Calibration Chamber Testing, New York, pp. 13-59.

Gregersen, O.S., AAS, G. and Dibiagio, E., (1973). "Load Tests on Friction Piles in Loose Sand", Proceedings of the Eigth International Canference on soil Mechanics, Vol. 2.1, pp 109-117.

Handy, Richard L., (1985). "The Arch in Soil Arching", Journal of Geotechnical Engineering, Vol. 111, No. 3, pp. 302-318.

Hanna, T.H. and Tan, R.H.S., (1973). "The Behaviour of Long Piles Under Compressive Loads in Sand", Canadian Geotechnical Journal, Vol. 10, No. 3, pp. 311-340.

Heerema, Edward P., (1980). "Predicting Pile Driveability: Heather as an Illustration of the friction fatigue theory", Ground Engineering, Vol. 13, April, pp.15-20.

Hettler, A., (1982). "Approximation formulae for piles under tension", Proceedings. IUTAM Conference on Deformation and Failure of Granular Materials, pp. 603-608.

Holden, J.C., (1971). "Laboratory Research on Static Cone Penetrometers", Department of Civil Engineering, University of Florida, Report No. CE-SM-71-1.

Hunter, A.H. and Davisson, M.T., (1969). "Measurements of Pile Load Transfer", Performance of Deep Foundations, ASTM STP444, American Society for Testing and Materials, pp. 106-117.

Ireland, H.O., (1957). "Pulling Tests on Piles in Sand", 4th International Conference on Soil Mechanics and Foundation Engineering, Vol. 8, No. 1, pp 43-45.

Jain, M.P., Rastogi, P.C. and Bhandari, R.K., (1979). "Comparative Behaviour of Tapered and Uniform Diameter Piles in Loose Sands", Indian Geotechnical Journal, Vol. 9, pp.154-162.

Jaky, J., (1948). "On the Bearing Capacity of Piles", Proceedings, Second International Conference on Soil Mechanics and Foundation Engineering, Vol. 1, pp. 100-103.

Kay, J.N., (1997). "Ultimate capacity of driven piles in sand", Proceedings of the Institution of Civil Engineers. Geotechnical Engineering, Vol. 125, pp. 65-70.

Kishida, H., (1967). "The Ultimate Bearing Capacity of Pipe Piles in Sand", Proceedings. 3rd Asian Regional Conference on Soil Mechanics and Foundation Engineering, Vol. 2, pp. 196-199.

Kishida, H. and Uesugi, M., (1987). "Tests of the interface between sand and steel in the simple shear apparatus", Geotechnique, Vol. 37, No. 1, pp. 45-52.

Klos, J. and Tejchman, A., (1977). "Analysis of Behaviour of Tubular Pipes in Subsoil", Proceedings of the International Conference on Soil Mechanics and Foundation Engineering, Tokyo, Japan, vol. 1, pp 605-608.

Kodikara, J.K. and Moore, I.D., (1993). "Axial Response of Tapered Piles in Cohesive Frictional Ground", Journal of Geotechnical Engineering, Vol. 119, No. 4, pp. 675-693.

Kraft, Leland M., (1990). "Computing Axial Pile Capacity in Sands for Offshore Conditions", Marine Geotechnology, Vol. 9, pp. 61-92.

Kraft, Leland M., (1991). "Performance of Axially Loaded Pipe Piles in Sand", Journal of Geotechnical Engineering, Vol. 117, No. 2, pp. 272-296.

Kulhawy, F. H., (1984). "Limiting Tip and Side Resistance: Fact or Fallacy?", Proceedings, Analysis and Design of Pile Foundations, ASCE, pp. 80-98.

Kurian, Nainan P. and Srinivas, Moola s., (1995). "Studies on the Behaviour of Axially Loaded Tapered Piles by the Finite Element Method" International Journal for Numerical and Analytical Methods in Geomechanics, Vol. 19, No. 12, pp. 869-888.

Last, N.C., (1979). "Cone Penetration Tests on Samples of Dry Hokksund Sand in a Rigid Walled Chamber", Norwegian Geotechnical Institute, Oslo, Norway.

Lehane, B.M., Jardine, R.J., Bond, A.J. and Frank, R., (1993). "Mechanisms of Shaft Friction in Sand from Instrumented Pile Tests", Journal of Geotechnical Engineering, Vol. 119, No. 1, pp. 19-35.

Leung, C.F., Lee, F.H. and Yet, N.S., (1996). "The role of particle breakage in pile creep in sand", Canadian Geotechnical Journal, Vol. 33, pp. 888-898.

Lindqvist, L. and Petaja, J., (1981). "Experiences of Tapered Priction Piles", Proceedings, Tenth International Conference on Soil Mechanics and Foundation Engineering, Vol. 2, pp. 759-766.

Lings, M.L., (1997). "Predicting the Shaft Resistance of Driven Pre-Formed Piles in Sand", Proceedings of the Institution of Civil Engineers. Geotechnical Engineering, Vol. 125, No. 4, pp. 71-84.

Lu, Bill T.D., (1988). "Effects of grain crushing on axial behavior of driven piles in calcareous sand", Engineering for Calcareous Sediments, pp. 231-238.

Mansur, Charles I. and Hunter, Alfred H., (1970). "Pile Tests - Arkansas River Project", Journal of the Soil Mechanics and Foundations Division, Vol. 96, No. SM5, pp. 1545-1582.

Mattes, N.S. and Poulos, H.G., (1971). "Model Tests on Piles in Clay", Proceedings, 1st Australian-New Zealand Conference on Geomechanics, Melbourne, vol. 1, pp. 254-260.

Mazurkiewicz, B.K., (1972). "Test Loading of Piles According to Polish Regulations", Royal Swedish Academy of Engineering Sciences Committee on Pile Research,, Report No. 35, Stockholm, 20 p.

McClelland, Bramlette, (1974). "Design of Deep Penetration Piles for Ocean Structures",

Journal of the Geotechnical Engineering Division, Vol. 100, No. GT7, pp. 709-747.

Meyerhof, G.G., (1956). "Penetration Tests and Bearing Capacity of Cohesionless Soils", Journal of the Soil Mechanics and Foundations Division, Vol. 82, No. SM1, pp. 1-21.

Meyerhof, G.G., (1959). "Compaction of Sands and Bearin Capacity of Piles", Journal of the Soil Mechanics and Foundations Division, Vol. 85, No. SM6, pp.1-29.

Meyerhof, G.G., (1976). "Bearing Capacity and Settlement of Pile Foundations", Journal of the Soil Mechanics and Foundations Division, Vol. 102, No. GT3, pp.197-228.

Meyerhof, G.G., (1979). "Scale Effects of Ultimate Pile Capacity", Journal of Geotechnical Engineering, Vol. 109, No. 6, pp.797-806.

Mitchell, J.K. and Solymar, Z.V., (1984). "Time-Dependent Strength Gain in Freshly Deposited or Densified Sand", Journal of Geotechnical Engineering, Vol. 110, No. 11, pp. 1559-1576.

Mohan. D.. (1989). "Pile Foundations", 1st Ed.,A.A. Balkema, Rotterdam, New York, pp. 7-8, 67-74.

Monotube Pile Performance Data, Form No. MP8., Monotube Pile Corporation.

Nauroy, J.F. and Le Tirant, P., (1983). "Model Tests of Piles in Calcareous Sands", Proceedings. Geotechnical Practice in Offshore Engineering, pp. 356-369.

Nordlund, R.L., (1963). "Bearing Capacity of Piles in Cohnesionless Soils", Journal of the Soil Mechanics and Foundations Division, Vol. 89, No. SM3, pp. 1-35.

Olson, R.E. and Long J.H., (1989). "Axial Load Capacity of Tapered Piles", The Art and Science of Geotechnical Engineering At the Dawn of the Twenty-First Century, pp. 417-436.

Parkin, A.K., (1991). "Chamber Testing of Piles in Calcareous Sand and Silt", Proceedings, 1st international Symposium of Calibration Chamber Testing, New York, pp. 289-302.

Peck, Ralph B., (1958). " A Study of the Comparative Behavior of Friction Piles", Highway Research Board, Vol. 36, pp. 1-72.

Pilyagin, A.V., (1995). "Improving the Effectiveness of Design Solutions for Pile Foundations", Soil Mechanics and Foundation Engineering, Vol. 32, No. 3, pp. 90-91.

Potyondy, J.G., (1961). "Skin Friction Between Various Soils and Construction Materials", Geotechnique, Vol. 2, No. 4, pp. 339-353

Prakash S. and Sharma H.D., (1990). "Pile Foundations in Engineering Practice", John Wiley and Sons Inc., New York.

Prandtl, L, (1921), "Uber die Eindringungsfestigkeit Plastisher Baustoffe und die Festigkeit von Schneiden", Zeitschrift fur Angewandte Mathematik und Mechanik, 1:1, pp. 15-20.

Rad, N.S. and Tumay, M.T., (1987). "Factores Affecting Sand Speciment Preparation by Raining", Geotechnical Testing Journal, Vol. 10, No. 1, pp. 31-37.

Randolph, M.F., (1979). "The Effect of Pile Type on the Desing Parameters for Driven Piles", Proceedings. 7th European Conference on Soil Mechanics, Vol. 2, pp. 107-114.

Randolph, M.F. and Dolwin, J., (1994). "Design of Driven Piles in Sand", Geotechnique, Vol. 44, No. 3, pp. 427-448.

Randolph, M.F., (1988). "The Axial Capacity of Deep Foundation in Calcareous Soil", Engineereing for Calcareous Sediments, pp. 837-857.

Randolph, M.F. and Wroth C.P., (1978). "Analysis of Deformation of Vertically Loaded Piles", Journal of the Geotechnical Engineering Division, Vol. 104, No. GT12, pp. 1465-1488.

Recommended Practice for Planning, Designing and Constructing Fixed Offshore Platforms, (1989). 18th Ed. API Recommended Practice 2, pp. 48-59.

Robinsky, E.I. and Morrison, C.F., (1964). "Sand Displacement and Compaction Around Model Friction Piles", Canadian Geotechnical Journal, Vol. 1, No. 2, 1964.

Rybnikov, A.M., (1990). "Experimental Investigation fo Bearing Capacity of Bored-Cast-In-Place Tapered Piles", Soil Mechanics and Foundation Engineering, Vol. 27, No. 2, pp. 48-52.

Saha, S. and Ghosh, D.P., (1986). " Vertical Vibration of Tapered Piles", Journal of Geotechnical Engineering, Vol. 112, No. 3, pp. 290-303.

Schnaid, F. and Houlsby, G.T., (1991). "An Assessment of Chamber Size Effects in the Calibration of in situ Tests in Sand", Geotechnique, Vol. 41, No. 3, pp. 437-445.

Singh, G., Lai, W.T. and Das, B.M., (1996). "Sensitivity of Probabilistic Pile Design to

Various Uncertainties", Proceedings of the Sixth International Offshore and Polar Engineering Conference, Vol. 1, pp. 506-513

Skempton, A.W., Yassin, A.A. and Gibson, R.E., (1953). "Theorie de la Force Portante des Pieux Dans le Sable", Annales de l'Institut du Batiment et des Travaux Publics, No. 63-64, pp. 285-290.

Smith, E.A.L., (1960). "Pile-Driving Analysis by the Wave Equation", Journal of the Soil Mechanics and Foundations Division, Vol. 86, No. EM4, pp. 35-61.

Smith, V.B., (1995). "Plugging of Model Piles", MSc. Thesis, University of Calgary, Calgary, Alberta.

Smits, F.P., (1982). "Cone Penetration Tests in Dry Sand", Proceedings, 2nd European Symposium on Penetration Testing, Vol. 2, pp. 877-881.

Sparrow, D.G., (1989). "Driven Model Piles in Sand", MSc. Thesis, University of Calgary, Calgary, Alberta

Sterin, V.S., Golubenkov, V.A., Rodov, G.S., Leikin, B.V. and Kurbatov, L.G., (1984). "Economics of Material and Energy Resources", Soil Mechanics and Foundation Engineering, Vol. 21, No. 3, pp. 108-111.

Sweeny, B.P. and Clough, G.W., (1990). "Design of a Large Calibration Chamber", Geotechnical Testing Journal, Vol. 13, No. 1, pp. 36-44.

Tabucanon, J.T., Airey, D.W. and Poulos, H.G., (1995). "Pile Skin Friction in Sands from Constant Normal Stiffness Tests", Geotechnical Testing Journal, Vol. 18, No.3, pp. 350-364.

Tan, R.H.S. and Hanna, T.H., (1974). "Long Piles Under Tensile Loads in Sand", Geotechnical Engineering, Vol. 5, pp. 109-124.

Tavenas, F. and Audy, R., (1972). "Limitations of the Driving Formulas for Predicting the Bearing Capacities of Piles in Sand", Canadian Geotechnical Journal, Vol. 9, pp. 47-62.

Teh, C.I., Wong, K.S., Goh, A.T.C., and Jaritngam, S., (1987). "Prediction of Pile Capacity Using Neural Networks", Journal of Computing in Civil Engineering, Vol. 11, No. 2, pp. 129-137.

Terzaghi, K., (1936). "Stress Distribution in Dry and in Saturated Sand Above a Yeilding Trap Door", Proceedings of the International Conference on Soil Mechanics and Foundation Engineering, Vol. 1, pp. 307-311.

Toolan, F.E., Lings, M.L. and Mirza, U.A., (1990). "An Appraisal of API RP2A Recommendations for Determining Skin Friction of Piles in Sand", Proceedings of the 22nd Offshore Technology Conference, pp. 33-42.

Touma, F.T. and Reese, L.C., (1974). "Behavior of Bored Piles in Sand", Journal of the Geotechnical Engineering Division, Vol. 100, No. GT7, pp. 749-761.

Veismanis, A., (1974). "Laboratory Investigation of Electrical Friction - Cone Penetrometers in Sand", Proceedings. E.S.P.T., pp. 407-419.

Vesic, A.S., (1963). "Bearing Capacity of Deep Foundations in Sand", National Academy of Sciences, National Research Council, Highway Research Record 39, pp. 44-56.

Vesic, A.S., (1964). " Investigations of Bearing Capacity of Piles in Sand",, Proceedings, North American Conference on Deep Foundations, Mexico City, Vol.1, pp. 197-224.

Vesic, A.S., (1967). "Ultimate Loads and Settlement of Deep Foundations in Sand", Proceedings, Symposium on Bearing Capacity and Settlement of Foundations, Duke University, Durham, N.C., pp. 53-68.

Vesic, A.S. and Clough, G.W., (1968). "Behavior of Granular Materials Under High Stresses", Journal of the Soil Mechanics and Foundations Division, Vol. 94, No. SM3, pp. 661-688.

Vesic, A.S., (1973). "On Penetration Resistance and Bearing Capacity of Piles in Sand", Discussion, Session 3, Proceedings, Eighth International Conference on Soil Mechanics and Foundation Engineering, Vol. 4-2, Moscow, pp. 78-81.

Vesic, A.S., (1977). "Design of Pile Foundations", National Co-Operative Highway Research Program Synthesis of Practice No. 42, Transportation Research Board, Washington D.C., pp. 1-68.

Vijayvergiya, V.N., (1980). "Soil Response During Pile Driving", Proceedings, International Conference on Numerical Methods in Offshore Piling, pp. 53-58.

Whitaker, T., (1957). "Experiments with Model Piles in Groups", Geotechnique, Vol. 7, pp. 147-167.

Wu, A.K.H., Kuhlemeyer, R.L. and To, C.W.S., (1989). "Validity of Smith Model in Pile Driving Analysis", Journal of Geotechnical Engineering, Vol. 115, No. 9, pp. 1285-1302.

Zil'berberg, S.D. and Sherstnev, A.D., (1990). "Construction of Compaction Tapered Pile

Foundations (From the Experience of the "Vladspetsstroi" Trust)", Soil Mechanics and Foundation Engineering, Vol. 27, No. 3, pp. 96-101.